THE DISTRIBUTION AND BEHAVIOUR OF GOLD IN SOILS IN THE VICINITY OF GOLD MINERALIZATION, NICKEL PLATE MINE, HEDLEY, SOUTHERN BRITISH COLUMBIA

by

STEVEN JOHN NORMAN SIBBICK

B.Sc. (Hons) The University of Western Ontario, 1986

A THESIS SUBMITTED IN PARTIAL FULFILMENT OF

THE REQUIREMENTS FOR THE DEGREE OF

MASTER OF SCIENCE

in

THE FACULTY OF GRADUATE STUDIES

DEPARTMENT OF GEOLOGICAL SCIENCES

We accept this thesis as conforming

to the required standard

THE UNIVERSITY OF BRITISH COLUMBIA

June, 1990

In presenting this thesis in partial fulfilment of the requirements for an advanced degree at the University of British Columbia, I agree that the Library shall make it freely available for reference and study. I further agree that permission for extensive copying of this thesis for scholarly purposes may be granted by the head of my department or by his or her representatives. It is understood that copying or publication of this thesis for financial gain shall not be allowed without my written permission.

Department of _GEOLOGICAL SCIENCES_

The University of British Columbia
Vancouver, Canada

Date _July 6 1990_

ABSTRACT

Sampling of soils and till are conventional methods of gold exploration in glaciated regions. However, the exact nature of the residence sites and behaviour of gold within soil and till are poorly known. A gold dispersion train extending from the Nickel Plate mine, Hedley, southwest British Columbia, was investigated in order to determine the distribution and behaviour of gold within soils developed from till.

Three hundred and twelve soil, till and humus samples (representing LFH, A, B and C horizons) were collected from fifty-two soil pits and thirty-four roadcut locations within the dispersion train. Soil and till samples were sieved into four size fractions; the resultant -212 micron (-70 mesh) fraction of each sample was analysed for Au by FA-AAS. Humus samples were ground to -100 micron powder and analysed for Au by INAA. Based on the analytical results, each LFH, A, B and C horizon was subdivided into anomalous and background populations.

Detailed size and density fraction analysis was carried out on soil profiles reflecting anomalous and background populations, and a mixed group of samples representing the

overlap between both populations. Samples were sieved to six size fractions; three of the size fractions (-420+212, -212+106, -106+53 microns) were separated into two density fractions using methylene iodide and analysed for Au by FA-AAS. The Au content of the -53 micron fraction was analysed by FA-AAS and cyanide extraction - AAS.

Results indicate that the Au content of soil profiles increase with depth while decreasing with distance from the minesite. Heavy mineral concentrates and the light mineral fraction Au abundances reveal that dilution by a factor of 3.5 occurs within the till over a distance of 800 metres. However, free gold within the heavy mineral fraction is both diluted and comminuted with distance. Recombination of size and density fractions indicate that the Au contents of each size fraction are equivalent; variation in Au abundance is not observed with a change in grain size. Seventy percent of the Au in the -53 micron fraction occurs as free gold.

Chemical activity has not altered the composition of gold grains within the soil profiles. Compositional and morphological differences between gold grains are not indicative of glacial transport distance or location within the soil profile. Relative abundances of gold grains between sample locations can be used as an indicator of proximity to the minesite.

The sampling medium with the best sample representivity and contrast between anomalous and background populations is the -53 micron (-270 mesh) fraction of the C horizon. Geochemical soil sampling programs in the vicinity of the Nickel Plate mine should collect a minimum mass of 370 grams of -2000 micron (-2 mm) soil fraction in order to obtain 30 grams of the -53 micron fraction.

TABLE OF CONTENTS

LIST OF TABLES

LIST OF FIGURES

ACKNOWLEDGEMENTS

Chapter One

Introduction

1.1 <u>Introduction</u>

Extensive portions of the Northern Hemisphere, including most of Canada, have undergone periodic glaciation during the past two million years. The effect of these glaciations has been to obscure large regions of bedrock with material derived from the glacial erosion of local or distant materials. As ore deposits found in regions of thin overburden have become depleted, emphasis has shifted to exploration in areas covered by glacial sediment. Till, the most common glacial sediment, has received the most attention. Exploration in till covered areas is further complicated by the development of soil, which can modify any geochemical signatures found in the till.

1.2 <u>Properties of gold</u>

Gold belongs to Group 1B of the periodic table, along with copper (Cu) and silver (Ag). The density of gold is high (density of pure gold = 19.3 g/cm^3), though solid solution with elements such as silver, copper, mercury and iron will decrease its density. Gold and silver exist in complete solid solution, with most native gold containing 5 to 15 percent Ag (Boyle, 1979). Native gold containing more than 20 percent silver is referred to as electrum. Visually,

electrum is distinguished from native gold by being pale yellow and becoming increasingly paler with increased silver content. At approximately 65 percent Ag, the colour of electrum becomes indistinguishable from pure silver (Boyle, 1979).

1.3 Statistical distribution of rare grains

The distribution of rare grains within a granular material is described by the Poisson distribution (Ingamells, 1981; Koch and Link, 1970):

$$P(n) = e^{-u} u^n/n! \qquad (1-1)$$

where u is the mean number of grains within a sample and P(n) is the probability of n grains being found within the sample. Confidence intervals for the mean (u) at a significance level (a) can be estimated using the X^2 (chi-squared) distribution (Zar, 1984):

$$(X^2(1-a/2),2N)/2 \quad < u < \quad (X^2(a/2),2(N+1))/2$$

where N is an estimate of u

The effect of rare grains upon soil sampling can be illustrated by a simple example. A gold dispersion train

derived from an auriferous quartz vein results in the
homogeneous distribution of 100 micron diameter gold grains
throughout the soil profile giving a bulk composition of 100
ppb (100 micrograms Au per gram). The host soil is composed
of grains close to 100 microns in diameter and possesses an
insignificant Au content. During a geochemical soil survey,
a 300 gram B horizon soil sample is taken from the
dispersion train. From this, a representative thirty gram
subsample is taken and analysed for Au by FA-AAS. Assuming
pure gold (density = 19.3 g/cm^3) spheres of 100 microns
diameter, the weight of each gold grain is 10.09 micrograms.
The weight of gold within the sample is 30 micrograms (100
ppb X 300 grams), resulting in the expected number of
particles (u) to be 2.972. The expected number of gold
particles in the representative thirty gram subsample will
be 0.297.

Using the Poisson distribution (equation 1-1) the
probability that the subsample will contain no particle of
gold (P(0), n=0) is 0.74 (Figure 1.1). Therefore, the chance
of not detecting the anomaly is 74%. Only a 26% chance
exists that one or more gold grains will be found within the
sample. Detection of a single gold grain would result in a
reported Au concentration of 337 ppb, three times higher
than the true Au concentration of 100 ppb. This feature has
led to the use of the term "nugget effect" to describe high
Au analyses generated by the random inclusion of a single

Probability

Figure 1.1 – Poisson probability of detecting N gold grains
in a 30 gram subsample.

(or a very few) gold particles within a small sample (Ingamells, 1981).

Variation in the size fraction and sample size used for analysis will have a dramatic effect upon the perceived Au concentration. In a modification of the previous example, the auriferous soil is now composed of six equally proportioned grain sizes (300, 150, 75, 50, 10 and 2 microns), each with a gold content of 100 ppb. All gold within the soil exists as free grains. A 1800 gram sample taken in the field provides 300 grams of each grain size for analysis. Representative ten and thirty gram splits are taken of each size fraction and analysed by FA-AAS for Au. The probability, using the Poisson distribution, of these samples (300, 30 and 10 gram) containing no gold grains (P(0), n=0) is shown in Figure (1.2). Chances of encountering a gold grain within a sample are strongly dependent upon the grain size and weight of sample analysed. There is a very high probability of not detecting Au within the coarse size fractions, while there is no chance of this occurring in the fine size fractions. Undersized field sample weights for the coarse size fractions results in a bias towards the finer size fractions; Au concentrations would be perceived to increase with decreasing grain size.

Variation of analytical precision with the number of gold particles in a sample was quantified by Clifton et al.
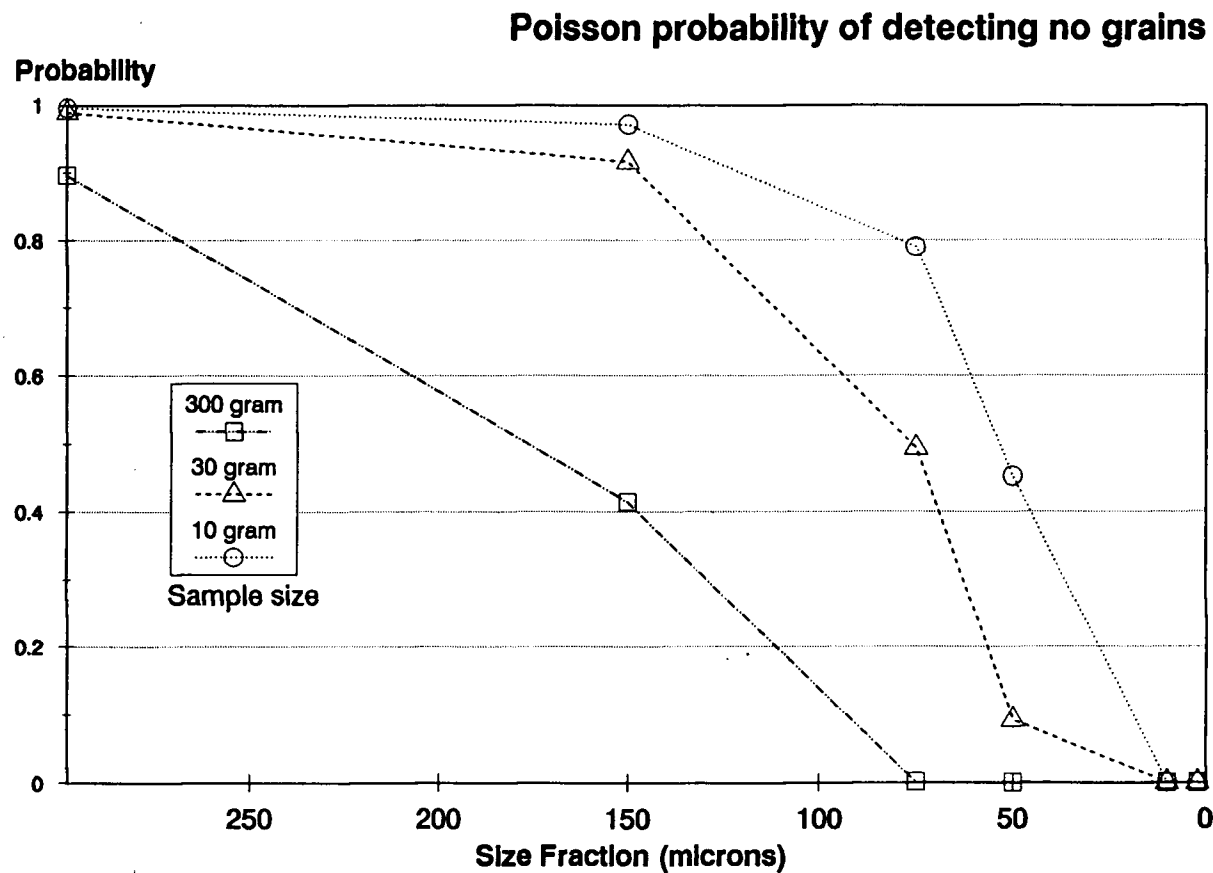
Figure 1.2 – Poisson probability of detecting no gold grains as a function of grain size and subsample weight.

(1969). Their work showed that the precision of an analysis is determined solely by the number of gold grains present in the sample as long as the following conditions are met:

1) Gold particle mass is uniform.
2) Gold particles make up less than 0.1% of all particles.
3) The sample contains at least 1000 particles.
4) Analytical errors are absent.
5) The gold particles are randomly distributed through the material being sampled.

Based on these conditions, to achieve a precision of 50%, a minimum of 20 particles of gold is required (Clifton et al., 1969). The relation between particle size and the size of sample required to contain 20 particles of gold is shown in Figure (1.3).

1.4 Statement of problem

At the Nickel Plate mine, Hedley, southwest British Columbia, a gold dispersion train extends downice and downslope from the minesite. The dispersion train is found in an oxidized basal till which has been altered by the formation of a poorly differentiated soil layer in the upper one metre of till.

Conventional methods of geochemical soil sampling rely upon analysis of the -80 mesh fraction of the B horizon. However, the exact nature of the residence sites and
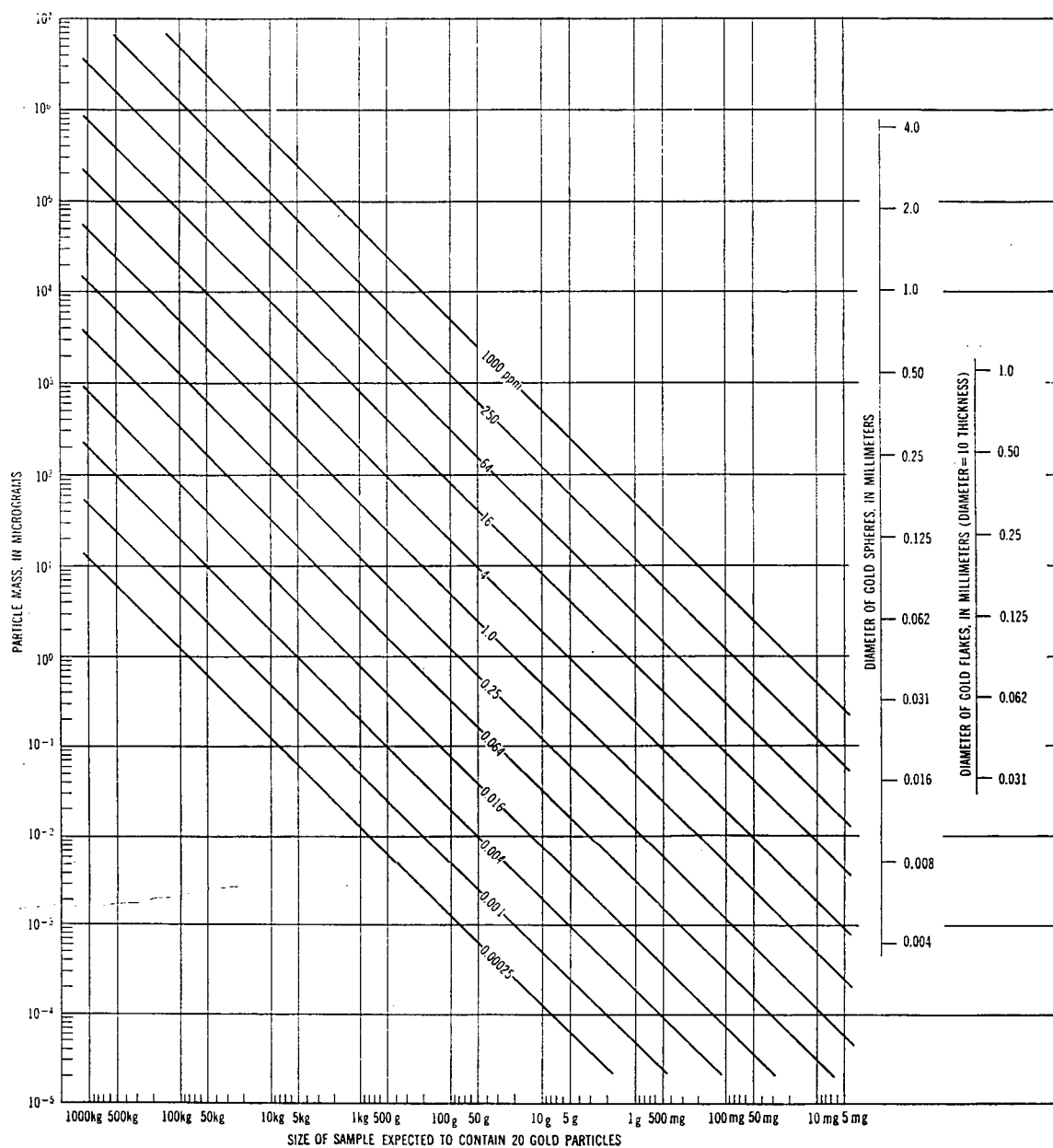
Figure 1.3 - Relationship between particle size and the size of sample required to contain twenty particles of gold. From Clifton et al. (1969)

dispersion characteristics of gold within soil are not well known. Improved techniques for detection of gold soil anomalies will result from a more detailed knowledge of the behaviour and characteristics of gold within the soil profile.

It is the goal of this thesis to examine the following:

1) Alpine glacial dispersion of gold away from gold mineralization.
2) The distribution and residence sites of gold within soil profiles.
3) The morphology and composition of glacially transported gold grains within soils.

Results of this examination should provide data which can be utilized to recommend:

1) Optimum sample size.
2) Optimum soil horizon for sampling.
3) Optimum size and / or density fraction for analysis.
4) Optimum analytical technique.

Chapter Two

Geochemical Dispersion in Tills

2.1 <u>Origin of till</u>

2.1.1 <u>Introduction</u>

Till is a form of glacial drift, a generic term which also includes glaciofluvial, glacioeolian and glaciolacustrine sediments. These materials differ from till by being sorted and reworked sediments, many of which exhibit the characteristics of reworking / redeposition by water (Goldthwait, 1971).

Dreimanis, (1976) defined till as a compact material which has a direct glacial origin, a variety of rock and mineral fragments of various sizes, poor sorting and a lack of stratification. Where this type of material composes more than fifty percent of a glacial drift exposure or stratum, then the entire unit may be referred to as till (Goldthwait, 1971).

2.1.2 <u>Till formation</u>

Three events contribute to the formation of till:

1) Erosion

2) Transport

3) Deposition

2.1.2.1 <u>Erosion</u>

Two forms of erosion are possible (Dreimanis, 1976):
(1) extraglacial debris, the passive collection of material
due to rocks (sand, gravel, etc.) falling and collecting
upon the glacier surface, and (2) active erosion, occurring
at the base of the glacier where material is abraded and
removed from the ground surface underlying the glacier.

Active erosion takes place by 1) plucking / quarrying,
where clasts or blocks of rock are removed from the bedrock
and carried either within the glacier or along the bedrock-
glacier interface (Flint, 1971); 2) abrasion, in which
entrained material at the base of the glacier acts to scrape
and polish the bedrock in a manner similar to a piece of
sandpaper moving across a block of wood (Flint, 1971), and
lastly 3) large scale block inclusions, wherein very large
(up to kilometers in size) blocks of bedrock are uplifted

and moved within or at the base of a glacier (Figure 2.1) (Moran, 1971).

Of these three methods of active erosion, quarrying / plucking appears to be the most important (Flint, 1971). The rate of erosion of material beneath a glacier depends upon the following factors (Flint, 1971):

1) glacier thickness,

2) rate of movement,

3) abundance, shape and hardness of rock fragments carried in the base of the glacier,

4) erodibility of ground beneath glacier.

5) state of flow (extending vs compressive)

6) hydrostatic flow

Susceptibility of the ground beneath a glacier to erosion will vary with depth. Weathered bedrock will erode much more rapidly than the underlying unweathered bedrock (Flint, 1971). Calculations carried out on two large glaciers in Iceland by Okko (1955) (see Flint, 1971) gave erosion rates of 6.4 cm / 100 years and 55 cm / 100 years.
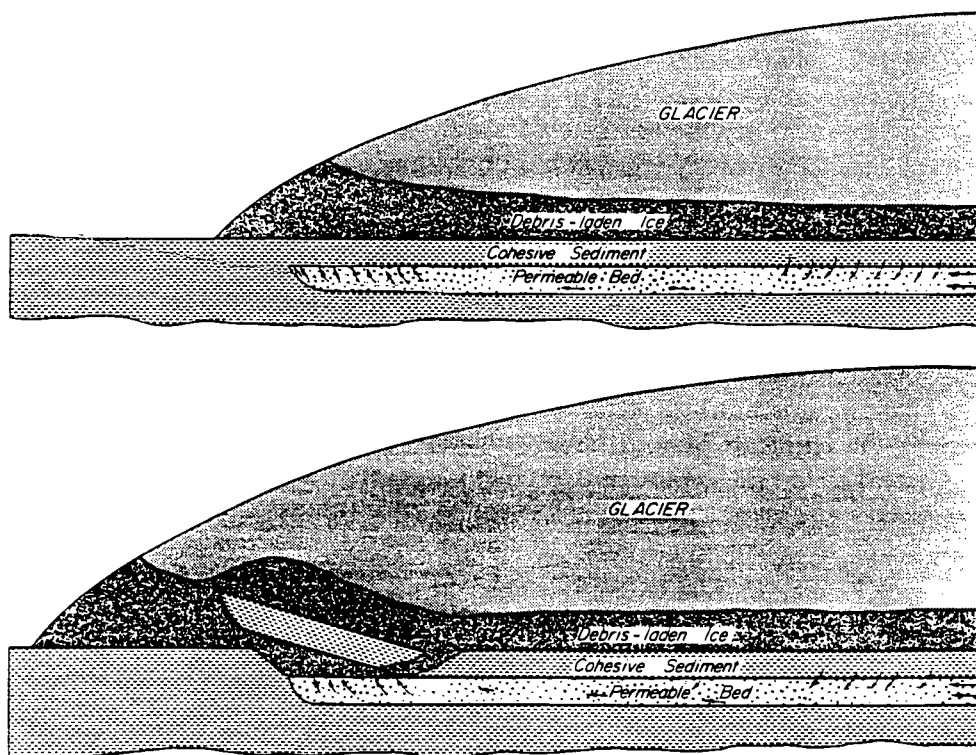
Figure 2.1 - Schematic diagram of large scale block
inclusions. From Moran (1971).

2.1.2.2 <u>Transport</u>

Drift may be transported by a glacier in three general ways:

1) Basal transport

2) Englacial transport

3) Superglacial transport

Basal transport

Basal transport occurs in the bottom 1 to 3 metres of a glacier (Figure 2.2). Most of the rock debris carried by a glacier are carried within this zone, usually as thin bands of material within the ice (Boulton, 1970). This is the main zone of crushing and comminution due to the high proportion of rock debris (Boulton, 1970). Less than 0.1% of all clasts survive more than 35 km of basal transport, most are comminuted to their constituent minerals prior to reaching this distance (Goldthwait, 1971). Studies by Drake (1971) showed that the breakdown of clasts is dependent upon lithology. Also, clast rounding increased greatly within the first mile of transport (Drake, 1971). Crushing (breakage) appears to be the most significant method of size reduction within the basal zone (Goldthwait, 1971).

The terminal size of material crushed within the basal
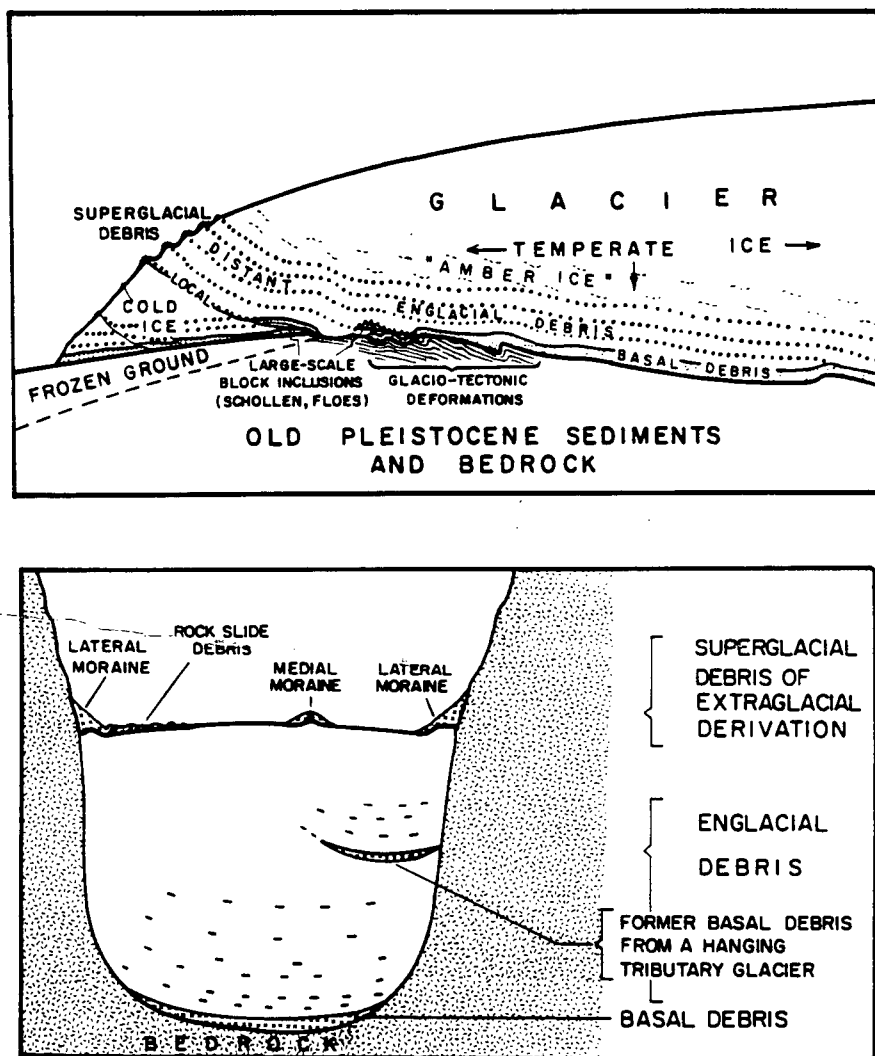
Figure 2.2 - Schematic diagrams of transport locations of debris within glaciers. From Dremanis (1976).
    A) Radial section of ice sheet in its terminal zone.
    B) Cross section of a valley glacier.

zone of a glacier was shown by Dreimanis and Vagners (1971) to be fine sand for granitic and metamorphic rocks, silt size for carbonate rocks, and clay size for shales.

Upon reaching a constriction or obstruction beneath or within a glacier, basal debris may move upwards to be emplaced within the englacial zone (Goldthwait, 1971).

Englacial transport

Debris is usually more diffused within the englacial zone (Figure 2.2) and therefore does not suffer the same degree of crushing and comminution as basal debris (Dreimanis, 1976). Soft, unresistant minerals, if rapidly uplifted out of the basal zone, may be preserved within the englacial zone (Dreimanis, 1976). Englacial material may survive hundreds of kilometers of transport before being comminuted (Dreimanis, 1976).

Superglacial transport

Material transported on the glacier surface may be derived from extraglacial sources, such as debris falling onto the glacial surface and from englacial debris uplifted to the surface near the glacial terminus (Figure 2.2)

(Dreimanis, 1976). Transport of this material may be by glacial movement, mechanical movement downslope, or localized transport in supraglacial meltwater streams (Sharp, 1949).

2.1.2.3 Deposition

The mode of transport of glacial debris determines its deposition (Figure 2.3). Englacially and superglacially transported debris are deposited by downmelting of glacial ice to form ablation till. Material transported within the basal zone and deposited beneath an active glacier is referred to as basal or lodgement till.

Ablation till

Shilts (1973, 1976) noted that ablation till generally contains more material transported from a distant source that does basal till, due to the greater distance of transport of englacial-superglacial debris. Ablation till is characterized by a lack of fine sediments (relative to basal tills), angular clasts, and loose compaction (Goldthwait, 1971). Ablation till has been defined by Boulton (1968, 1970) to be composed of two forms, flow till and melt-out till (Figure 2.3).

| GLACIAL DRIFT IN TRANSPORT | GLACIAL DRIFT DEPOSITED AS TILL | |
| | BY GLACIERS AGROUND | UNDERNEATH ICE SHELVES |

SUPERGLACIAL DEBRIS → ABLATION — FLOWTILL

ENGLACIAL DEBRIS TILL ABL. MELT-OUT TILL

BASAL DEBRIS BASAL BASAL MELT-OUT TILL — LODGMENT TILL TILL DEFORMATION TILL

WATER-LAID TILL

GLACIAL ICE

DEFORMED BEDROCK, OR SEDIMENTS RELATED TO GLACIATION
———— AND/OR ————
GLACIALLY ERODED SURFACE OF ROCKS OR SEDIMENTS

Figure 2.3 - Classification of tills and their relationship to mode of transport (Bolviken and Gleeson, 1979 after Dremanis, 1969).

Flow till is produced during the melting out of superglacial debris. The high proportion of glacial meltwater mixed with the debris creates a highly fluid till which can flow downslope (Boulton, 1971). Flow tills may show a greater similarity to glaciofluvial material than till and thus straddle the border between till and stratified drift (Boulton, 1971). Melt-out till forms at the surface of a glacier by in situ melting under a cover of overburden, generally flow till (Boulton, 1971).

Basal till

Basal till, or lodgement till, is deposited subglacially by the "plastering" of material under actively moving glaciers and is characterized by moderate to high compactness (due to the compaction of rock flour into void spaces) and striated, abraded clasts (Flint, 1971). Varieties of basal till are basal melt out till, which forms by the melting out of basal debris in a stagnant glacier (Goldthwait, 1971) and deformation till, which is lodgement till and / or bedrock characterized by dynamic structures such as folds, shear planes and breccias (Figure 2.3) (Dreimanis, 1976).

Three possible origins have been suggested by Boulton

(1971) for the origin of lodgement till:

1) Lodgement of glacial debris: friction between glacier and underlying bedrock cause till to melt out by pressure melting.

2) Lodgement of sheets of basal ice: a portion of the glacier becomes attached to the bedrock while the remainder of the glacier continues movement. The till is then deposited through basal melting of the ice block or expulsion of the ice by pressure melting.

3) Basal Melting / regelation: ice at the bottom of a moving glacier melts to form a rock / water slurry which is preferentially deposited on the lee side of rock knobs and large clasts.

2.2 Geochemical dispersion in till

2.2.1 Introduction

Within a till sheet, the dispersion of gold can be separated into two different classes; mechanical dispersion during glaciation and post-glacial dispersion due to

weathering. The latter can occur through both mechanical transport and chemical translocation (Bolviken and Gleeson, 1979).

The factors which make till useful as a geochemical sampling medium are (Shilts, 1975; Bolviken and Gleeson, 1979):

1) till is the most widespread form of glacial drift,

2) till sheets are easily related to ice movement directions,

3) unweathered till is a direct, representative derivative of its source bedrock,

4) till is easily identified, and

5) dispersal trains of till are larger than their source.

2.2.2 Mechanical dispersion

Glaciers tend to disperse material in the form of a negative exponential curve (Figure 2.4) (Shilts, 1976). The highest concentrations appear near the source with a rapid exponential decrease in concentration downice. The exact shape of this exponential curve is determined by the type of transport (subglacial, englacial, etc.) and the physical characteristics of the material in question (Shilts, 1976).
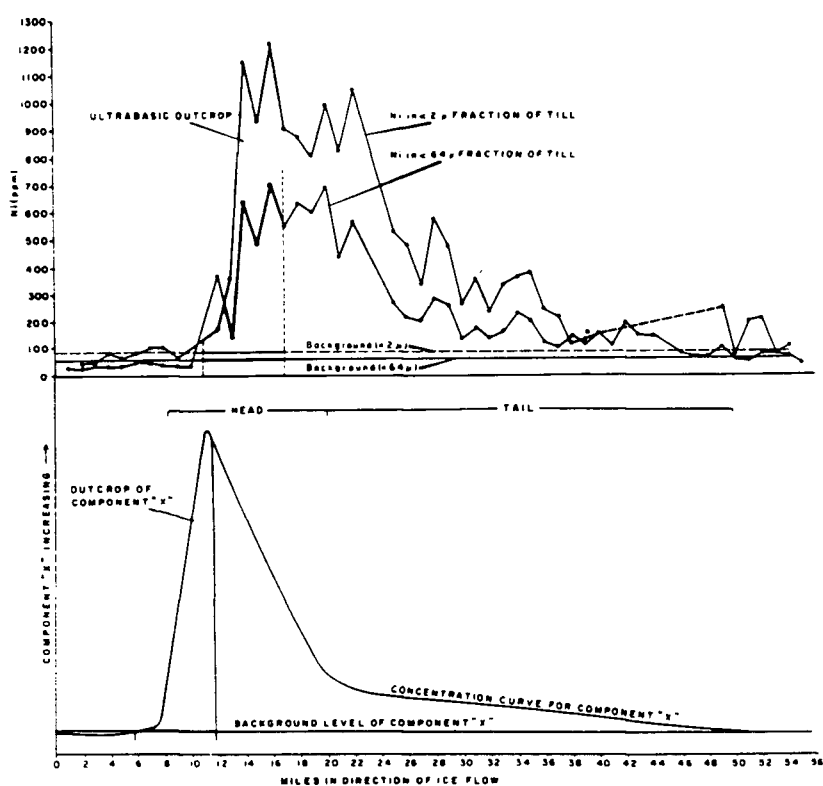
Figure 2.4 – Actual (A) and idealized (B) glacial dispersal curves showing negative exponential decrease. From Shilts (1976).

Debris carried englacially will be dispersed further than material transported along the glacier-bedrock interface. Studies of glacial transport distances by Strobel and Faure (1987) of granitic and metamorphic clasts derived from the Canadian Shield indicated that some englacially carried clasts travelled over 800 kilometers before final deposition.

Material dispersed by a glacier from a single source generally has a ribbon or fan shaped form (Figure 2.5 and 2.6) (Bolviken and Gleeson, 1979). Fan shaped dispersion trains may be caused by radial spreading of glaciers within lowlands, near an ice front or changing directions of ice flow with time (Flint, 1971). Irregularly shaped dispersion trains may be due to rough subglacial topography (Shilts, 1976). Most dispersion trains of economic minerals, however, generally have a ribbon shape (Shilts, 1976). The area of a dispersion train is roughly proportional to the source area exposed to glacial erosion and its orientation to the direction of glaciation (Holmes, 1952). Studies of geochemical dispersion in alpine terrain by Evenson et al. (1979) and Hicock (1986) indicate that valley topography and movement of individual ice lobes determines the pattern of geochemical dispersion.

Dispersion trains are three dimensional features; they may reach the surface near their source or may not appear at
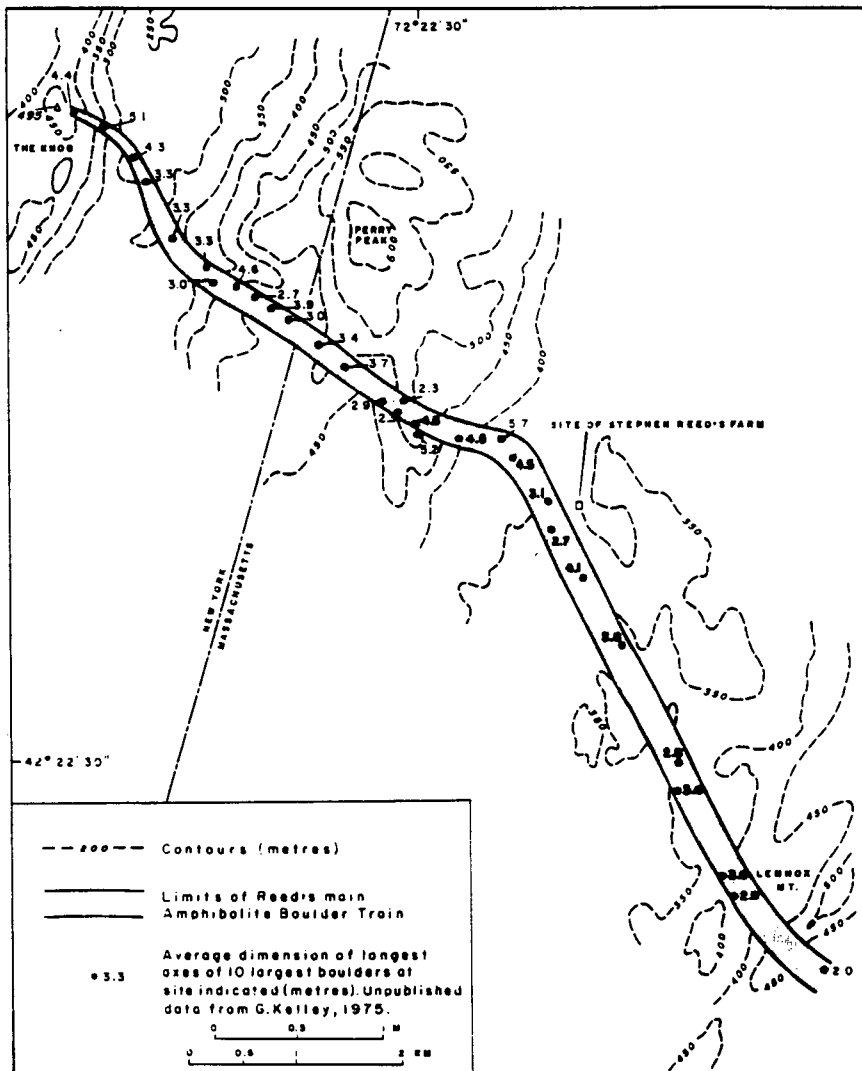
Figure 2.5 - Ribbon shaped train of amphibolite boulders. From Shilts (1976).
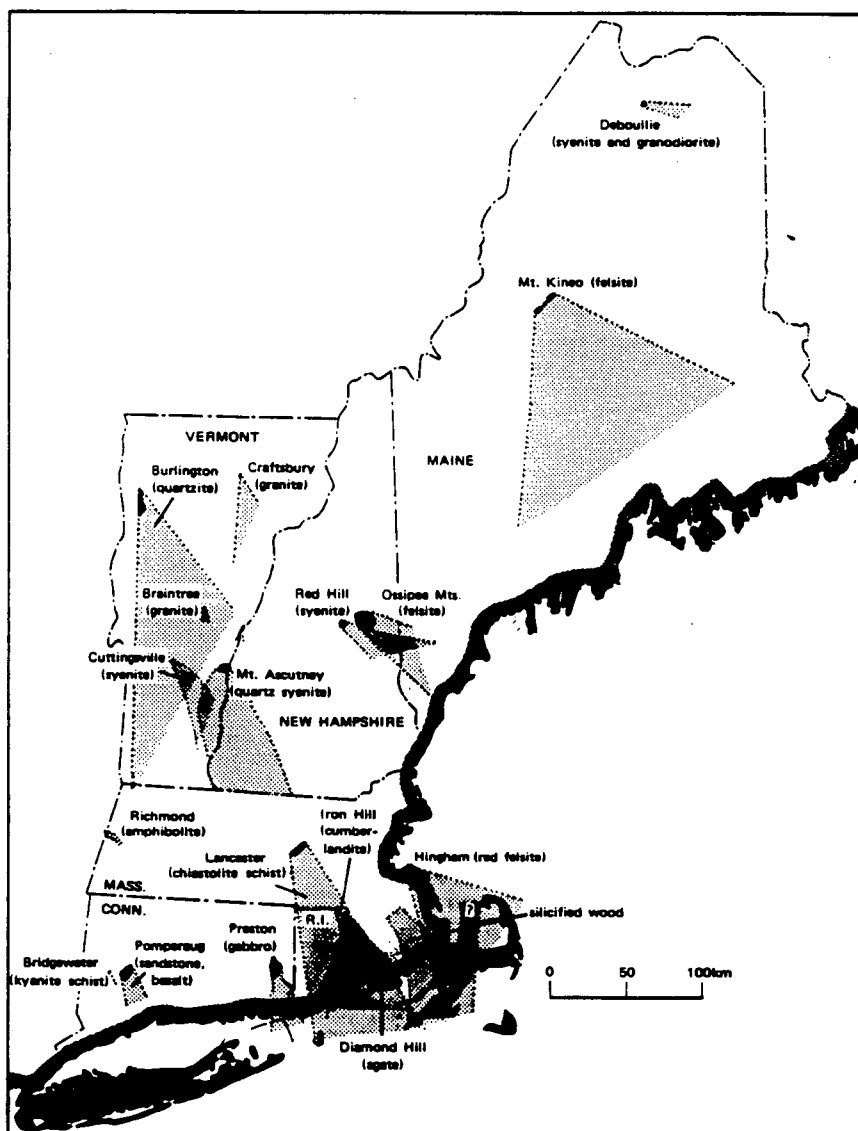
Figure 2.6 - Regional sized, fan shaped dispersion trains. From Flint (1971).

surface for several hundreds of metres downice (Bolviken and Gleeson, 1979; Drake, 1983). Miller (1984) described Pb dispersion trains in till at Bathurst Norsemines N.W.T. and Lough Derg, Ireland in which anomalous lead values were displaced 500 to 1000 metres downice from lead mineralized outcrop. Detailed sampling in three dimensions at both sites indicated thin (1-3 metre thick) ribbon anomalies which rose on shallow angles towards the surface (Figure 2.7). In addition, steep angle, diapiric anomalies were also delineated within the till sheets. Miller (1984) proposed that these anomaly patterns were due to dispersion trains rising through the till at angles of 2-3 degrees along thrust or smear planes. Diapiric type anomalies were regarded as being the result of steeper thrusting angles, perhaps due to bedrock irregularities, which would act to deflect the dispersion trains towards the surface (Miller, 1984). Drake (1983), likened dispersion trains to plumes of smoke rising downwind from a chimney, or alternatively, to stacks of till slabs aligned stair-step fashion in a downice direction.

Generally, in till less than one metre in thickness, an anomaly will be found directly above its source, with very little downice movement evident (Govett, 1973). In till up to 5 metres thick, the anomaly is usually detectable at surface above its source, but may be displaced several tens of metres downice (Rose, Hawkes and Webb, 1979). Downice Au
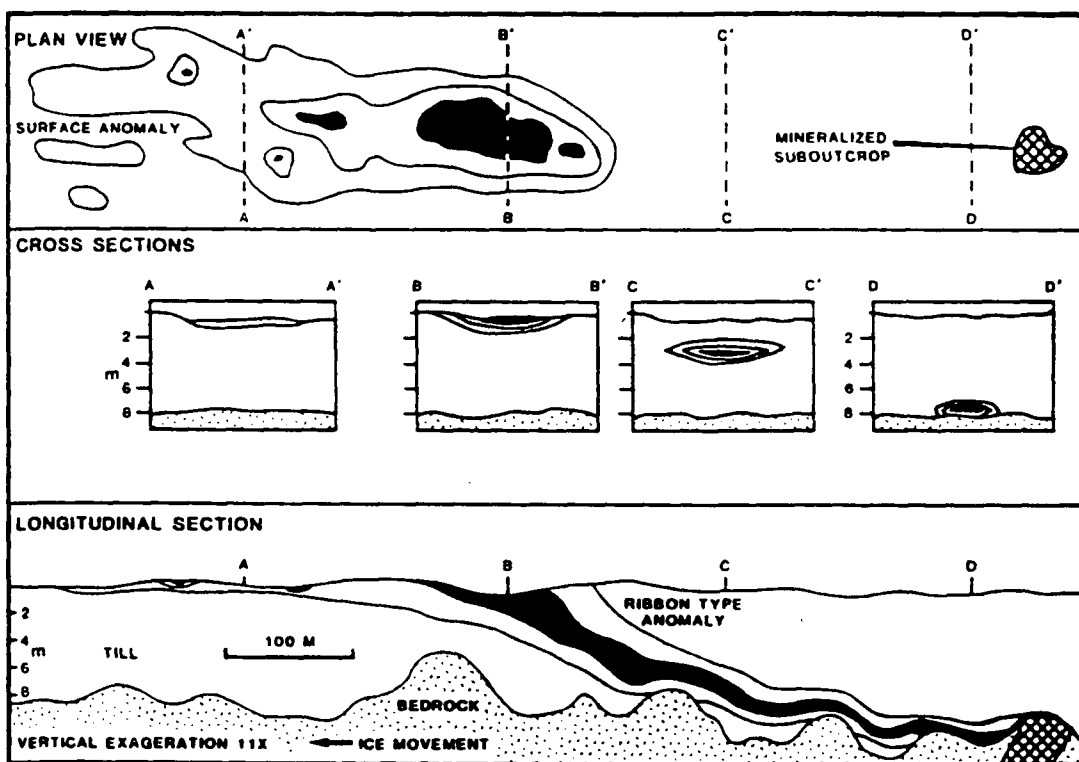
Figure 2.7 – Idealized model of glacial dispersal. From Coker and DiLabio (1987), modified from Miller (1984).

dispersion of 25 to 100 metres was observed in thin tills overlying the Shasta Au-Ag deposit, British Columbia (Downing and Hoffman, 1987). As noted by Miller (1984), displaced anomalies appear to be more prevalent in till greater than 6 meters in thickness. At the QR gold deposit, British Columbia, Au anomalies in till are displaced up to 200 metres from their source and extend up to 3 kilometres downice (Fox et al., 1987). In areas where multiple sheets of till are present, anomalies may not be expressed at surface or may be offset due to different glacial episodes (Rose, Hawkes and Webb, 1979). Stratified drift or distantly transported till may cover and block syngenetic anomalies within underlying till (Klassen, 1987; Bradshaw, 1975).

The morphology of free gold within unoxidized till appears to change with distance of transport. Sauerbrei et al. (1987) studied a glacial dispersion train emanating from the Golden Pond Zone, Casa Berardi area. Gold grains found within the basal till lying directly above the auriferous zone were composed of very delicate grains which showed few signs of abrasion. Gold grains found 100 metres downice from the source were still delicate in form; those found 400 metres downice from the mineralized zone were irregular in form and abraded, indicating transport over greater distances.

The comminution and crushing to the terminal size of gold grains is poorly understood. Dreimanis and Vagners (1971) determined the terminal size for heavy minerals in basal till to be 250 to 30 microns. However, it is doubtful that the resistate nature of the majority of the particles (garnets) within these samples is representative of the behavior of gold. Sauerbrei et al.(1987) reported abundant gold grains in the 50 to 150 micron range. Analysis of unoxidized basal tills by Shelp and Nichol (1987) revealed that the majority (75%) of gold within the till was concentrated in the -125 micron fraction. These may, however, reflect the fine grain size of the source gold and not a mechanical size reduction.

2.2.3 Modification by soil forming processes

The controlling factor in the post depositional dispersion of gold in till is weathering; the most important feature of the weathering of till is the development of a soil profile. This results in the transformation of the upper part of the till into a series of layers which have different properties and compositions (Bolviken and Gleeson, 1978). Soil formation is governed by the factors:

1) parent material,

2) relief,

3) climate

4) biological activity, and

5) time

In alpine glaciated areas, time for soil development has been limited (approx. 10 Ka). Therefore, soil development is usually poor, resulting in soil profiles with similar characteristics to their parent till (Bolviken and Gleeson, 1978). Gold may be transported mechanically or chemically (hydromorphic transport) within the soil profile. Mechanical transport may be by mass movement, compaction due to soil development, or soil creep (Bolviken and Gleeson, 1978). Pedoturbation, by various mechanisms, may also physically move material within soil. Chemical transport (pedotranslocation) is largely due to the movement of water within the soil profile (St. Arnaud, 1976).

Gold in unoxidized till is most common in size fractions which represent the original grain sizes of the source deposit or of the glacially comminuted particles. It is found as native gold or as a component of an original oxide or sulphide host mineral (DiLabio, 1985; 1988). In oxidized till and soils DiLabio (1988) found Au mainly within finer size fractions, commonly of silt size (-63 microns) or finer. However, it is possible that sampling

bias, in the form of inadequate sample sizes for the coarse fractions, may have influenced these results (section 1.2). Study of a till profile downice from a gold-scheelite occurrence at Waverly, Nova Scotia, led DiLabio (1982b, 1985) to speculate that native gold and gold liberated from sulphides during oxidation were absorbed onto iron and manganese oxides, hydroxides and clay minerals. An apparent enrichment of Au within the upper layer of the weathered till / soil was interpreted as a result of hydromorphic transport of Au towards the surface (Figure 2.8) (DiLabio, 1985). Coker et al.(1988) found gold dispersed from the Beaver Dam gold deposit, Nova Scotia, to be most abundant in the coarser fractions of the oxidized and unoxidized till, a reflection of the original grain size of gold within the deposit.

MacEachern (1983) noted compositional differences between gold from till and gold from a bedrock source at the Fifteen Mile Stream area, Nova Scotia and interpreted this as being caused by hydromorphic redistribution of Au within the till (MacEachern and Stea, 1985). Analysis of gold dispersal within till at the Forest Hill District, Nova Scotia by (MacEachern and Stea, 1985) revealed enrichment of Au, Cu, Pb, Zn and As within the fine (-63 micron) fraction of a Fe-Mn cemented unit. No enrichment was found within the coarser (sand) sized fraction. This has been interpreted as a secondary emplacement, indicating a hydromorphic origin
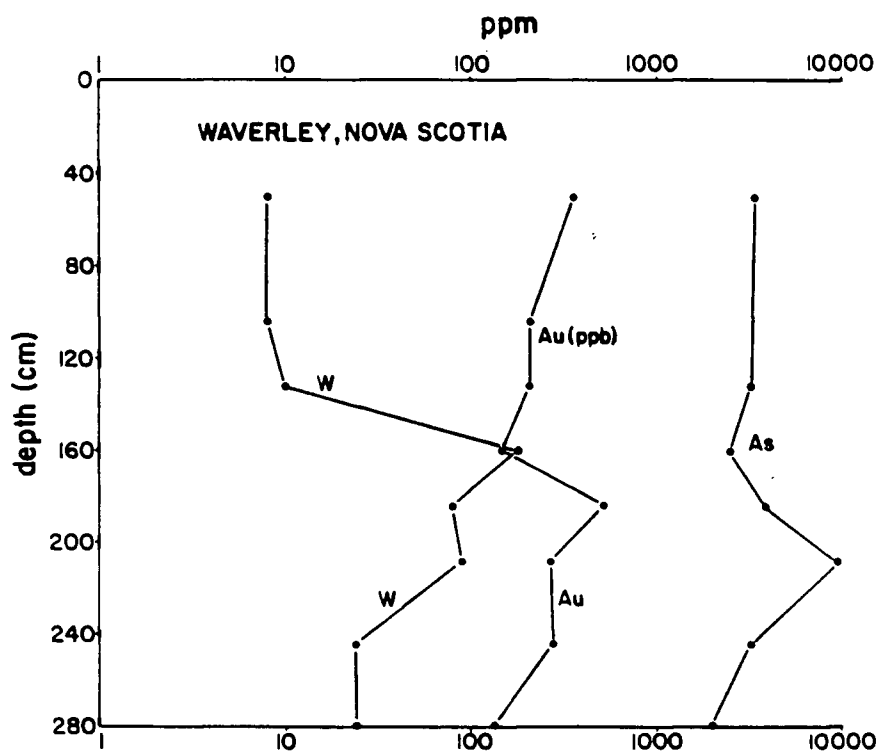
Figure 2.8 - Plot of depth versus concentration for W, Au and As in till. The change in sympathetic behavior between Au / As and W is interpreted as being due to a hydromorphic enrichment of Au and As in the upper section of the till. From DiLabio, (1985).

for the Au (MacEachern and Stea, 1985).

Hydromorphic movement of Au within the surficial environment involves the dissolution and transport of Au followed by its precipitation due to a change in physiochemical conditions. Complexing of elemental Au with an anion is necessary to achieve dissolution and transport (Webster and Mann, 1984). A number of gold complexes have been cited as possible transporting agents of Au in solution (Krauskopf, 1951; Shacklette et al., 1970; Lakin et al., 1974; Boyle et al., 1975; Mann, 1984; Stoffregen, 1986):

Gold Halides	$AuCl^{-4}$, $AuBr_4^{-2}$, AuI^{-2}
Gold Thiosulphate	$Au(S_2O_3)_2^{-3}$
Gold Thiocyanate	$Au(CNS)^{-4}$
Gold Cyanide	$Au(CN)^{-2}$

The increasing ease of oxidation of gold by the various anions of the gold complexes is:

$$Cl^- < Br^- < CNS^- < S_2O_3^{-2} < I^- < CN^-$$
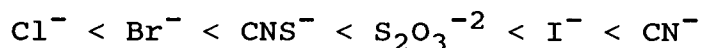
Formation of gold chloride is restricted to highly acidic, chloride ion rich areas which contain a strong oxidizing

agent such as MnO_2, O_2, Fe^{+3}, or Cu^{+2} (Krauskopf, 1951).
Such regimes exist only within oxidizing sulphide deposits
(Krauskopf, 1951; Lakin et al., 1974) and are not expected
in till sheets or soil profiles. Gold bromide and gold
iodide both have a greater stability than gold chloride, but
are exceptionally rare within the natural environment, due
to the low natural concentrations of Br and I (Lakin et al.,
1974).

Thiosulphate ions occur in sulphur-rich environments,
but usually in low concentrations. Lakin et al. (1974)
suggested that the oxidation of pyrite in an alkaline
environment may produce sufficient $S_2O_3^{-2}$ or HS^- to dissolve
gold. Such a solution may be a significant complexing agent
for gold around and within sulphide orebodies, but is
probably not of much consequence within till and soil. The
thiocyanate ion readily dissolves gold to form gold
thiocyanate, which is stable across a wide range of pH
(Lakin et al., 1974). Unfortunately, thiocyanate does not
appear to be useful as a large scale complexer of gold, as
it appears to be relatively rare in nature (Lakin et al.,
1974).

The gold cyanide complex may be best suited to
transport gold in soils (Lakin et al., 1974; Girling and
Peterson, 1978). Hydrogen cyanide can be produced from plant
material by the hydrolysis of cyanoglycosides, which have

been found in approximately 1000 species of plants (Lakin et al., 1974). However, no direct proof of gold transport by complexing with cyanide is available. Evidence such as thermodynamic data (Groen, 1987) or the singular observation of close spatial association of gold crystals with cyanogenic plants (Warren, 1982) is used as the argument for this hypothesis.

In weakly acidic to basic environments, free gold can bind with a variety of compounds to form colloidal gold. Colloidal gold is formed when fine (<0.05 micron) gold acquires a coating of organic material, iron-manganese hydroxides, or silica (Boyle, 1979). The negative charge inherent to these colloids increases their movement through the soil profile until interaction with free cations causes their precipitation (Boyle, 1979).

Organic compounds, such as humic and fulvic acids, have also been suggested as complexing agents for gold (Freise, 1931; Baker, 1973; Roslyakov, 1984). Baker (1978) proved experimentally that gold could be dissolved, complexed and transported by humic acid. The reaction of $AuCl^{-4}$ with humic acid was found to produce colloidal gold, with the humic acid forming a protective colloid for the gold (Ong and Swanson, 1969). Roslyakov (1984) found fulvic acids to possess a greater capacity for forming gold complexes than humic acids. Gold humic complexes do not appear to be

susceptible to the problems of stability and solubility which ionic and colloidal gold complexes are subject to (Baker, 1978).

Mineyev (1976) found that various microorganisms in alkaline solutions can dissolve and uptake gold in the soil profile. Doxtader (in Lakin et al., 1974) analysed the ability of bacteria to uptake gold; a wide variety of solubilization abilities were revealed. Many bacteria are able to solubilize gold (Boyle, 1979), although no direct information is available on their behaviour in the soil.

Lakin et al.(1974) observed that gold values in a group of soil profiles in the western United States were highest in the surficial (humus) and basal horizons. High concentrations of gold within the bottom horizons of the soil profiles were explained by Lakin et al. (1974) as being due to the in situ breakdown of gold bearing rock fragments and the downward migration of gold particles as a result of the churning action of soil during downslope creep.

Enrichment of Au within the humus layer is a result of the uptake of Au by vegetation (Lakin et al., 1974). Girling and Peterson (1978) determined that Au absorbed through the root systems of plants was either concentrated within the leaf tips / ridges or was flushed from the leaves. Au in gold complexes washed from the plant onto the surface would

be concentrated within the humus layer, due to the reducing nature of the decaying plant material. Gold complexes retained within the plant would encounter the same fate upon the death of the host plant.

2.2.4 <u>Summary of factors which effect the dispersion of gold within soil and till</u>

A number of relevant observations and conclusions can be derived from the literature cited:

1) Mode of transport within a glacier (basal, englacial, superglacial) will determine the type of till formed.

2) Dispersion trains in till are three dimensional features which are ribbon or fan shaped in plan view.

3) Experience with other minerals indicates that gold values generally decrease exponentially away from source.

4) Dispersion trains increase the anomaly size of an orebody.

5) The comminution effects on gold grains and terminal size of the comminuted grains is not well known, although gold grains appear to be abraded during glacial transport.

6) The ultimate appearance of a gold dispersion train is determined by the varying effects of transport and weathering processes upon the host till sheet.

7) Any chemical or physical movement of gold in deposited till is controlled by weathering and the development of a soil profile.

8) Gold in unweathered till is usually found as its original grain size or as grains representative of the degree of glacial comminution.

9) Gold in the weathering environment has a much more complex distribution which reflects original grain size, comminuted grain size, grain size of gold released from weathered sulphides and precipitated or adsorbed gold.

Chapter Three

Description of Study Area

3.1 Location and access

The Nickel Plate mine lies within the Hedley gold camp, approximately 40 kilometers east-southeast of Princeton, B.C. (Figure 3.1). Access to the mine is provided by the Hedley Road, which connects the mine to nearby Hedley and to Penticton, to the east. Several other mines with significant gold mineralization are found in the Hedley Camp, namely the Canty, French, Good Hope, Banbury, Peggy and Gold Hill properties (Figure 3.2).

3.2 History

Attention was first directed to the Hedley area in the 1860's by prospectors travelling from California to the newly discovered gold placer deposits of the Cariboo District (Camsell, 1910). Economic concentrations of placer gold in the vicinity of Twenty Mile Creek were discovered and worked for several years before being exhausted (Camsell, 1910). Afterwards, the region was overlooked until 1894, when several claims were staked near the peak of Nickel Plate Mountain (Camsell, 1910). Permanent work began on the claims in 1899 with the first milling of ore beginning in 1904 (Camsell, 1910). Production ceased in 1963, due to depleted reserves and rising mining costs (Ray
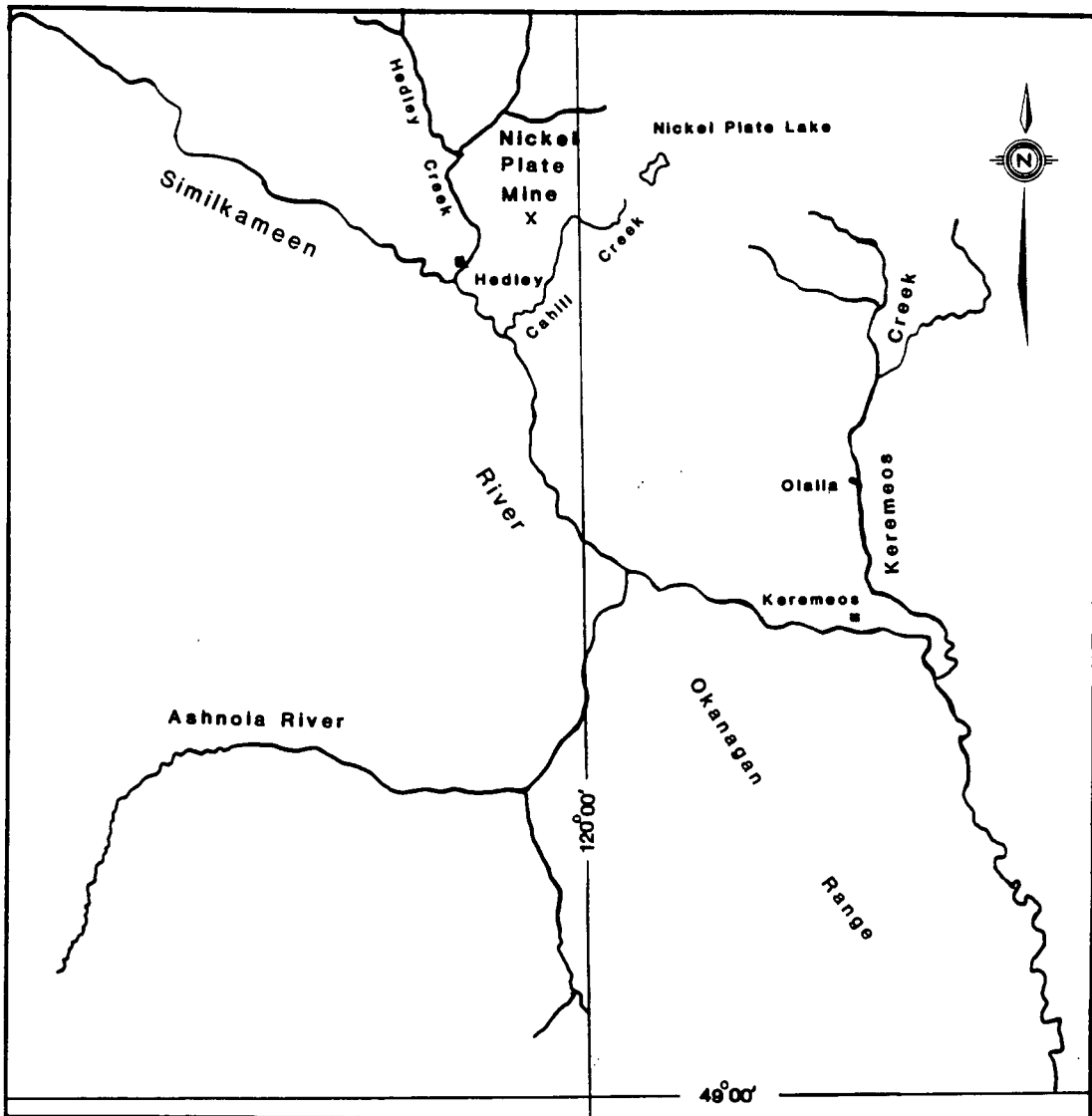
Figure 3.1 - Map of the Hedley region, southwest British Columbia. Scale: 1 cm = 3.5 km.
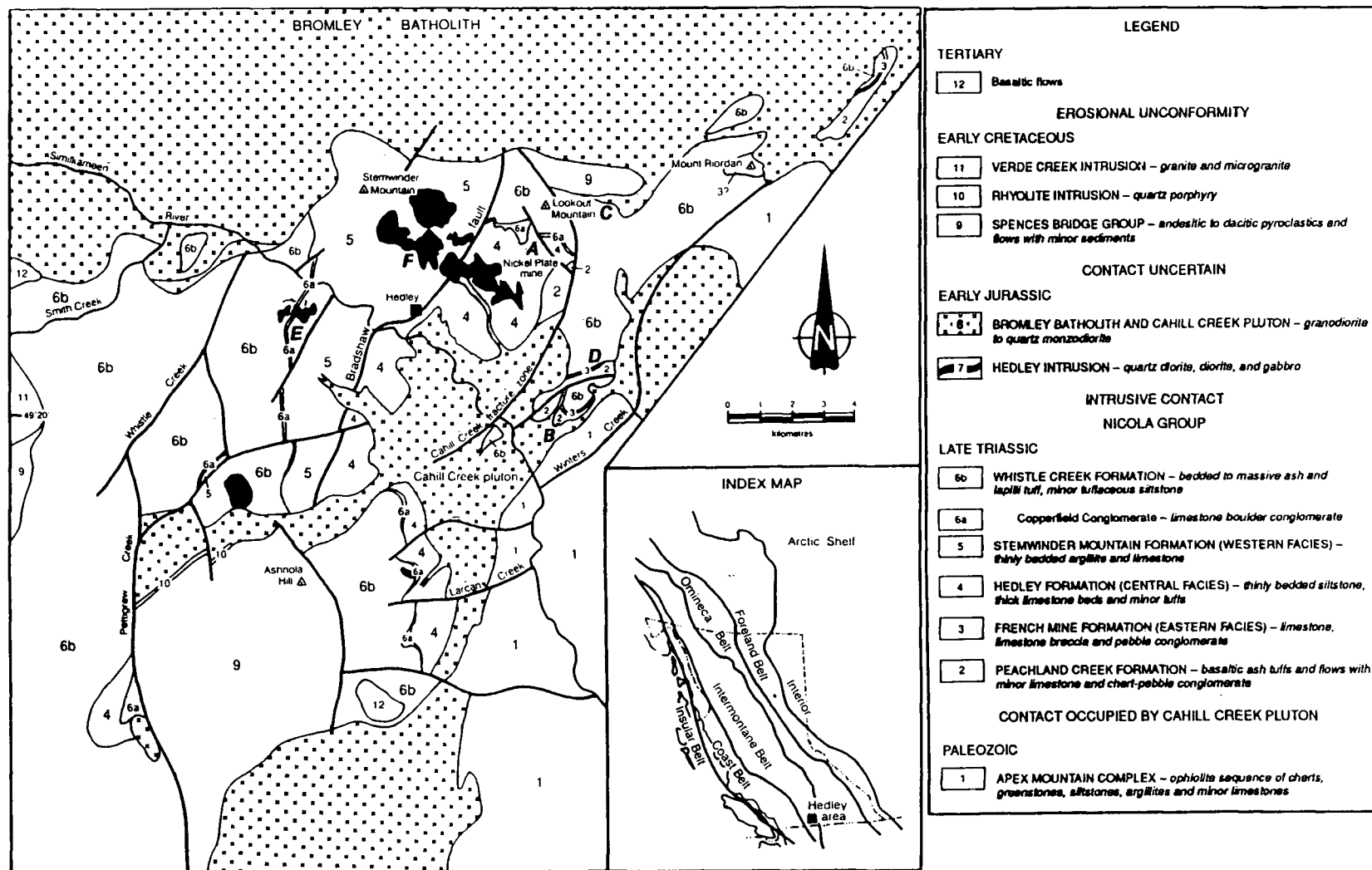
Figure 3.2 - Regional geology and location of gold bearing properties, Hedley region. From Ettlinger and Ray (1989) and Ray et al (1987). A: Nickel Plate Mine; B: French Mine; C: Canty Mine; D: Goodhope Mine; E: Banbury Gold Mine; F: Peggy Mine.

et al., 1987). During this period, 2.9 Mt of ore was mined,
producing 41.6 million grams of Au and 4.1 million grams of
Ag (Ray et al., 1986). In 1971 , Mascot Gold Mines (now part
of Corona Corporation) acquired the Nickel Plate property.
In August, 1987, the mine was officially reopened, as a bulk
tonnage, open pit operation. Minable reserves as of January
1, 1989 stood at 5.1 million tonnes grading 2.98 grams Au
per tonne (Corona Corporation Annual Report for 1988).

3.3 <u>Regional geology</u>

The Hedley region has been mapped by a number of
geologists since the early 1900's (Camsell, 1910; Bostock,
1930, 1940a, 1940b; Ray and Dawson, 1988, 1990). The Nickel
Plate mine lies within predominantly sedimentary rocks of
the Nicola Group. Flanking this section of the Nicola Group
to the east are rocks of the Cache Creek Group represented
by the Apex Mountain complex. Granodioritic to quartz
monzonitic Similkameen intrusions, are found on both the
eastern contact (Cahill Creek pluton) and north-northwestern
edge (Bromley batholith) of this Nicola Group pendant.

The Apex Mountain complex consists of a sequence of
highly deformed argillites, cherts, tuffs and minor
limestones that Milford (1984) has interpreted to be a
highly deformed ophiolite sequence formed above a subduction

zone dipping towards the east. Fossils from rocks in this group range in age from Upper Devonian to Late Triassic (Ray et al. 1987). Based on the work of Ray and Dawson (1988; 1990) the overlying Nicola Group begins with basalt tuffs, argillite, chert pebble conglomerate and limestone olistostrome (Peachland Creek Formation), succeeded by limestone and limestone conglomerate of the French Mine Formation; siltstone and limestone of the Hedley Formation; and finally argillite and limestone of the Stemwinder Mountain Formation. The Whistle Creek Formation, consisting of andesite ash and lapilli tuff, with minor silstone, marks the top of the group. Lying between the Stemwinder Mountain and Whistle Creek Formations is the Copperfield conglomerate, a 1-200 meter thick limestone-boulder conglomerate.

Rocks of the Hedley and Whistle Creek sequences are cut by the quartz diorites and gabbros of the Hedley Intrusions with K-Ar ages of 170-190 Ma (Roddick et al. 1972). Recently, a U-Pb zircon age date of 199 Ma has been determined by Ray and Dawson (1990) for a quartz diorite of the nearby Banbury Stock. These rocks appear as stocks with diameters up to 1500 meters and as dense swarms of sills and dykes up to 200 meters thick (Camsell, 1910; Ray et al., 1987). Camsell (1910) noted that gabbro dykes cut the quartz diorite-diorite sills and appear to be closely related

temporally, as the gabbro dykes seem to have cut the diorites while they were still plastic and deformable (Camsell, 1910). Camsell (1910), Billingsley and Hume (1941), Dolmage and Brown (1945), Lee (1951) and Ray et al. (1987) all associate the intrusion of the diorites with the gold mineralization at the Nickel Plate Mine.

The Similkameen intrusions consist of granites and granodiorites with a K-Ar age of 150 Ma (Roddick et al., 1972). Zircon dates of 168 Ma and 206-210 Ma have been established for the Cahill Creek pluton and Bromley batholth respectively (Ray and Dawson, 1990). Hornfels and minor skarn are associated with the plutons, but with the possible exception of the French Mine, there seems to be no related Au mineralization (Ray et al., 1987).

3.4 Deposit geology

The Nickel Plate mine is located within the upper units of the Hedley Formation (Figure 3.3) (Ray et al., 1987). Ore is stratabound and generally follows the bedding planes of the tuffaceous-calcareous siltstones and limestones (Camsell, 1910; Billingsley and Hume, 1941). The beds generally dip to the west at 20-30 degrees (Camsell, 1910). Quartz diorite to diorite sills are interlayered with the sedimentary rocks and are cut by gabbro or diorite dykes
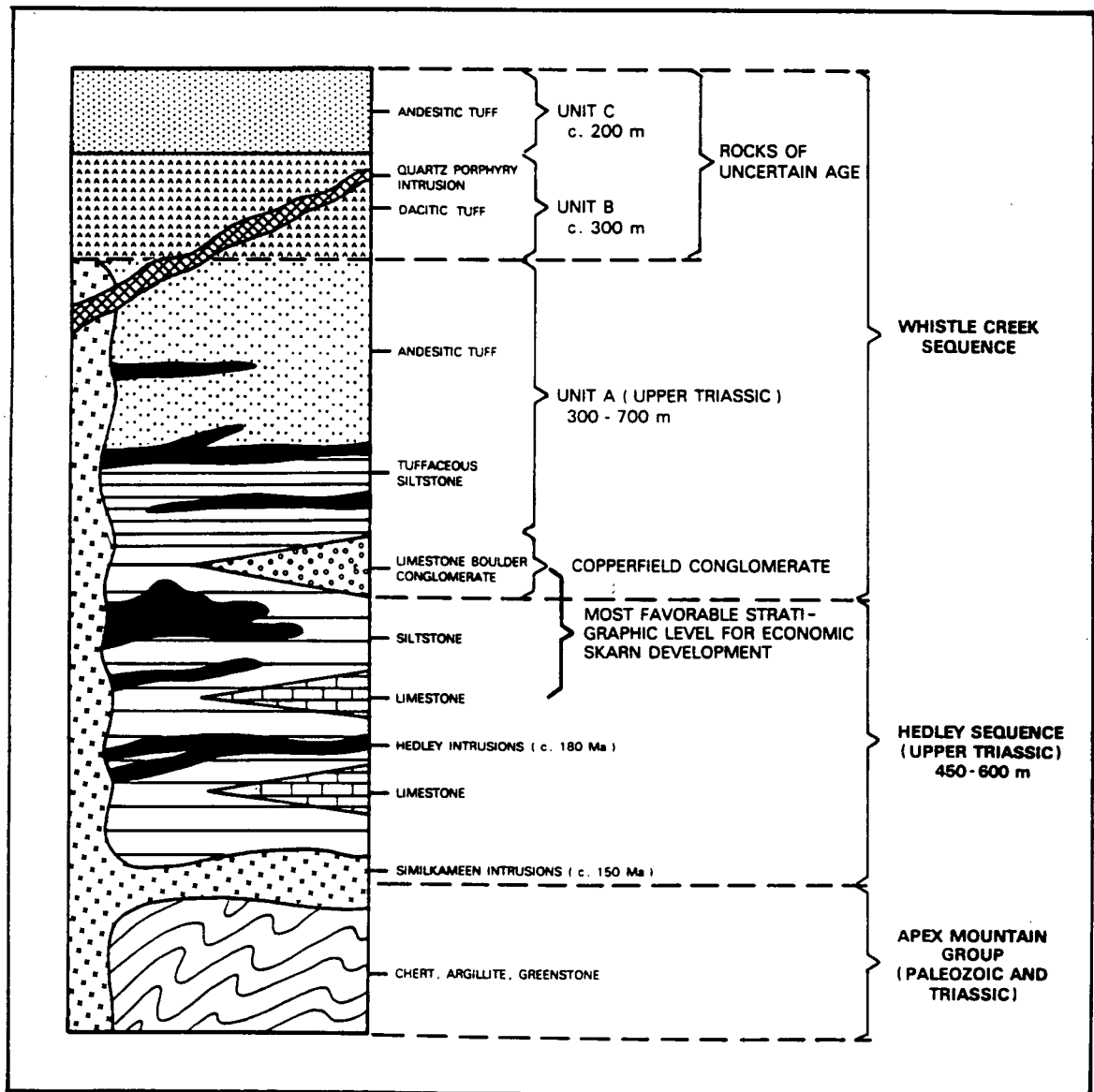
Figure 3.3 – Stratigraphy of the Hedley region. From Ray et al (1987).

(Camsell, 1910; Billingsley and Hume, 1941). Dominating the local geology is a large mass of diorite known as the 'Toronto Stock', an oblong body approximately 1200m x 2100m in size (Rice, 1947). However, contacts of the 'stock' with the rocks of the Hedley sequence are generally conformable and not crosscutting (Lee, 1951). The 'Toronto Stock' is in fact a large, irregular sill or lopolith (Lee, 1951). Swarms of smaller sills and dykes, from centimetres to metres in thickness, emanate eastwards from the Toronto Stock into the surrounding sediments (Figure 3.4) (Camsell, 1910).

Skarn alteration occurs in both the calcareous sediments (exoskarn) and within the diorites/gabbros (endoskarn) and extends up to 1850 metres from the Toronto Stock (Camsell, 1910; Dolmage and Brown, 1945). It ends abruptly along a boundary known as the Marble Line (Figure 3.4) (Billingsley and Hume, 1941), a zone ranging up to thirty metres in width (Dolmage and Brown, 1945). Scapolite is common within the boundary of the Marble Line (Dolmage and Brown, 1945). Minor non-calcareous sediments within the zone of skarn alteration have been altered to quartzites (Dolmage and Brown, 1945). Garnet-rich and pyroxene-rich assemblages are the predominant varieties of skarn alteration found in the area (Ray et al. 1987). Initial hornfels alteration has been overprinted, first by pyroxene-rich skarn which was in turn overprinted by garnet-rich skarn alteration which forms the core of the alteration
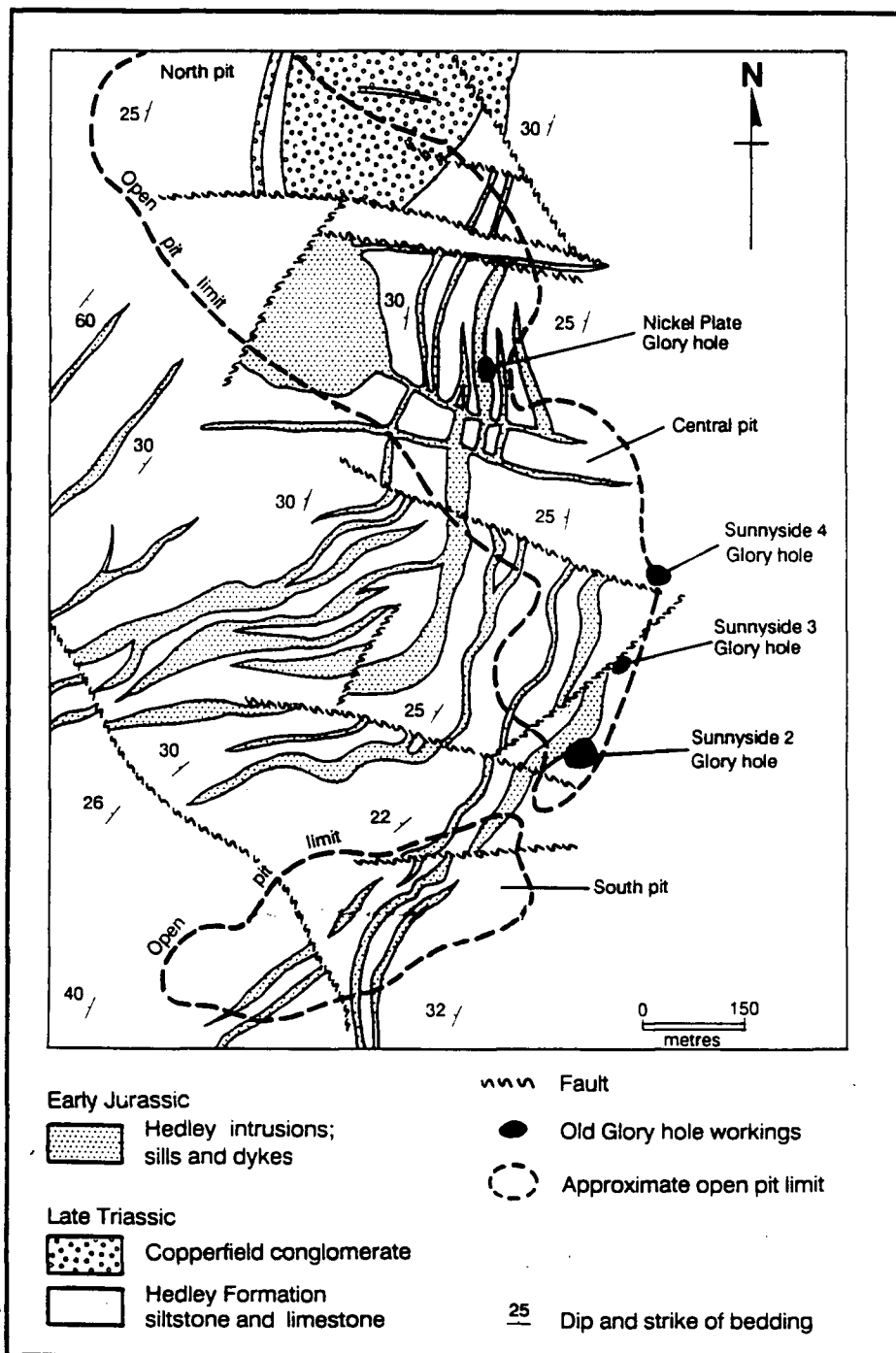
Figure 3.4 – General deposit geology of the Nickel Plate mine. From Ettlinger and Ray (1989).

envelopes (Ray et al., 1987). Composition of garnets found within the exoskarn (Figure 3.5) range between 25 and 80 mole percent andradite, whereas pyroxenes (Figure 3.6) generally are between 40 and 75 mole percent hedenbergerite (Ettlinger and Ray, 1989).

Within the thesis area, a few outcrops of Hedley Formation siltstone and basaltic tuffs of Peachland Creek Formation are exposed along the Hedley Road (Figure 3.7). Hedley formation is confined to the western half of the thesis area, while Peachland Creek occupies the eastern and southern regions. A 1 to 2 metre wide outcrop of granodiorite is found along the Hedley Road, near the contact between the Peachland and Hedley formations (Figure 3.7).

3.5 Ore deposits and mineralogy

Ore deposits of the Nickel Plate Mine are stratabound, lenticular bodies that preferentially follow the bedding planes of the sediments (Camsell, 1910; Billingsley and Hume, 1941). The majority of the mineralized zones are found within the apices of fold structures, within fractures parallel to the sills, or at the intersection of sills and dykes (Billingsley and Hume, 1941; Ray et al., 1987). All the mineralized zones are located within the exoskarn,
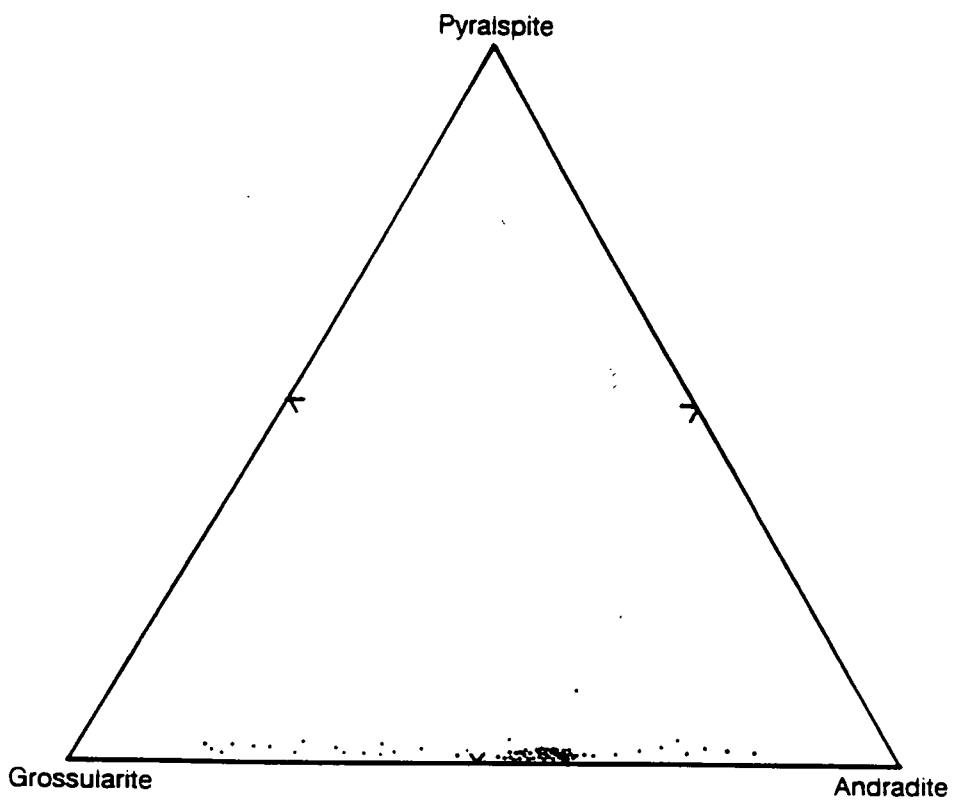
Figure 3.5 – Garnet composition of the exoskarn, Nickel Plate mine. From Ettlinger and Ray (1989).
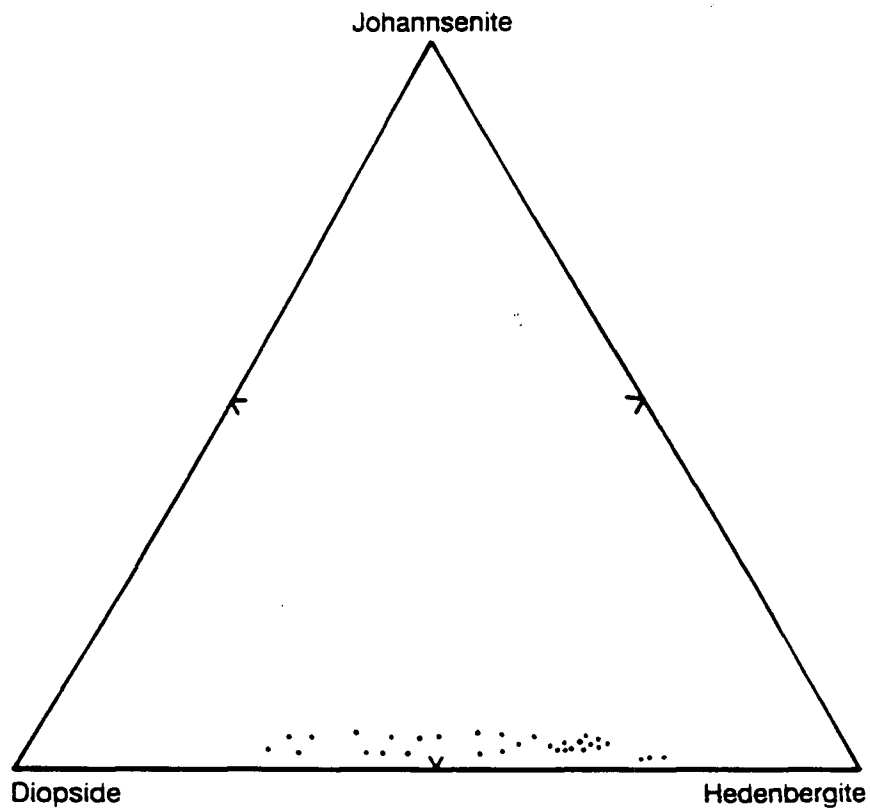
Figure 3.6 - Pyroxene composition of the exoskarn, Nickel Plate mine. From Ettlinger and Ray (1989).

Legend

Granodiorite

Diorite

Hedley Formation

Peachland Creek

Formation

Faults

Scale 200 m

Thesis area

Marble Line

North

Hedley Road

Thesis Area
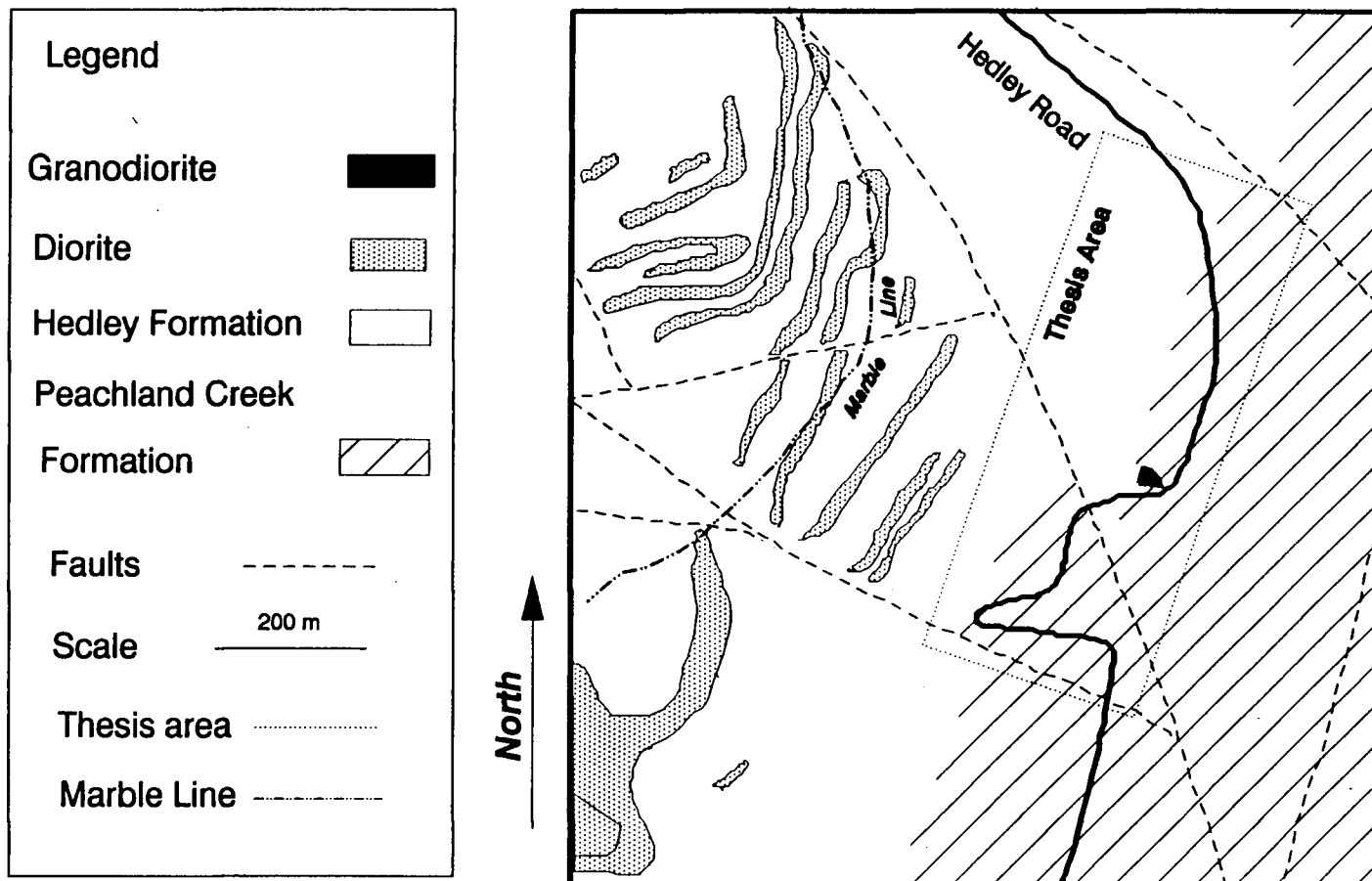
Marble Line

Figure 3.7 - Geology of the thesis area. Modified from Ray and Dawson (1988).

approximately 75-100 metres inside the Marble Line (Camsell, 1910; Billingsley and Hume, 1941; Dolmage and Brown, 1945). Some irregular pods of gold bearing massive sulphide, containing chalcopyrite, pyrite, pyrrhotite and arsenopyrite, are found in the mine area (Ray et al., 1987). Of the three varieties of skarn lithology found in the area (garnet-rich, pyroxene-rich and cherty quartzite), gold mineralization appears to occur in the pyroxene-rich exoskarn lithology and not in the brittle quartzites (Dolmage and Brown, 1945).

Gold is found primarily within arsenopyrite as minute grains generally less than 7 microns in size (Warren and Cummings, 1936). Occasional grains of gold are also found within pyrrhotite; more than 75% of the grains are less than 45 microns in diameter (Warren and Cummings, 1936). Minor gold is also found within late stage, crosscutting calcite veins (Bostock, 1930; Dolmage and Brown, 1945). Warren and Cummings (1936) concluded that the deposition of the gold and arsenopyrite were contemporaneous. After reviewing the work of Warren and Cummings (1936), and their own work, Billingsley and Hume (1941) suggested that the gold-arsenopyrite was deposited closely after the development of skarn alteration. Based on grain boundary relationships, Simpson (in Ettlinger and Ray, 1989) concluded that three stages of sulphide deposition occurred: (1) pyrite; (2) arsenopyrite and gersdorffite (NiAsS); and (3) pyrrhotite,

chalcopyrite and sphalerite. Gold mineralization was associated with the final two sulphide stages.

Visible gold was panned by early prospectors from gossans marking the surface projections of the orebodies (Camsell, 1910; J. Bellamy, personal communication, 1989). Free gold was observed by Camsell (1910) to be associated with arsenopyrite or tetradymite. Where the sulphide host had oxidized, ragged, sharp pointed gold grains with a dull rusty appearence were observed. When freshly cut, these grains had a bright lustre. Very fine gold grains were found in drift derived from the gossans and could be traced for a very short distance downslope (Camsell, 1910).

3.6 Glacial history

In south-central British Columbia, there have been two major glacial periods and two non-glacial periods over the past 51,000 years (Fulton and Smith, 1978). The first of these events, the Okanagan Center Glaciation, ended no later than 43,800 years BP and was follwed by the Olympia Interglacial period with a duration of approximately 20,000 years (Fulton and Smith, 1978).

Radiocarbon dating of organic samples by Fulton and Smith (1978) and Clague et al.(1980) indicates a readvance

of glaciers (Fraser Glaciation) into the major valleys of
southern British Columbia 22,000 years BP and a complete ice
cover sometime after 19,000 years BP. Advance to the maximum
extent of the Fraser Glaciation began approximately 18,000
years BP (Clague et al., 1980) and ended 15,000 years BP
(Mullineaux et al. 1965). At this point, the Cordilleran Ice
Sheet extended southwards into the northern United States as
far as the forty-seventh parallel (Mullineaux et al., 1965).
Glacial striae mapped by Rice (1960) in south-central
British Columbia indicate a regional ice flow in a northwest
- southeast direction.

Retreat of the Cordilleran sheet began almost
immediately after its maximum extension (Mullineaux et al.,
1965). In south-central British Columbia, deglaciation was
well underway 11,000 years ago (Fulton and Smith, 1978), and
had retreated to its modern day confines by 9,500 years BP
(Ryder, 1978). Work by Mathews (1944) indicated that in the
Princeton area the ice lobe filling the Similkameen Valley
retreated towards the northwest. A sample of charcoal taken
near Keremeos from a soil pit in the alpine zone (2480
metres elevation) gives a radiocarbon date of 9120+/-540
years, indicating that this area was deglaciated and
forested by that time (Lowdon et al., 1971), and warmer than
present day (Clague, 1980). Alley (1976) showed that climate
within the nearby Okanagan Valley was warmer and drier than
present conditions between 8400 and 6600 years ago.

Surficial mapping indicates that the glacier residing
in the Cahill Creek valley and the Nickel Plate Lake area
downwasted during deglaciation. The region surrounding
Nickel Plate Lake became ice-free first, depositing a veneer
of glaciofluvial outwash upon the bedrock. Coincident to
this, the ice lobe filling the Cahill Creek valley forced
meltwaters to flow southwards through Winters Creek. At some
later time, the meltwaters shifted their flow back to Cahill
Creek, cutting a channel through the glaciofluvial deposits
accumulated through downwasting of the ice. During
deglaciation, water saturated ground on the east and south
facing slopes of a small drainage entering Cahill Creek
underwent solifluction.

3.7 Surficial geology

The surficial geology of the Nickel Plate mine area can
be divided into two distinct areas (Figure 3.8, back
pocket). West of the mine, along the valley slopes of Hedley
Creek, topography is steep and overburden is thin or non-
existent. Bedrock, thin colluvium, and minor amounts of
colluvium modified till comprise the surface materials.
Talus slopes occur in the lower reaches of the steep valleys
which dissect the area. Fluvial deposits of sand and gravel
are found in the drainages of Hedley Creek and the

Similkameen River.

East of the mine, including the thesis area, the
overburden is generally thicker and the upland topography is
rounded and rolling. Till is the dominant surficial material
and rock outcrop is very minor, totalling no more than five
percent. In general, the thickness of till increases towards
the center of the Cahill Creek valley floor. Thus, till in
the vicinity of the Nickel Plate mine is from less than one
to three meters thick, whereas near the west bank of Cahill
Creek, it is on the order of sixty metres. This blanket of
till acts to cover and subdue the surface expression of the
underlying bedrock topography.

Several moraines are found within the valley of Cahill
Creek. The largest of these is located immediately south of
the tailings dam and stretches across the valley. It has
been modified by erosion and is cut in several places by
glacial and postglacial streams, including Cahill Creek. The
presence of granodiorite outcrop within this moraine
suggests that a ridge of bedrock underlies this feature. A
second, smaller moraine is located downstream from the
confluence of Sunset and Cahill Creeks. This moraine may
also be due to the presence of an underlying bedrock ridge,
as outcrop is found where this ridge is truncated by Cahill
Creek. On the eastern slope of Cahill Creek, three low,
southwesterly trending ridges, each approximately four

hundred meters long are interpreted to be lateral moraines.

A small kame deposit occurs on the northwest corner of the thesis area, adjacent to the minesite. Based on visual inspection, this material is similar in composition to the basal till, but has a coarser overall grain size. Minor glaciofluvial and kame deposits occur within the Cahill Creek valley. These deposits are associated with present day creeks but appear to be the result of modification by meltwater during deglaciation. In the vicinity of Nickel Plate Lake, an extensive blanket of sandy outwash, ablation till and minor lacustrine silts and clays cover the bedrock. Solifluction lobes are observed on the east and south facing slopes of a small creek valley east of Lookout Mountain.

Two outcrops displaying glacial striae were found within the confines of Cahill Creek. One location on the east slope of the creek gave eight striae measurements between 030 and 045 degrees with a mean of 039 degrees. A second location on the west slope gave five striae measurements ranging from 035 to 040 degrees with a mean of 038 degrees. Chattermarks observed at the first location indicate ice movement from northeast to southwest (Figure 3.9), paralleling the axis of the lower reach of Cahill Creek and the creek valleys of adjoining Hedley and Winters Creeks.

Figure 3.9 - Glacial striae and chattermarks on granodiorite outcrop, 2.5 kilometres east of the Nickel Plate mine.

Granodiorite erratics are ubiquitous throughout the Cahill Creek valley. Their most likely source is the Bromley batholith to the north of the mine area, and apophyses of the Cahill Creek pluton. The abundance of granodiorite as erratics is likely due to the greater outcrop area of the granodiorite within the region and the tendency of granodiorite to weather along preexisting fractures or planes of weakness into large blocks. These granodiorite blocks would have been readily plucked from their source outcrop by an overriding glacier. Faces of the granodiorite erratics resting on the surface are commonly flat and striated.

Within the thesis area, overburden is composed mainly of a hard packed till consisting of a subangular collection of rock fragments in an oxidized, red-brown silty-clay matrix. In the south end of the area, the till is saturated by water from a seepage / stream, is less indurated and greenish-grey in colour. Rock fragments in the till are generally of local origin, with diorite and skarn altered rock being the most prevalent. Cobbles of weathered, friable granodiorite were also found in the till and the overlying soil horizons. Pebble counts carried out on five C horizon samples (Table 3-1) indicate that local rock types (diorite, siltstone, limestone and skarn) dominate the clast

# of sample	Diorite	Grano-diorite	Silt-stone	Quartz	Skarn	Limestone	Other	# Clasts
12	21.7	0.0	24.4	0.0	30.8	20.5	2.6	78
58	28.6	0.0	25.4	0.0	22.2	23.8	0.0	63
105	28.6	0.0	33.9	0.0	21.4	10.7	5.4	56
135	28.8	1.7	20.3	1.7	37.3	6.8	3.4	59
202	63.6	0.0	9.1	0.0	22.7	4.5	0.0	22

Table 3-1 - Pebble count (+2000 micron fraction) results on five selected C horizon samples. All values in percent. Skarn catagory includes clasts containing pyroxenes and / or garnet. Other catagory includes lamprophrye, aplite, limestone / hornblende or feldspar / quartz clasts.

assemblage. No changes in overall clast (grains > 10 mm diameter) shape or composition were observed with depth in the pit profile.

The bimodal grain size distribution of the till indicates two distinct sources for the till components. Subangular rock and mineral fragments within the till are presumably of local origin, having experienced little glacial comminution. The silty-clay matrix, however, either represents material which has originated from the incorporation of lacustrine sediments into the till, or represents the final product of the comminution of less resistate rock types, such as fine grained sedimentary (shale, siltstone, carbonate) rocks. The latter case is the most likely, as tuffaceous siltstone and tuff units of the Whistle Creek Formation are found upice from the thesis area.

Carbonate precipitate was noted in 45 of 52 sample pits as coatings on roots and rock fragments, and as infillings within shale-like partings of the matrix. The carbonate precipitate does not appear to have acted as a matrix cement, as both the calcareous and non-calcareous tills were noted to have the same degree of compaction during excavation of the sample pits.

3.8 <u>Physiography, climate, vegetation and soils</u>

The Nickel Plate mine lies within the Okanagan Range of
the Intermontane Belt of the Western Canadian Cordillera.
The topography is generally strongly sloping and moderately
rolling, with elevations rarely exceeding 1800 meters. South
of the mine, the Similkameen River flows east-west through a
steep valley; the slopes of which are precipitous and over
1200 meters high. The Similkameen River also serves to
divide the rolling topography of the Okanagan Range from the
higher, more rugged terrain of the Cascade Range to the
south.

The climate of the Nickel Plate area is characterised
by hot, dry summers and cold dry, winters. Recorded
temperatures for the years 1904-17 and 1939-55 range from a
maximum of $33^{O}C$ in the summer and to a minimun of $-39.2^{O}C$
during the winter with a mean annual temperature of $1.7^{O}C$.
Precipitation for these years averaged 597 mm, with 62% of
the precipitation occurring as snowfall during the winter.
On average, the Nickel Plate mine area experiences a 32-day
frost free period (Mackie, 1961).

Tree cover is generally sparse; northern slopes are
mostly heavily wooded. Common trees are Douglas Fir
(*Pseudotsuga menziesii*), Englemann spruce (*Picea englemanni*)
and lodgepole pine (*Pinus contorta*). Grasses include bunch

grass (*Agropyron spicatum*) and pine grass (*Koeleria cristata*). In open meadows, sagebrush (*Artemista tridentata*) is common.

Soils developed on the tills of the thesis area are restricted to Eutric Brunisols and Gray Luvisols. The Eutric Brunisol soils generally display thin to nonexistent Ah horizons gradational to Bm horizons underlain by a C or Ck horizon. Also present are profiles possessing only Bm1, Bm2 and C or Ck horizons. Gray Luvisols have moderately well defined Ae and Bt horizons overlying a C or Ck horizon. Soils developed within a seepage zone in the south of the study area are probably best classed as Gleyed Eutric Brunisols. They are water saturated, contain mottles and display weak partitioning between Ahk and Bmk horizons or possess only a Bmk horizon above the Ck layer. Soil pH for the profiles ranges from 5.5 to 8.2 (average pH = 7.09), and consistently increases with depth (Table 3-2).

Sample	Horizon	pH (in H_2O)
14	A	5.9
15	B	6.0
16	C	7.5
41	A	6.2
42	B	6.4
43	C1	6.6
44	C2	7.1
122	A	6.9
123	B	7.1
124	C1	7.6
125	C2	7.8
127	A	7.3
128	B	7.7
129	C1	8.0
130	C2	8.1
162	A	6.9
163	B	8.0
164	C	8.2
186	A	7.2
187	B	7.3
188	C1	7.4
189	C2	8.0

Table 3-2 - pH values of selected soil profiles.

Chapter Four

Sampling Methods

4.1 Site selection

Selection of the Nickel Plate mine site was based on the results of a geochemical soil survey by Placer Development Ltd. during the 1984 field season (Young, 1984) and an orientation survey carried out by W.K. Fletcher during the 1986 field season. Data from the Placer Development Ltd. survey indicated a gold dispersion train parallel to the local ice direction and extending downice from the Nickel Plate mine for a distance of approximately one kilometre (Figure 4.1). Orientation surveys carried out on the anomaly by W.K. Fletcher consisted of profile sampling several exposures of the anomaly to determine relative gold contents of the various soil horizons.

4.2 Field sampling methods

Sampling pits were located fifteen metres apart on a series of five parallel lines which traversed the dispersion train (Figure 4.2). In total, 52 pits were excavated, in most cases to a minimum depth of one metre. All pits were located in areas of undisturbed, forested ground. Till samples were taken every 50 metres from roadcut exposures at 33 sites along the Hedley Road.
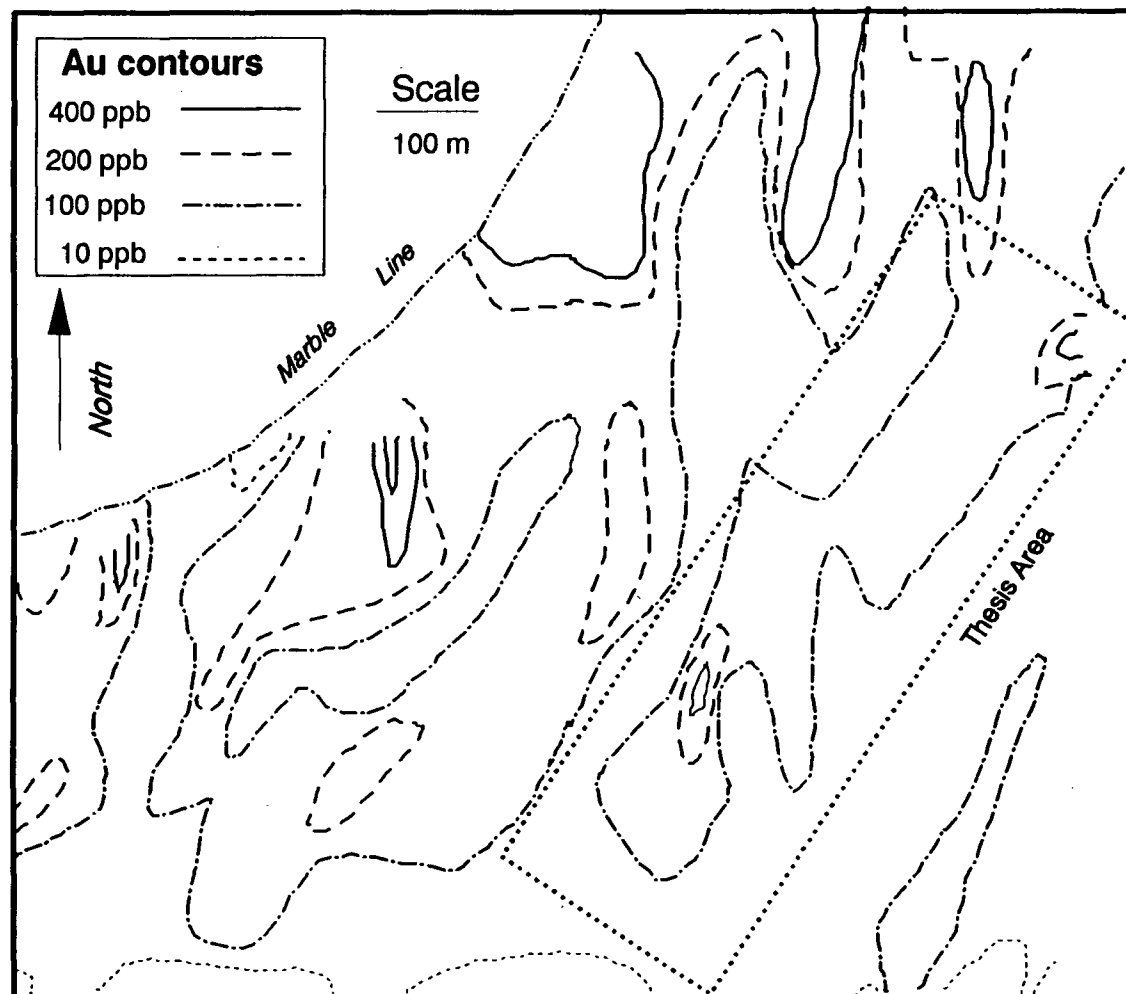
Figure 4.1 – Gold dispersion trains delineated by Placer Development, Ltd..
Thesis area defined by stippled box
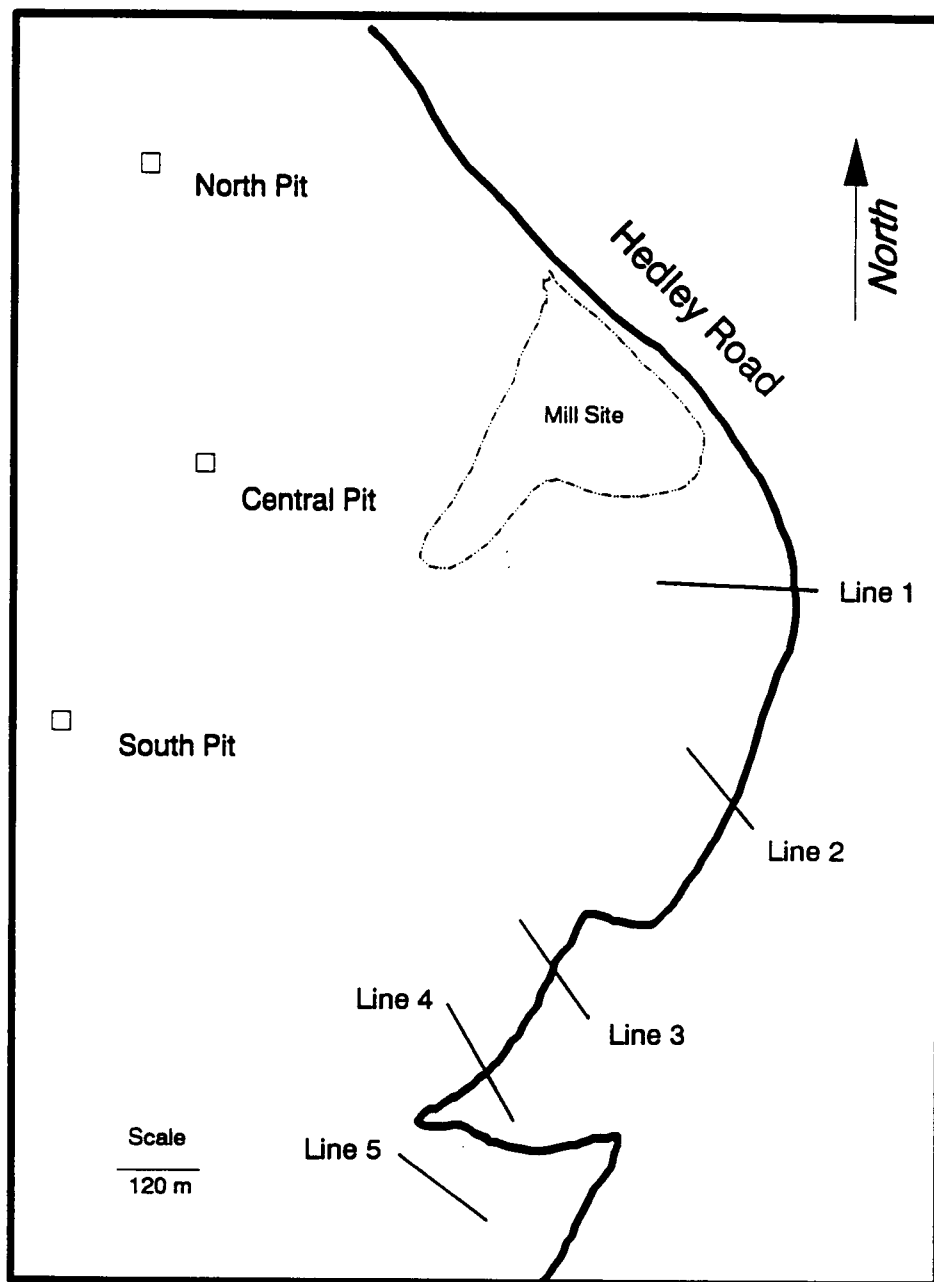
Figure 4.2 – Location of sampling pit traverse lines relative to the minesite.

Before digging each pit, the overlying layer of humus was removed and sampled using a gardening trowel taking care to avoid contamination by the mineral soil. The pit was then excavated and the soil profile was subdivided on the basis of compaction, colour and root density of the soil. The presence of secondary carbonate was determined with dilute HCl.

Soil horizons greater than ten centimetres thick were sampled (from the bottom up in order to avoid contamination from overlying horizons) using a geologists' hammer (pick end) and a ten litre plastic bucket. Two five litre samples were obtained from each horizon: a first duplicate ('A') sample and a second duplicate ('B') sample. Rocks, greater than three centimetres in diameter, were removed from each sample by hand.

4.3 Laboratory preparation and analysis

4.3.1 Humus

One half of each dried humus sample was ground to a fine (100 micron) powder in a Wiley mill. Between each sample, the mill was cleaned with both a brush and a jet of compressed air. Once reduced to a powder, ten gram splits of each sample were taken using a Jones riffle splitter. The

ten gram subsamples were then packaged in plastic vials and
sent to Chemex Labs, Ltd. (Vancouver, B.C.) for neutron
activation analysis.

4.3.2 <u>Soils</u>

4.3.2.1 <u>Minus 212 micron sample preparation</u>

Labratory preparation of the soils is represented
schematically in Figure 4.3. A one-quarter split of each
soil horizon sample was taken by carefully mixing the entire
sample on a large, clean nylon sheet. The sample was then
split in half, with one half being returned to the bag. The
procedure was then repeated to produce a one-quarter split
of the sample for wet sieving. A small (ten gram) portion of
the remaining sample was retained for determination of soil
pH.

The one-quarter splits were then wet sieved through
2000, 420, and 212 micron sieves using a recirculating water
system (Figure 4.4). Except for the -212 micron slurry, the
resulting size fractions (+2000, -2000+420, -420+212 micron)
were placed in an oven and dried at 70° - 80° C until all
excess water had been evaporated. After the samples were
dry, the +2000, -2000+420, and -420+212 micron size
fractions were weighed and stored for reference.
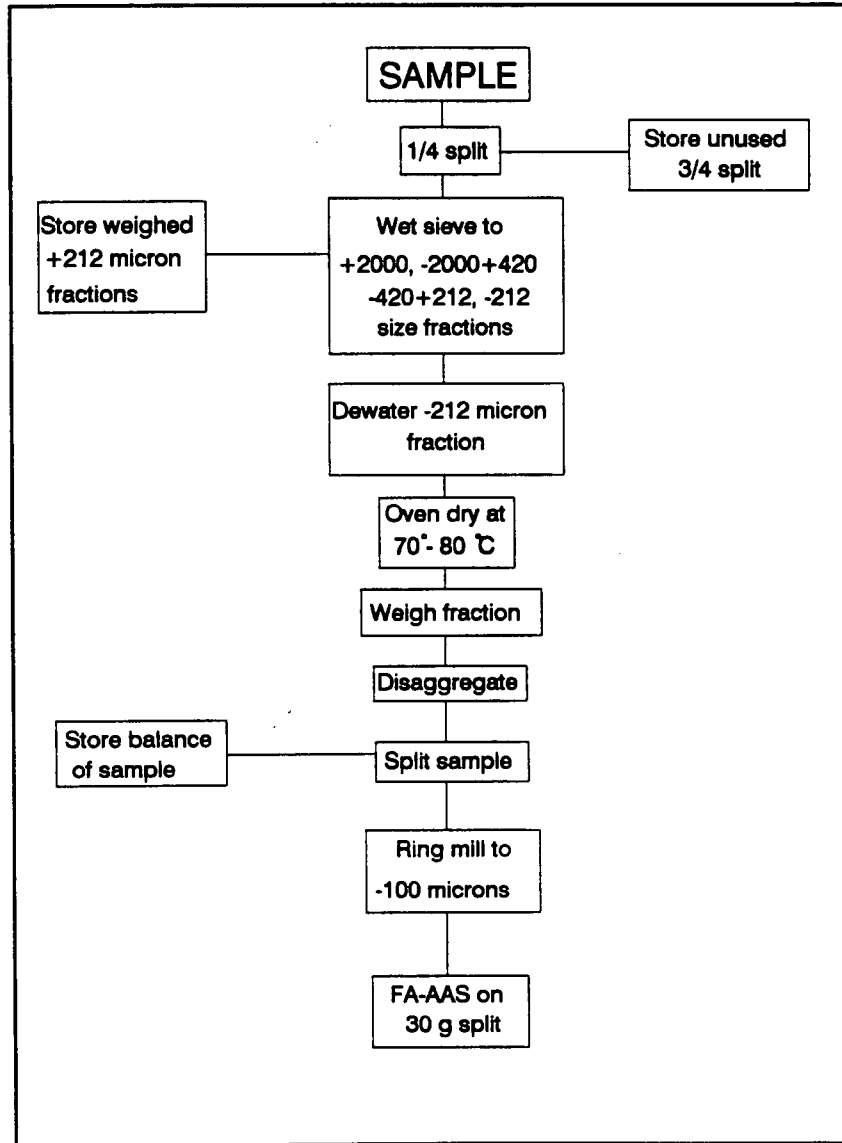
Figure 4.3 - Schematic diagram of sample preparation.

Recirculated water

| 2000 micron |
| 420 micron |
| 212 micron |

Sieves

Plastic bucket

water & -212 sediment

-212 sediment
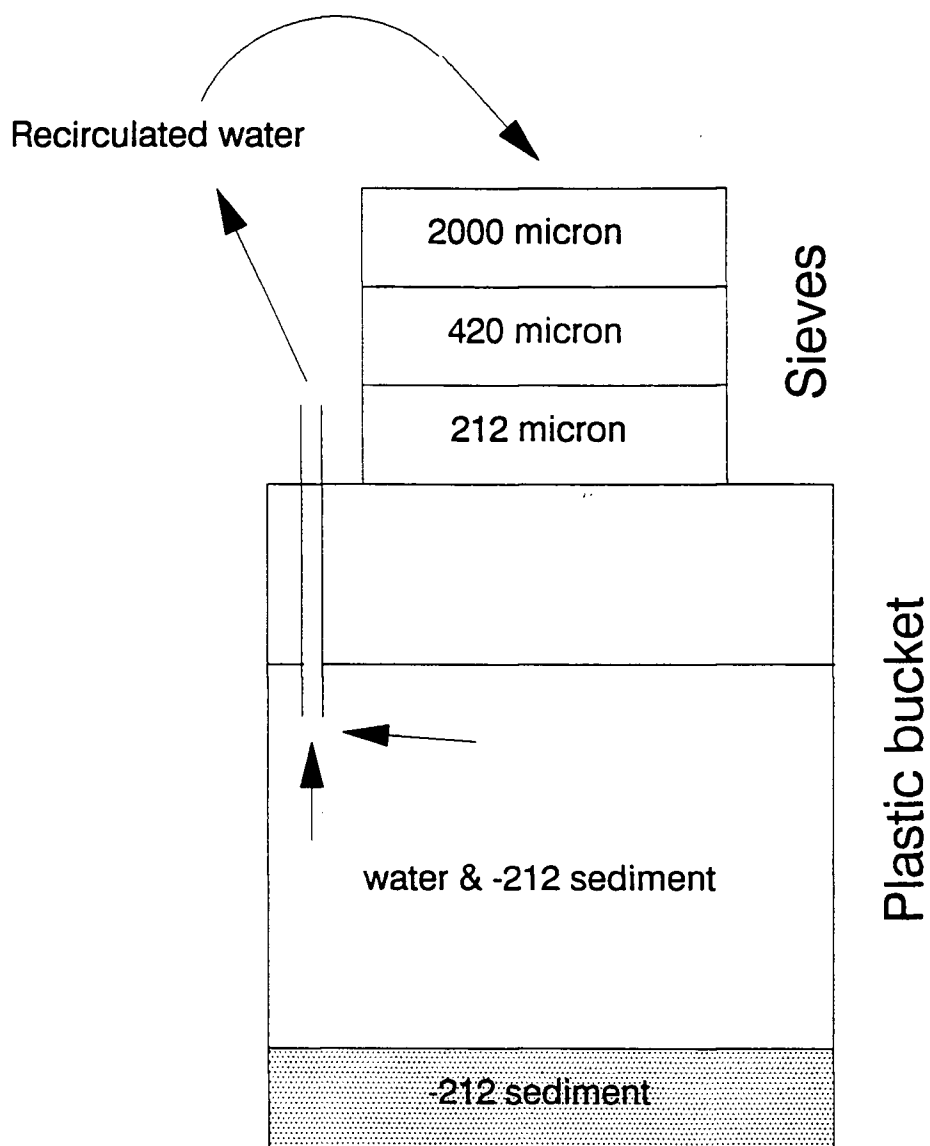
Figure 4.4 - Wet sieving system.

The -212 micron slurry was dewatered in a large pressure filter. This consisted of a two centimetre thick, thirty centimetre diameter plastic cylinder with removable aluminium plates at either end. A sheet of wetted white paper, wider than the cylinder, was placed between the bottom baseplate and the cylinder. The slurry was poured into the filter and the upper plate was bolted down. Compressed air was then introduced into the cylinder until the interior pressure had increased to approximately 500 kPa. This pressure was maintained until dry air was observed to emanate from the drain hole in the baseplate. The dewatered -212 micron fraction was dried in an oven at 70° - 80° C, separated from the paper filter, and disaggregated. Each sample was weighed before taking a thirty gram split using a Jones riffle splitter. These splits were ground to less than 100 microns in a ring mill, then sent to Chemex Labs, Ltd. (Vancouver, B.C.) for gold analysis by fire assay - atomic absorption. Fifty-six duplicate splits were also prepared and sent for analysis. The remainder of the sample material was retained for any further work.

4.3.2.2 <u>Size fraction, density fraction and</u>

<u>cyanide extraction samples</u>

Samples were sieved using 2000, 420, 212, 106 and 53 micron sieves and a recirculating water system as shown in Figure 4.4. Once sieved, the +2000 and -2000+420 micron size fractions were dried and stored. The -420+212, -212+106 and -106+53 micron size fractions were dried and set aside for heavy mineral separation. The -53 micron slurry was dewatered in the pressure filter; the resulting cake was then dried in a low temperature oven and pulverized in a ring mill. Two thirty gram splits were taken from each sample, plus additional thirty gram splits for duplicate analyses.

Twenty-two of the thirty gram -53 micron subsamples was submitted to Chemex Labs, Ltd. for FA-AAS while another set of twenty-two subsamples were submitted for Au determination by cyanide extraction, solvent extraction into MIBK and atomic absorption spectrophotometry. Four duplicate samples were submitted for each of the analytical techniques. Sample residues were then analysed for Au by FA-AAS.

Heavy and light mineral concentrates of the -420+212, -212+106, and -106+53 micron size fractions were separated using methylene iodide (CH_2I_2; S.G.= 3.3). Methylene iodide

was recovered from the samples by repeated washings with acetone.

After the samples were dry, they were placed within plastic bags or vials (depending on sample size) and weighed. Heavy and light mineral fraction samples weighing more than 30 grams were ground in a ring mill (to -100 micron grain size) and split to a subsample size of 30 grams. Any remaining material was stored for further use. Samples weighing less than 30 grams were not ground, but sent directly for analysis.

One hundred and thirty-two heavy and light mineral size fraction subsamples were sent to Chemex Labs, Ltd. for FA-AAS. Six duplicate subsamples were also submitted for FA-AAS.

4.3.3 Scanning electron microscope and electron microprobe sample preparation and analyses

Seven 'B' (second duplicate series) samples were sieved through 212 and 53 micron sieves. The +212 and -53 micron fractions were discarded, while the resultant -212+53 micron size fraction was subjected to heavy mineral separation using methylene iodide. A hand magnet was then used to remove any magnetics from the heavy mineral fractions.

Isolation of free gold grains in each sample was achieved by repeatedly passing the samples through a Franz isomagnetic separator. An initial current level of 0.1 amps was raised in 0.2 amp increments after each pass to a maximum of 1.1 amps. The resultant concentrate consisted of a restricted number of mineral types, of which zircon appeared to be the most prevalent. This concentrate was then examined for free gold under a binocular microscope by sprinkling a small portion of the grains on a black cardboard tray. Gold grains were removed from each sample by using a few strands on a modified fine haired brush to pick up the grains. The grains were then placed in 7 dram glass vials (one vial per sample) for further use.

Gold grains were mounted on S.E.M. stubs coated with a thin layer of nail polish (J. Knight, personal commmunication, 1988). The gold grains were placed on the polish and immersed in acetone vapour. Once the grains were observed to begin settling into the polish, the acetone vapour was removed, allowing the partially embedded gold grains to set within the rehardened polish.

Mounted gold grains were studied using a SEMCO NANOLAB 7 scanning electron microscope operating at 15 kV. Qualitative energy dispersive spectrometry (EDS) was carried out using a Kevex Unispec System 7000. Axial measurements of

each grain were determined from photographs and SEM imagery. EDS and backscatter secondary electron imaging was used to ascertain the surface composition of each grain.

A cross-section of each gold grain was prepared using a method developed by J. Knight and Y. Douma at U.B.C. Eight grains were not sectioned, while one grain was lost during the process. Once the sectioning was complete, the plugs were coated with carbon for electron microprobe analysis.

Electron microprobe analyses of the sectioned grains was carried out on a Cameca SX-50 electron microprobe, using operating conditions modified from Knight and McTaggart (1986): a specimen current of 100 nA on aluminium and an accelerating potential of 20 kV. Counting time for peaks was 30 seconds and 15 seconds for each side of background. Data were reduced with Cameca PAP program utilizing the phi-rho-xi data reduction method (J. Knight, personal communication, 1989). The elements Au, Ag, Cu and Hg, were assumed to be present in sufficient concentrations to be analysed for (Knight and McTaggart, 1986). Detection limits for Au and Ag are 0.05% (Knight and McTaggart, 1986), whereas Cu had a detection limit of 0.025% and Hg a limit of 0.65% (J. Knight, personal communication, 1989). Where possible, each grain was analysed in two places ; one analysis in the centre of the grain, and a second analysis within the outer

rim of the grain.

Chapter Five

Results

5.1 Minus 212 micron fraction results

5.1.1 Reliability and analytical precision

5.1.1.1 Introduction

Reliability and analytical precision were estimated using 56 duplicate pairs of Au analyses. Duplicates were prepared by taking two representative 30 gram splits of the -212 micron (ASTM -70 mesh) fraction. An initial group of thirty-two randomly selected duplicates were renumbered and analysed along with 171 primary samples. A second set of twenty four duplicates were submitted five months later as an independent batch, without accompanying primary samples.

Estimation of the reliability and analytical precision of the data was carried out using scatterplots, a bias test, a one-way analysis of variance (ANOVA) test and the Thompson and Howarth (1973, 1976, 1978) method of estimating precision.

5.1.1.2 Scatterplots / correlations

A scatterplot of primary versus duplicate Au analyses is shown in Figure 5.1. The Pearson correlation coefficient (r) for all fifty-six pairs is 0.133. Inspection of the scatterplot reveals an outlier (6350 ppb, 130 ppb) which
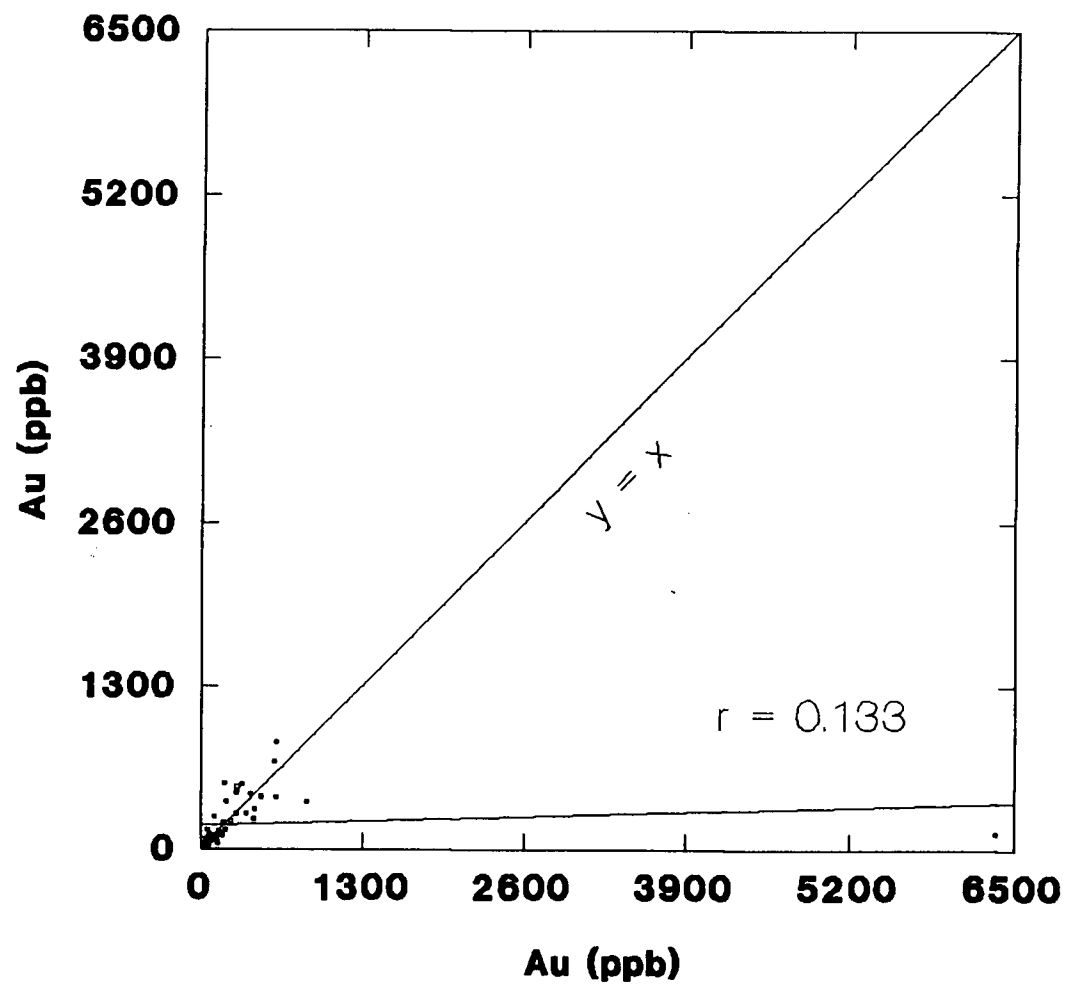
Figure 5.1 – Scatterplot of duplicate Au analyses, –212 micron fraction.

strongly skews the regression line towards the outlier. Removal of this outlier results in a regression line which better fits the entire data set (Figure 5.2) and gives a correlation coefficient of 0.806.

5.1.1.3 Systematic bias

Error in measurement due to non-random, systematic errors was estimated by the use of a bias test. Use of this test for determining systematic error on geological samples is detailed in Matysek and Sinclair (1984) and Matysek (1985). In this test, the number of positive differences between duplicate pairs is determined; if no bias is present, then the number of positive values (m) should be close to one-half the total number of pairs. A normal distribution is assumed for the data, where n is the total number of data points, n/2 is the mean and $n^{-1/2}$ is the standard deviation. To determine the probability of obtaining a specific deviation from the mean, the number of positive differences (m) is first converted to the standard normal form (Z) through the formula:

$$Z = [m - (n/2)]/(n^{-1/2}) \qquad (5-1)$$
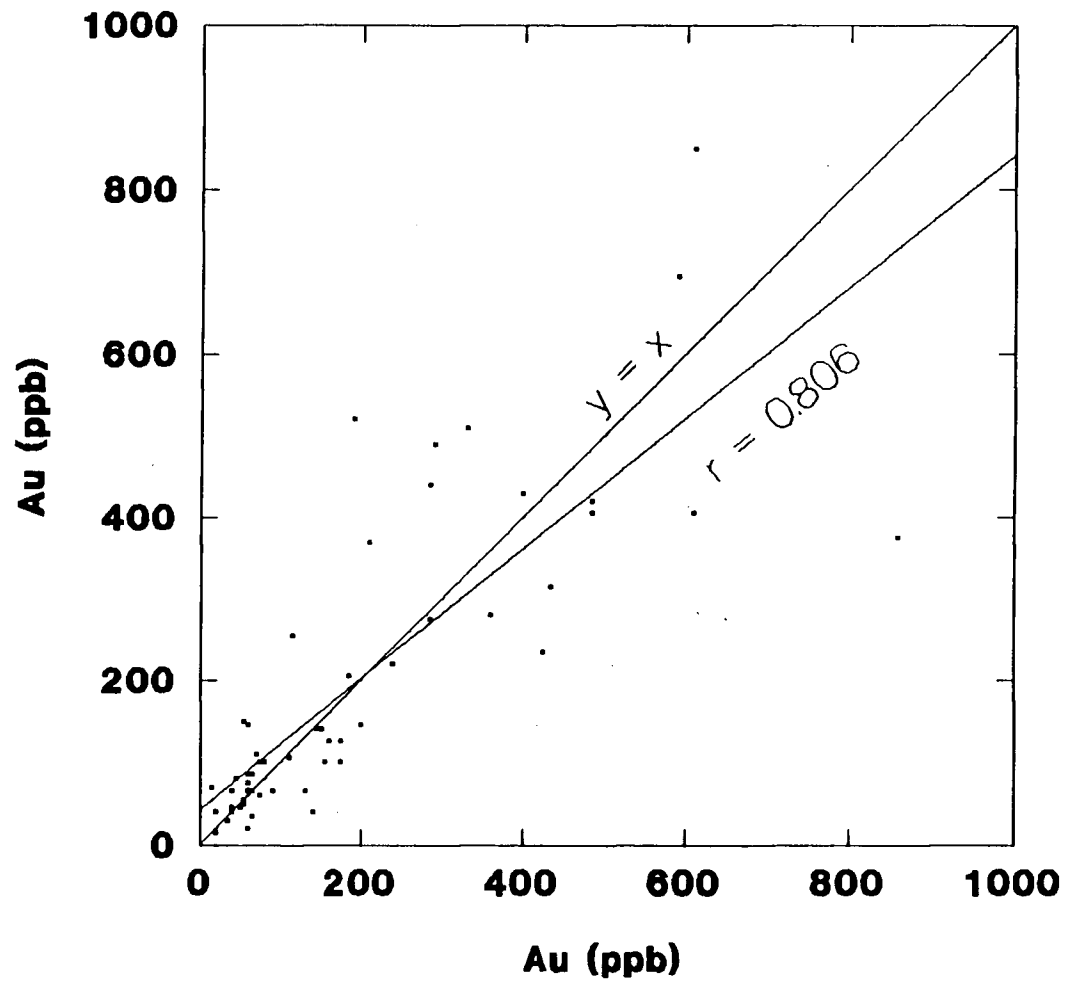
Figure 5.2 - Scatterplot of duplicate Au analyses, -212 micron fraction. Large outlier (6350 ppb) and corresponding duplicate analysis removed.

Probability is then calculated using the formula:

$$p = X - Z(s) \qquad\qquad (5\text{-}2)$$

where p is the probability of obtaining a particular deviation, X is the cumulative probability (0.50) of the standard normalized distribution where the deviation equals zero, Z is the result of equation (5-1), and s is the standard deviation (0.6826) of the standard normalized distribution .

Using values of n = 56 and m = 28, the calculated probability (p) of obtaining this particular deviation is 0.50. Under ideal situations where no systematic bias is present (ie., Z = 0), the maximum obtainable probability (p) is 0.50. From this, it is determined that systematic bias has not influenced the results. Inspection of Figure 5.1 confirms this, as 28 scatterplot points (Anal1 vs. Anal2) are found on or above the Anal1 = Anal2 line, whereas 28 are found on or below this line.

5.1.1.4 <u>Analysis of variance</u>

One way analysis of variance can be utilized to determine whether variability between both sets of duplicate analyses (ie. primary analyses and duplicate analyses) is greater than the variability within each set. If the null hypothesis ($u_0 = u_1 = \ldots = u_n$) is accepted, then analytical variability between sets is indistinguishable from analytical variability within each set.

Analysis of variance (calculated at the 95% confidence level) results in a calculated F ratio (0.865) less than the F ratio (1.53) required for a significant difference. Thus the primary analyses cannot be distinguished from the duplicate analyses (Table 5-1).

5.1.1.5 <u>Thompson and Howarth precision method</u>

Precision of geochemical data is an estimate of the relative variation due to sampling and analytical error. This is specified as the percent relative variation at the two standard deviation (95%) confidence level, or:

Group	Mean	N
1	298.214	56
2	190.893	56
Grand mean	244.554	112

Source of Variation	Sum of Squares	Degrees of Freedom	Mean Square
Between groups	322500.9	1	322500.9
Within groups	41029376.8	110	372994.3
Total	41351877.7	111	

$$F_{calc} = 0.865; \quad F_{(60,60,0.05)} = 1.53$$

Null hypothesis accepted

Table 5-1 - Analysis of variance results for primary and duplicate -212 micron Au analyses.

$$P_c = 200S_c/c \qquad\qquad (5-3)$$

where P_c is the precision (in percent) at concentration c, and S_c is an estimate of the standard deviation at concentration c.

In order to determine precision using geochemical samples, Thompson and Howarth (1973,1976,1978) devised a rapid method using a minimum of 50 randomly selected duplicate pairs. Briefly, this method is as follows (Thompson and Howarth, 1978):

1) From the duplicate analyses obtain a list of the means $(X_1+X_2)/2$ and the corresponding absolute differences $|X_1-X_2|$.

2) Sort the list in increasing order of concentration means.

3) Select the first 11 results and calculate the mean of the concentration means and determine the median value of the absolute differences.

4) Repeat this procedure for each successive group of eleven results and obtain corresponding lists of means and medians. Reject any group with less than eleven results.

5) Calculate the intercept and slope of the regression line fitting a plot of median absolute differences versus concentration means. Multiply the intercept and

slope by 1.048 to obtain S_0 (standard deviation at zero concentration) and k (slope), respectfully.

Use of this method is restricted to data which follows a normal distribution; data drawn from non-normal populations will likely result in erroneous conclusions (Thompson and Howarth, 1976).

Five sets of eleven analyses were utilized to determine precision. Figure 5.3 graphically represents the distribution of duplicate analyses (dots), the mean absolute difference versus median value for each group of eleven duplicates (squares) and the fitted regression line. The calculated intercept for the regression line is -0.822, with a corresponding slope of 0.309 and a correlation coefficient of 0.967. The presence of a negative intercept implies that at some concentration the standard deviation (S_c) is equal to zero, a result which is neither realistic or possible to achieve. Evidently, the duplicate dataset follows a non-normal distribution, likely a result of the nugget effect. The Thompson and Howarth (1973, 1976 and 1978) precision method is invalid for this dataset.
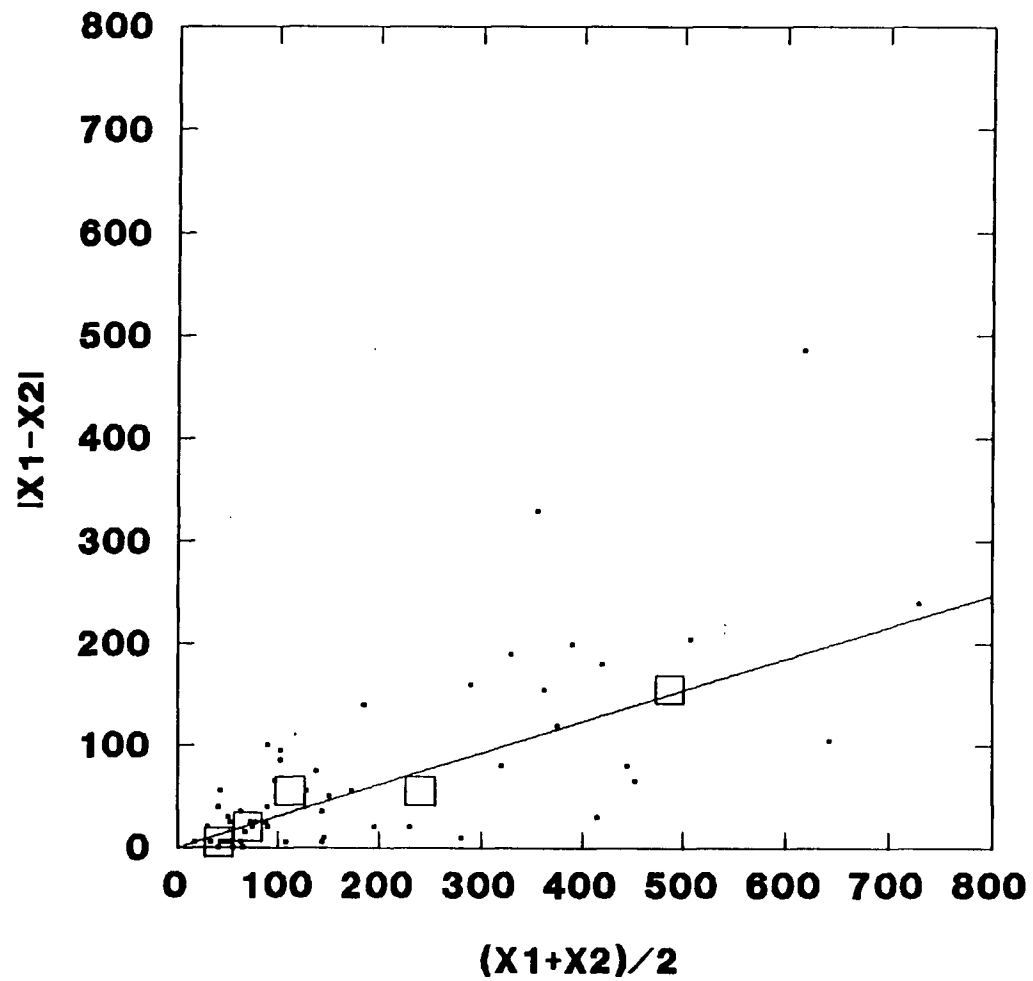
Figure 5.3 - Thompson and Howarth error plot, -212 micron fraction duplicate data.

5.1.2 <u>Grain size distribution of the -2000 micron fractions</u>

Grain size distribution within the -2000 micron (ASTM - 10 mesh) fraction was determined from labratory sieving of each sample into three subfractions (-2000+420 microns, -420+212 microns, and -212 microns). Results of this sieving (Figure 5.4) indicates that the majority of the mass of each soil horizon resides in the -212 micron fraction. The proportion of -212 micron material is observed to increase with depth.

5.1.3 <u>Soil pit results</u>

For statistical evaluation of results, the classification of the soil profiles was simplified into four discrete horizons: LFH, A, B and C. The uppermost mineral horizon of each profile was designated as the A horizon, whereas the underlying soil layer was denoted the B horizon. C horizon was used to specify the lowest unit(s) exposed within each soil pit which exhibited the characteristics of weathered parent material. In cases where two or more C horizons were encountered within a profile, the values were combined and a mean value taken. LFH samples were not affected by this regrouping.
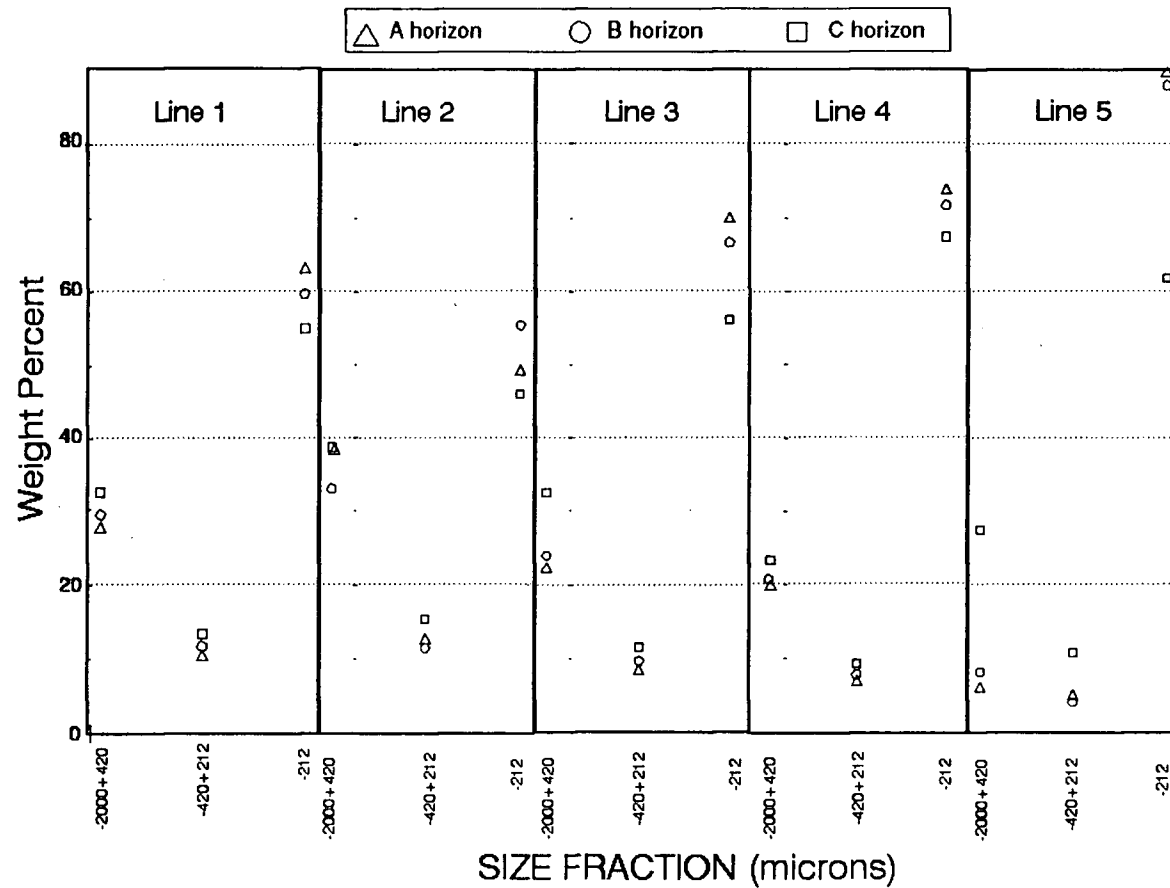
Figure 5.4 - Mean grain size distribution of the -2000 micron fraction for the A, B and C horizons of each traverse line.

Results of FA-AAS on thirty gram splits of the -212
micron fraction for each soil horizon are shown in the
Appendix. A strongly skewed arithmetic histogram of these Au
analyses (Figure 5.5) indicates the presence of a single
outlier (6350 ppb). Examination of a logarithmic histogram
(Figure 5.6) indicates a slightly skewed, normal
distribution of Au values with isolated outliers.

Plots of the data by traverse line (Figures 5.7a-e)
shows the Au content of each horizon. Results are generally
erratic, no noticable patterns of Au distribution are
observed along each traverse line. As shown in Table 5-2,
the (logarithmic) mean Au content of each horizon increases
with depth. Mean (antilog) Au concentrations for each
horizon range from a low of 8.2 ppb (Line 5, LFH horizon) to
a high of 413 ppb (Line 1, C horizon). Comparison of
corresponding logarithmic horizon means from each traverse
line indicates that with increasing distance from the mine,
the Au concentration within each horizon decreases (Figure
5.8).

5.1.4 Roadcut samples

FA-AAS results for forty-four C horizon till samples
taken along the Hedley Road are listed in the Appendix. A
summary table of these results is shown in Table 5-3. The

n = 189

mean = 196.8

σ = 489.2
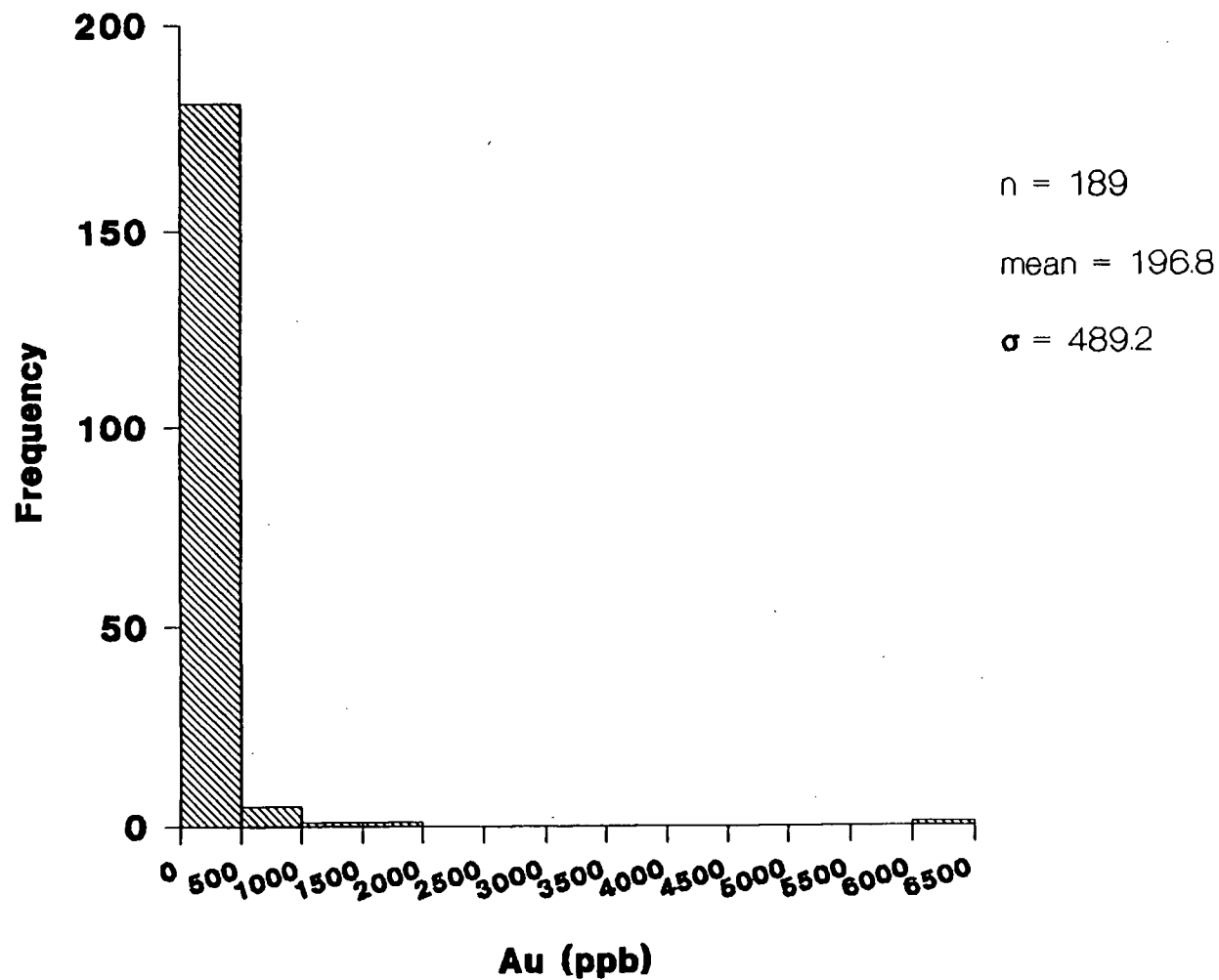
Figure 5.5 - Arithmetic histogram of all A, B and C horizon -212 micron fraction Au analyses.
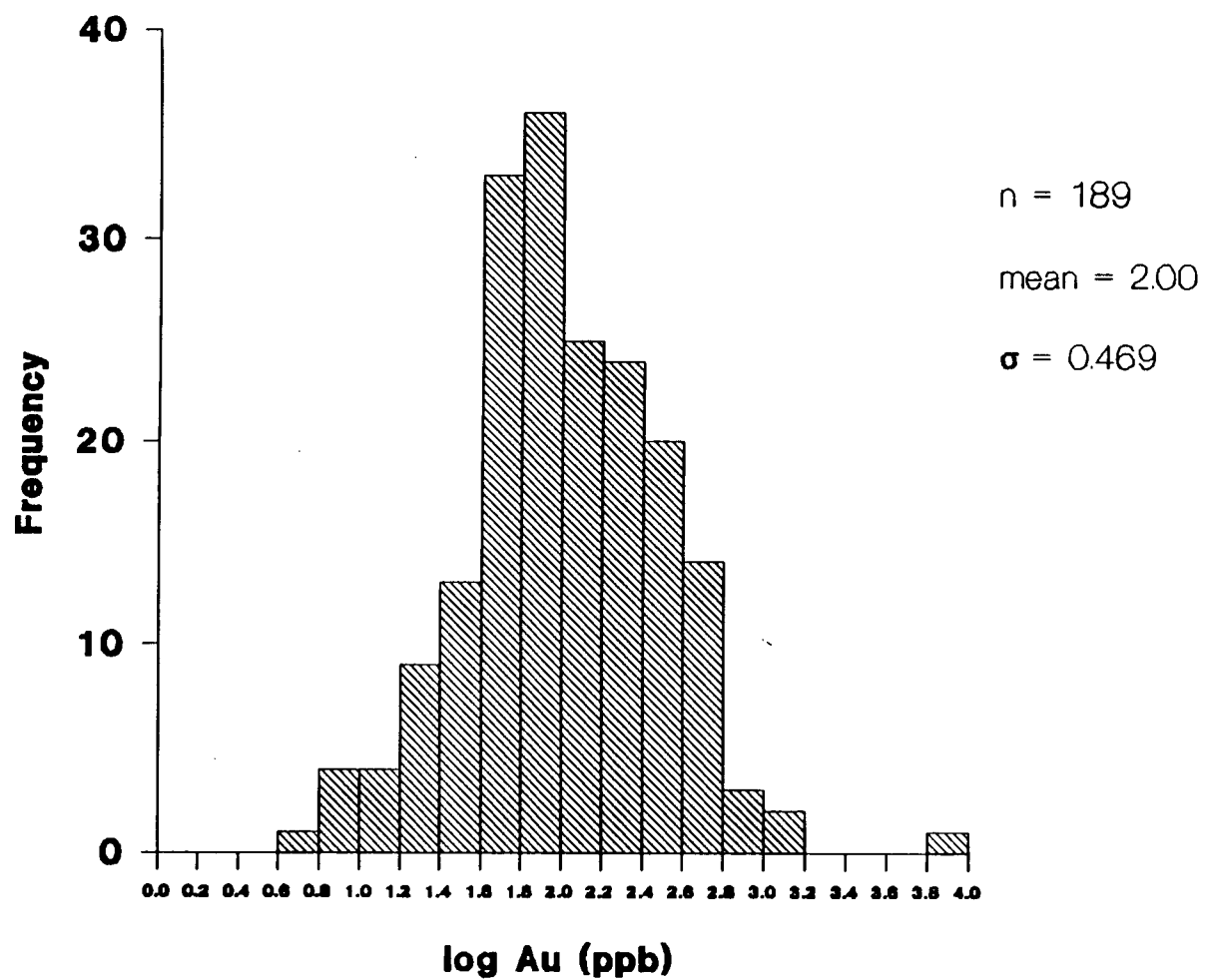
Figure 5.6 – Logarithmic histogram of all A, B and C horizon -212 micron fraction Au analyses.
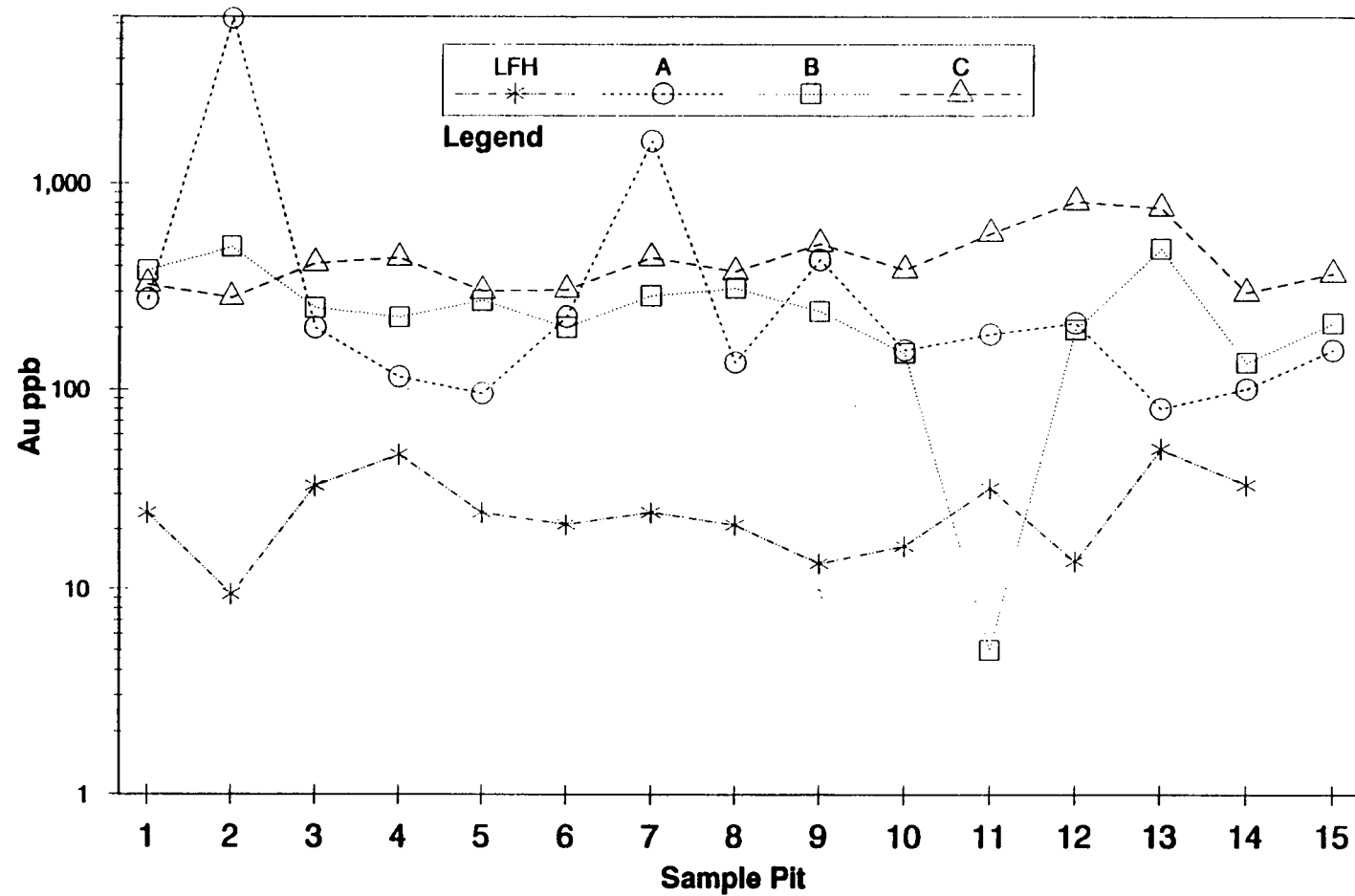
Figure 5.7a - Au content of the LFH, A, B and C horizons, -212 micron fraction, traverse line 1.
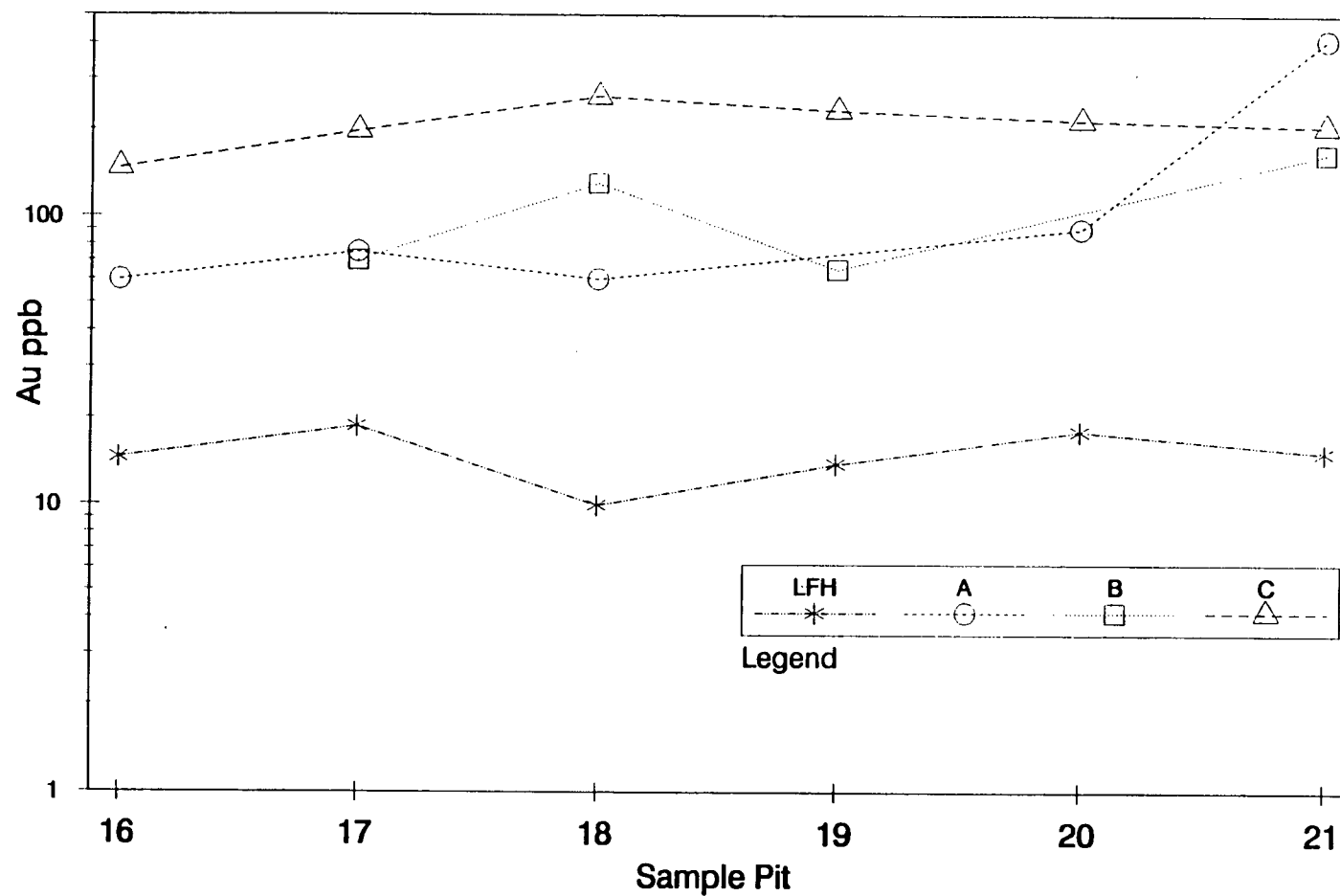
Figure 5.7b – Au content of the LFH, A, B and C horizons, -212 micron fraction, traverse line 2.
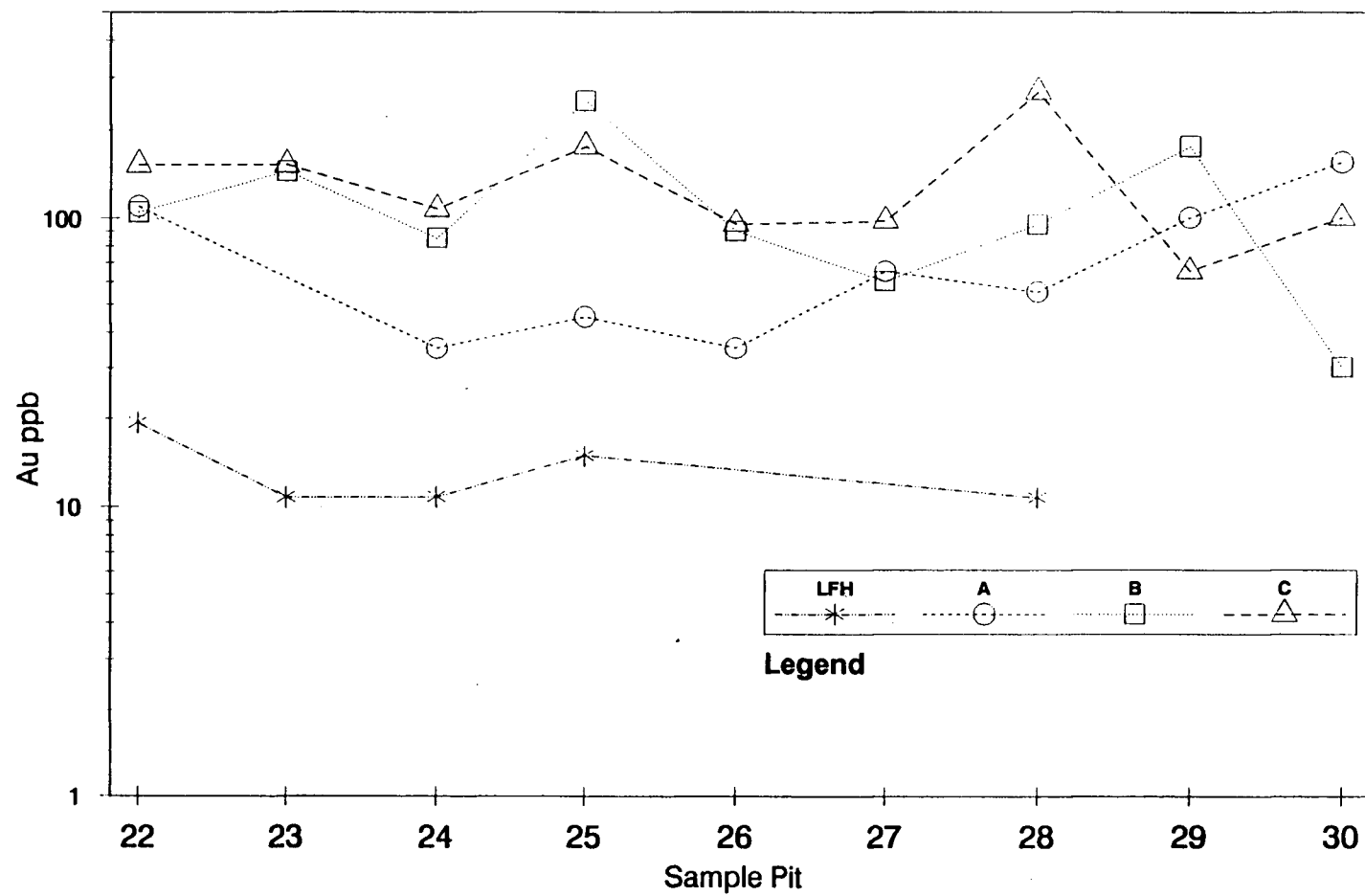
Figure 5.7c - Au content of the LFH, A, B and C horizons, -212 micron fraction, traverse line 3.
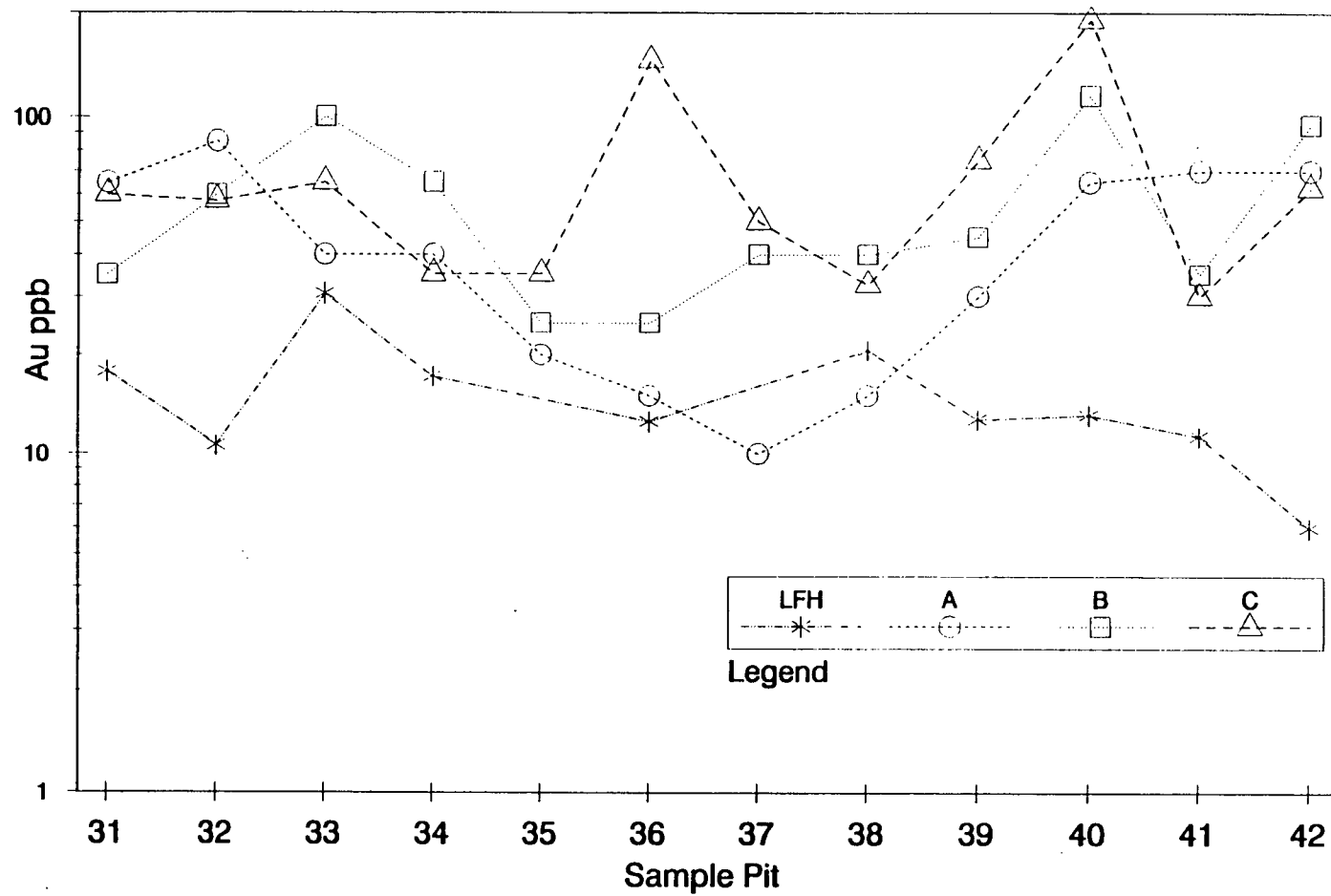
Figure 5.7d - Au content of the LFH, A, B and C horizons, -212 micron fraction, traverse line 4.
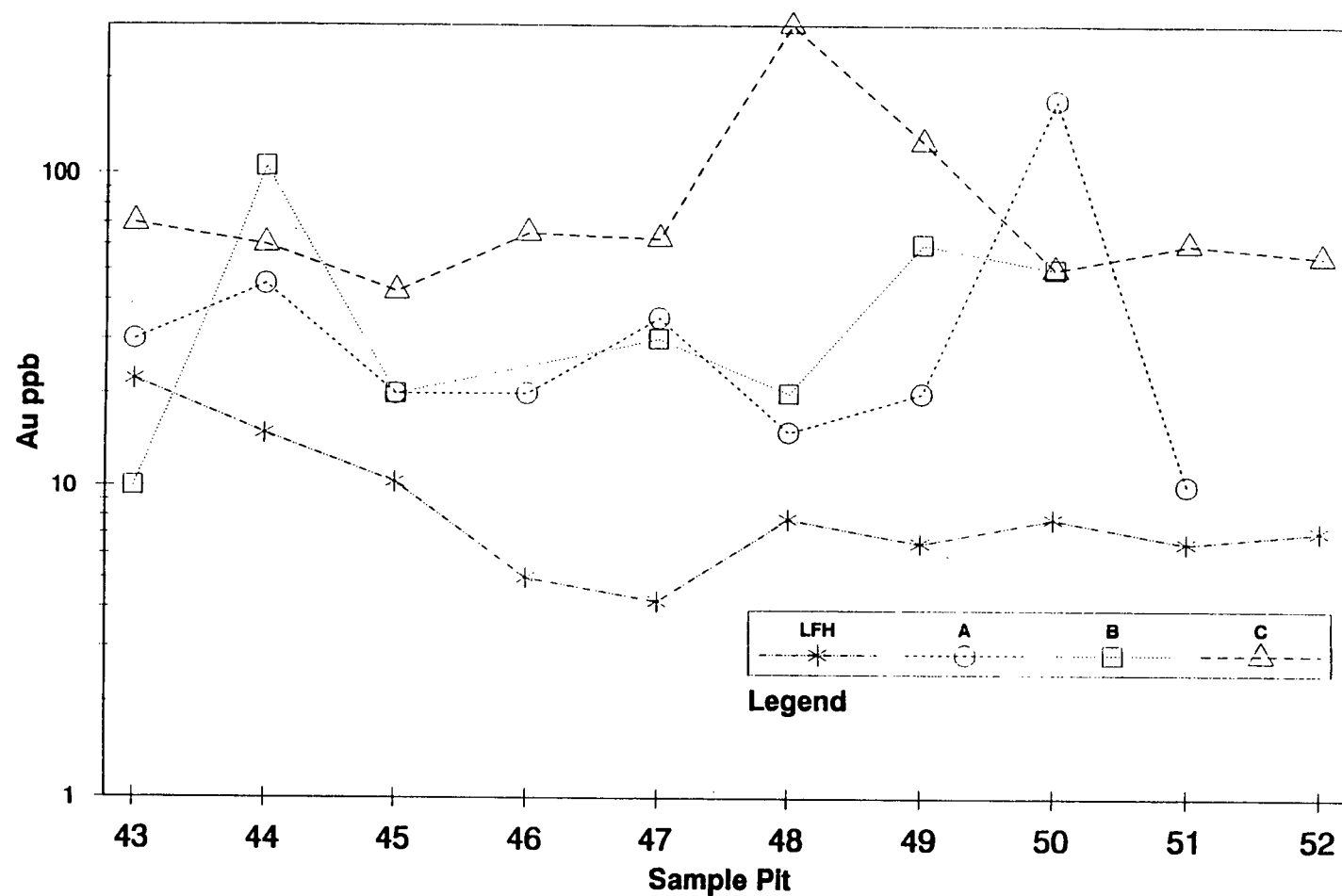
Figure 5.7e - Au content of the LFH, A, B and C horizons, -212 micron fraction, traverse line 5.

Horizon	LFH	A	B	C
Line				
1	23.4	162	257	417
2	14.8	100	99	209
3	12.9	66	98	123
4	14.1	35	58	59
5	8.1	28	32	74

Table 5-2 - Mean (antilog) Au content of each soil horizon by traverse line. All values in ppb.
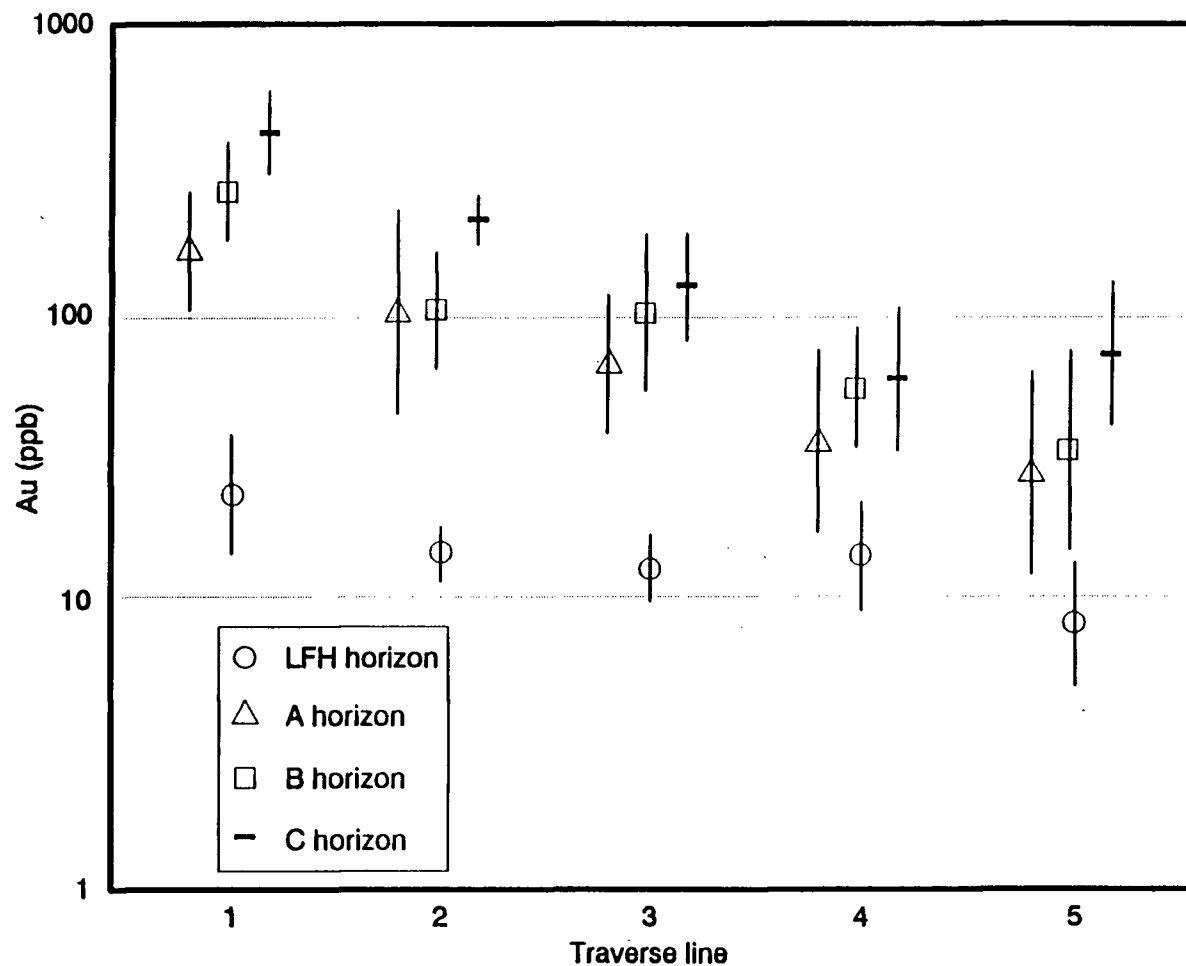
Figure 5.8 - Plot of the mean logarithmic Au content of the LFH, A, B and C horizons as a function of distance. Error bars indicate one standard deviation. Results are staggered to eliminate overlap of points.

Number of Samples	Mean	Minimum	Maximum	Standard Deviation
44	210	10	5070	(-) 59
				(+) 748

Table 5-3 - Summary table for (antilog) Roadcut C horizon (till) sample Au analyses. Analytical values in ppb.

same general trend is observed with the roadcut samples as with the soil pit samples: ie. a decrease in Au values with increasing distance from the mine (Figure 5.9).

5.1.5 Population distributions of the minus 212 micron results

Separation of the Au data into anomalous and background populations was achieved using logarithmic probability plots generated by the PROBPLOT program (Stanley, 1987). Logarithmic probability plots were selected as the data approximates a normal logarithmic distribution (see Figure 5.6). Data were first separated into subsets by horizon (LFH, A, B, and C), and C horizon samples taken along the Hedley Road (Roadcut samples) were treated as a separate set of data. A bimodal population distribution (anomalous and background populations) was assumed for each subset. Attempts to subdivide the data into a greater number of populations was considered unreliable due to the small number of samples analysed (n = 51, maximum). Data which could not be placed confidently within either the anomalous or background populations were categorized as belonging to mixtures of the populations. Thresholds used by the PROBPLOT program were based upon the method described by Sinclair (1976) and were defined as the mean +/- two standard deviations for each partitioned (anomalous and background)
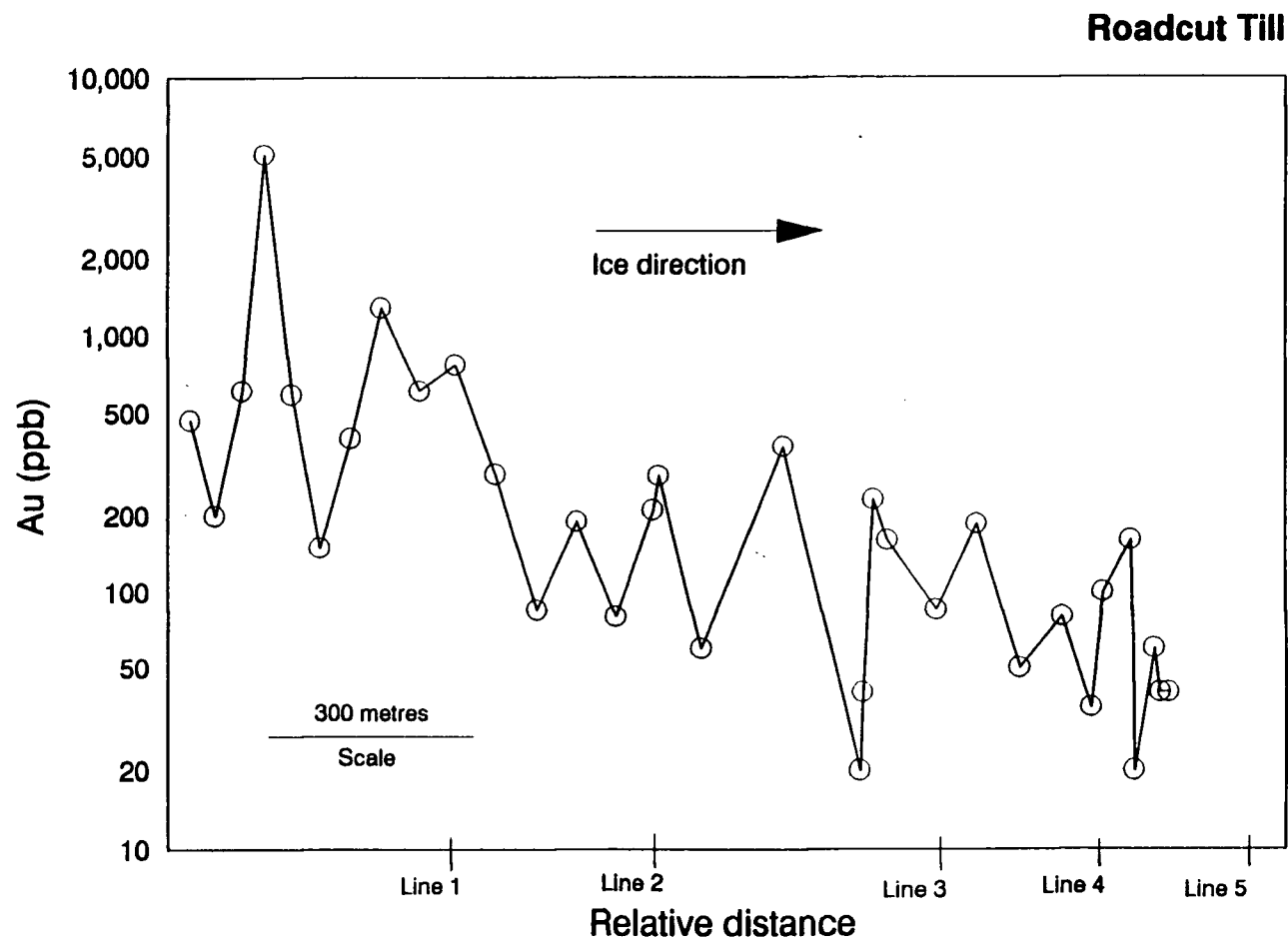
Figure 5.9 - Plot of the -212 micron fraction Au content of the Roadcut till samples with increasing distance from the minesite.

population (Stanley, 1987). Mixed samples were defined as those values which fell above the cumulative 98.5 percentile of the background population and below the cumulative 2.5 percentile of the anomalous population.

Results of logarithmic probability plots generated for each horizon and the Roadcut C horizon samples are shown in Figures 5.10a-e. Visual inspection of the probability plots and calculated threshold values indicates that the bimodal population model best fits data from the C horizon and the Roadcut C horizon samples. Partition of the LFH, A and B horizons into anomalous and background populations, although plausible, is not as distinct. The lower five to eight percent of each dataset (excluding the LFH horizon) poorly fits a bimodal curve and appears to represent a third population. However, only two to four samples are represented by five to eight percent of the data. It is possible that these data are spurious and are due to field sampling problems or analytical difficulties for Au. Conversely, a third population may exist within the dataset, but is not sufficiently represented to be conclusive.

Calculated threshold values for each horizon and the resultant ranges for the corresponding anomalous, mixed and background populations are listed in Table 5-4. Contrast values generated for the A, B and C horizons (where contrast equals the mean of the anomalous population divided by the
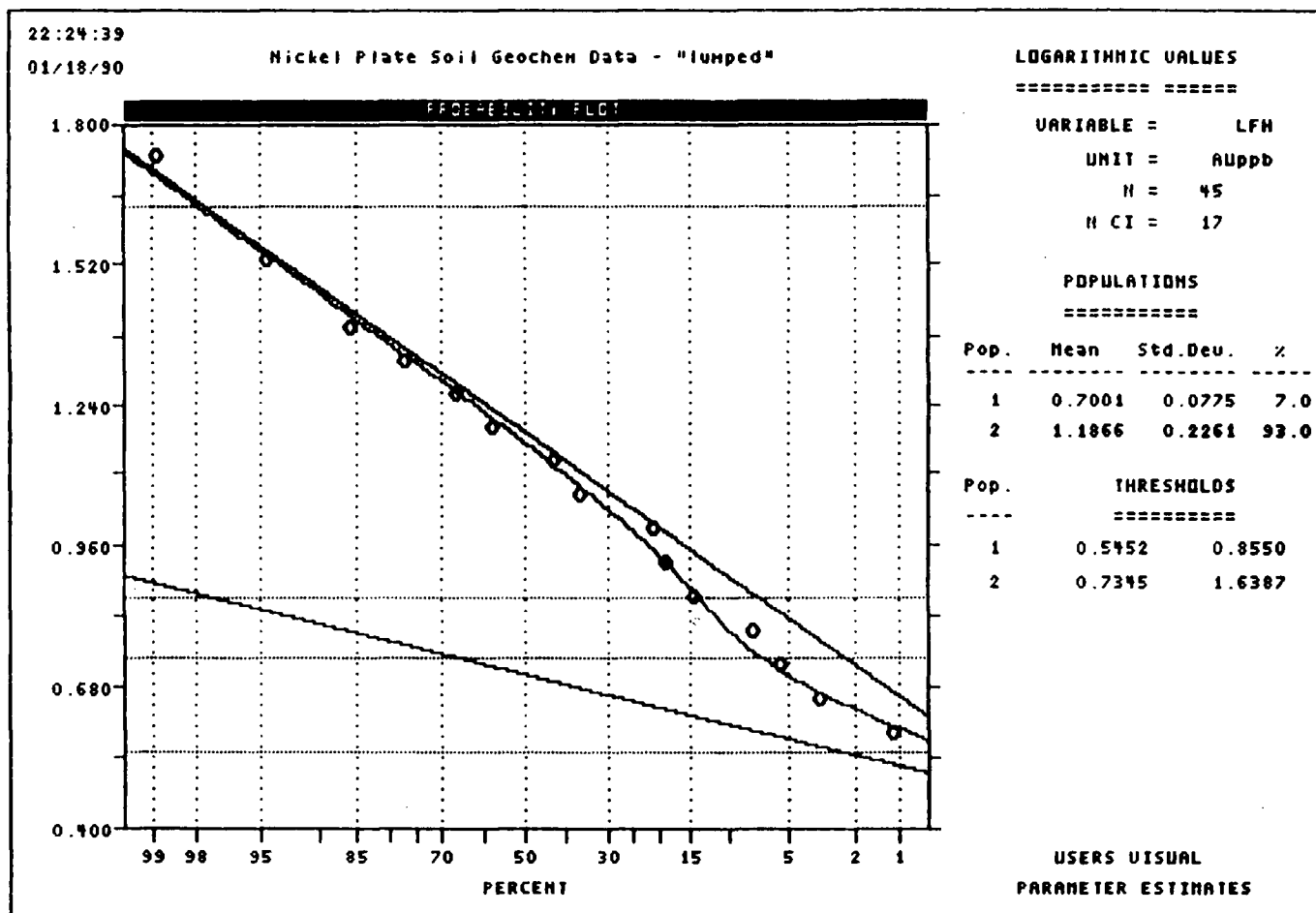
Figure 5.10a - Probability plot with thresholds, LFH horizon Au content.
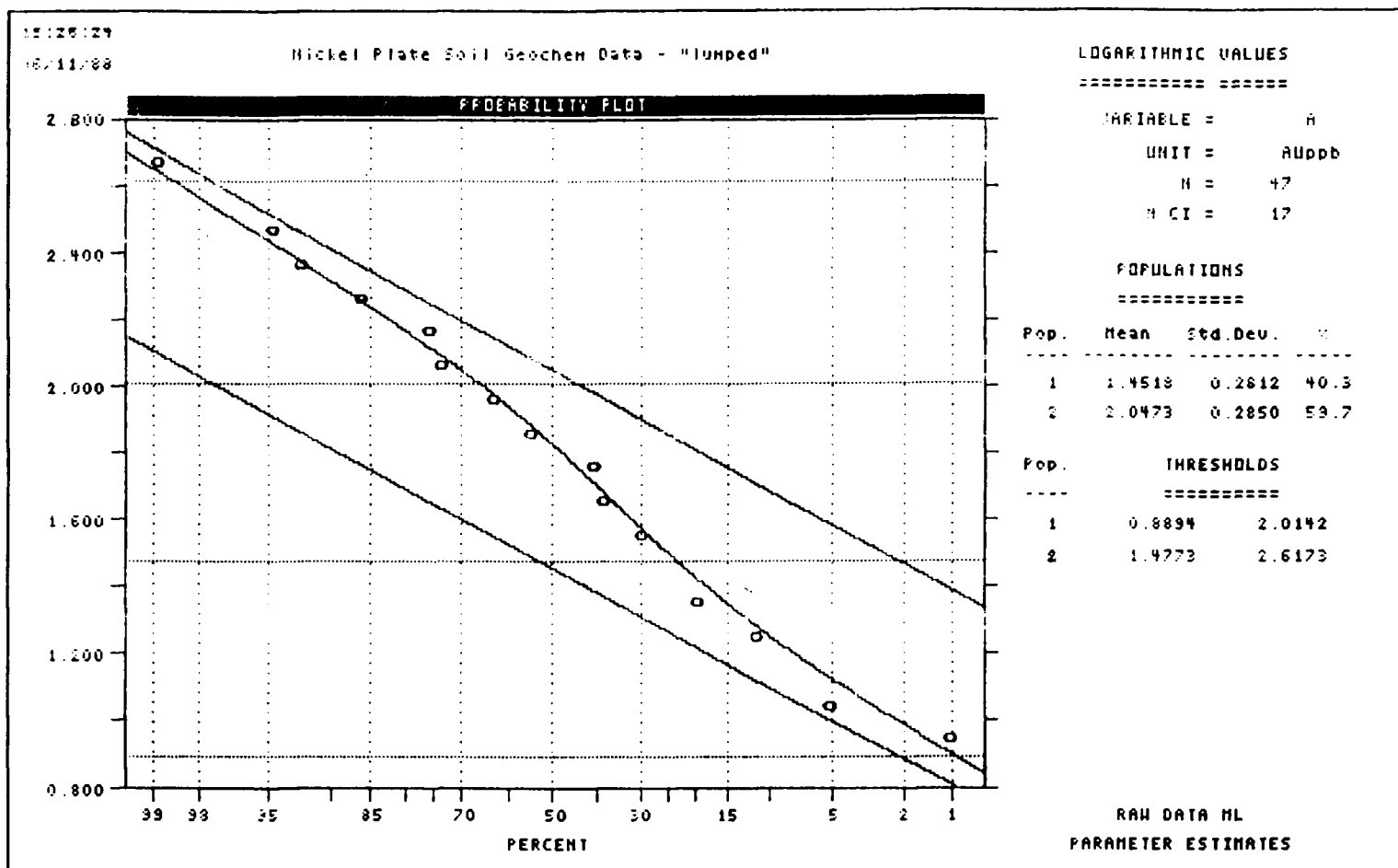
Figure 5.10b - Probability plot with thresholds, A horizon -212 micron fraction Au content.
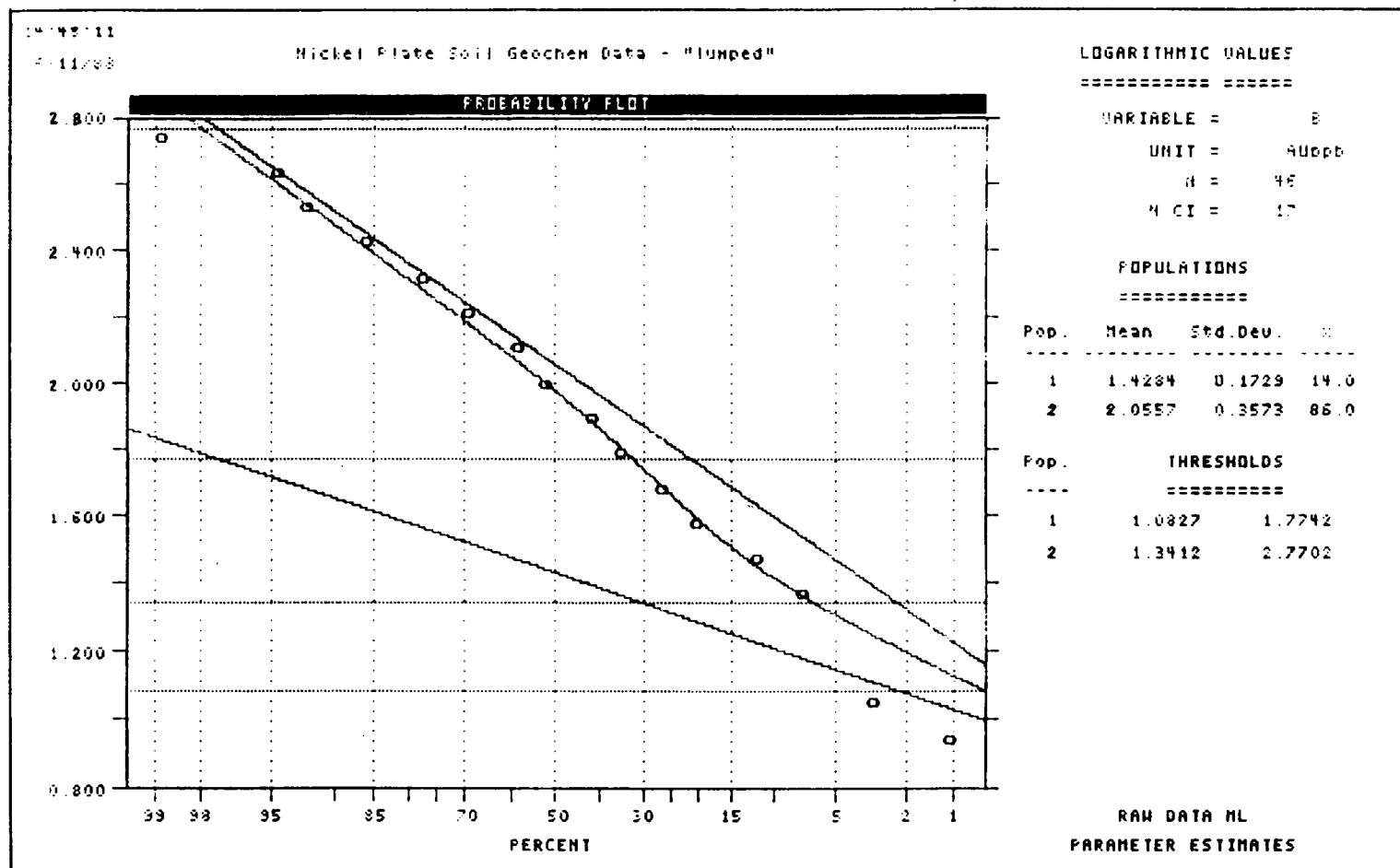
Figure 5.10c - Probability plot with thresholds, B horizon -212 micron fraction Au content.
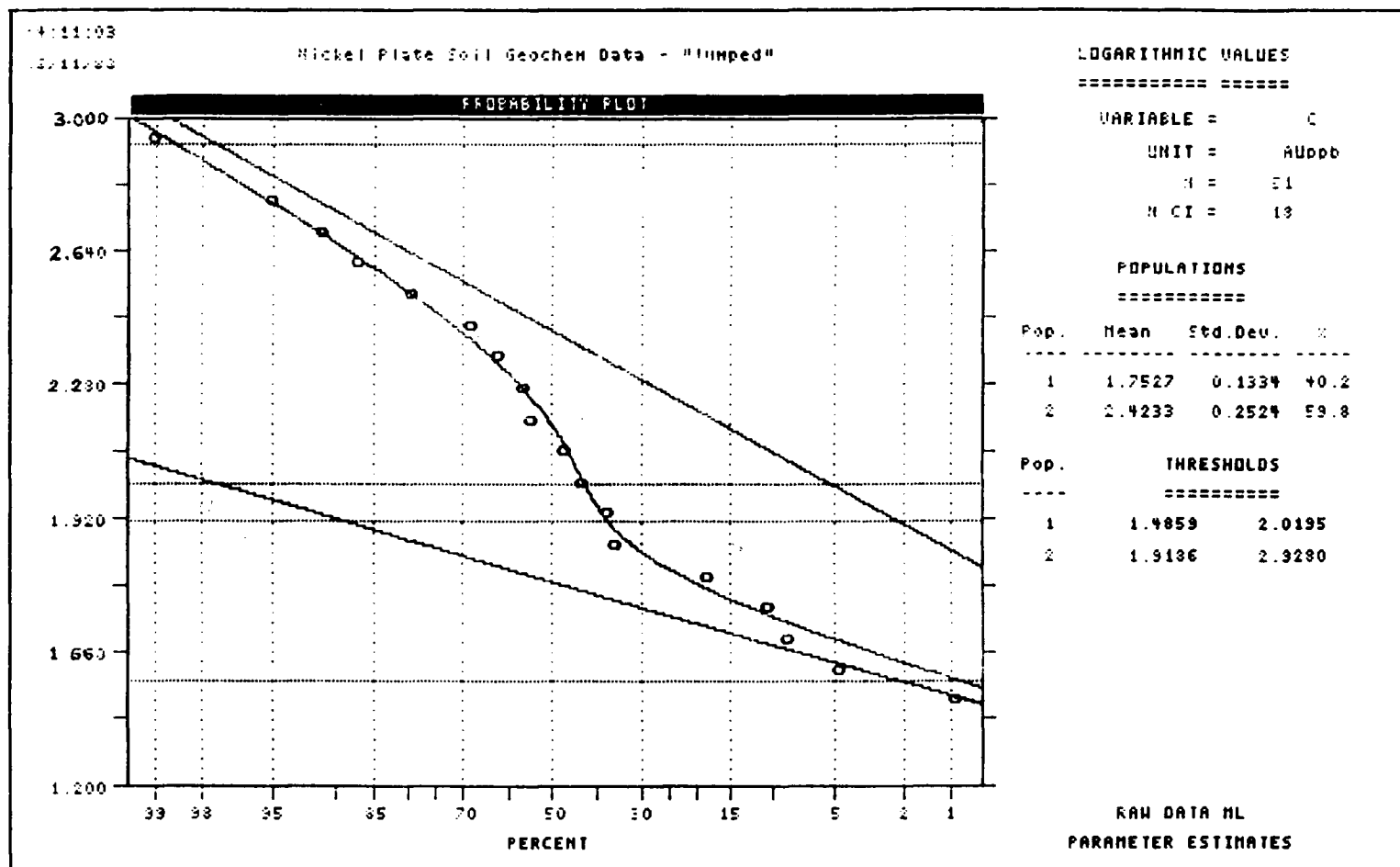
Figure 5.10d - Probability plot with thresholds, C horizon -212 micron fraction Au content.
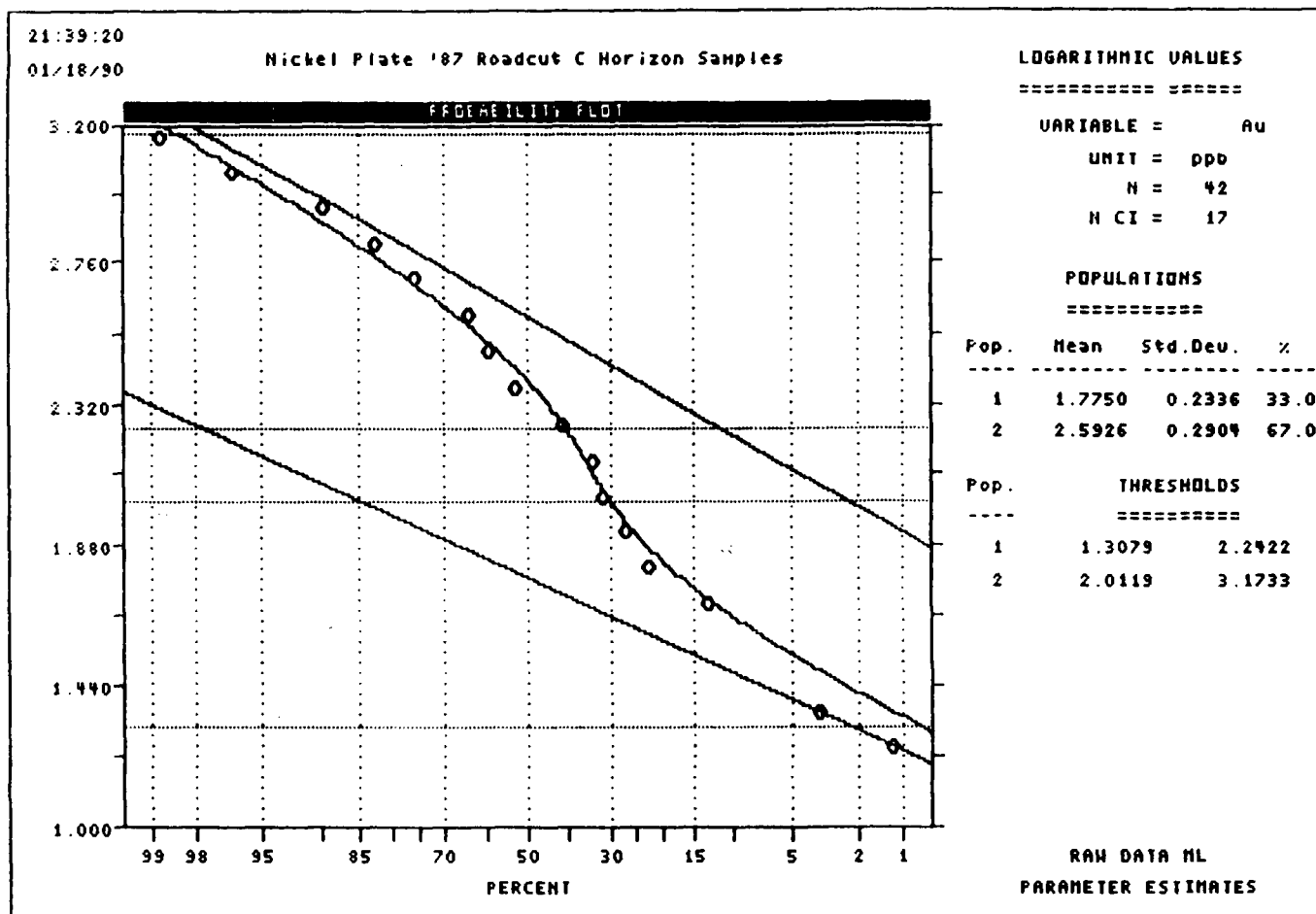
Figure 5.10e - Probability plot with thresholds, Roadcut C horizon samples, -212 micron fraction Au content.

Mean or Threshold	Horizon				
	LFH	A	B	C	Road C
Anomalous (mean)	15.4	111	114	265	392
Anomalous (X + 2s)	43.6	414	589	847	1489
Anomalous (X - 2s)	5.4	30	22	83	103
Background (mean)	5.0	28	27	57	60
Background (X + 2s)	7.2	103	59	104	175
Background (X - 2s)	3.5	8	12	31	20
Contrast ratio	2.1	1.1	1.9	2.6	2.2
% population anomalous	93.0	59.7	86.0	59.8	67.0
% population background	7.0	40.3	14.0	40.2	33.0

Table 5-4 - Calculated (antilog) means and thresholds for the anomalous and background populations of each soil horizon. (Contrast ratio = mean anomalous population divided by mean plus two standard deviations background population). Also included are the percentages of anomalous and background populations.

mean plus two standard deviations of the background
population) reveals that contrast between anomalous and
background populations increases down the soil profile
(Table 5-4).

5.2 Size / density fraction results

5.2.1 Introduction

Six pit profiles were chosen for detailed size and
density fraction analysis. Pit selection was based upon
separation of the -212 micron C horizon Au data into
anomalous and background populations. Two profiles were
chosen from the anomalous C horizon population (referred to
as the Proximal pits) and two from the background population
(Distal pits); the remaining two pits were picked to
represent the mixed group of samples (Intermediate pits).
All profiles were selected to represent the observed
increase in Au content with depth. A distance of 780 metres
separates the Proximal and Distal pits.

5.2.2 Reliability and analytical precision

Reliability of the size / density fraction analyses was

estimated using a total of eighteen duplicate samples. Duplicate splits of the light mineral and -53 micron fractions indicate good reproducibility (Figures 5.11, 5.12). Poor reproducibility (r = 0.61, $r_{crit(0.05)}$ = 0.74) is displayed for duplicate pairs of the heavy mineral fraction (Figure 5.13), and is presumably a result of the nugget effect.

Analysis of variance carried out on the three duplicate subsets (LMC, HMC and -53 micron) is shown in Table 5-5. In all cases, the null hypothesis is accepted: ie. there is no evidence to suggest that the primary and duplicate analyses have originated from separate populations.

5.2.3 Grain size distribution of the -2000 micron fraction

Grain size distribution within the -2000 micron fraction (in weight percent) of the detailed samples is represented in Table 5-6a. All samples have a nearly identical bimodal grain size distribution, with most of the sample weight being concentrated in the -2000+420 micron and -53 micron size fractions.

Distribution of light and heavy mineral fractions within the -420 micron fraction is listed in Table 5-6b. The
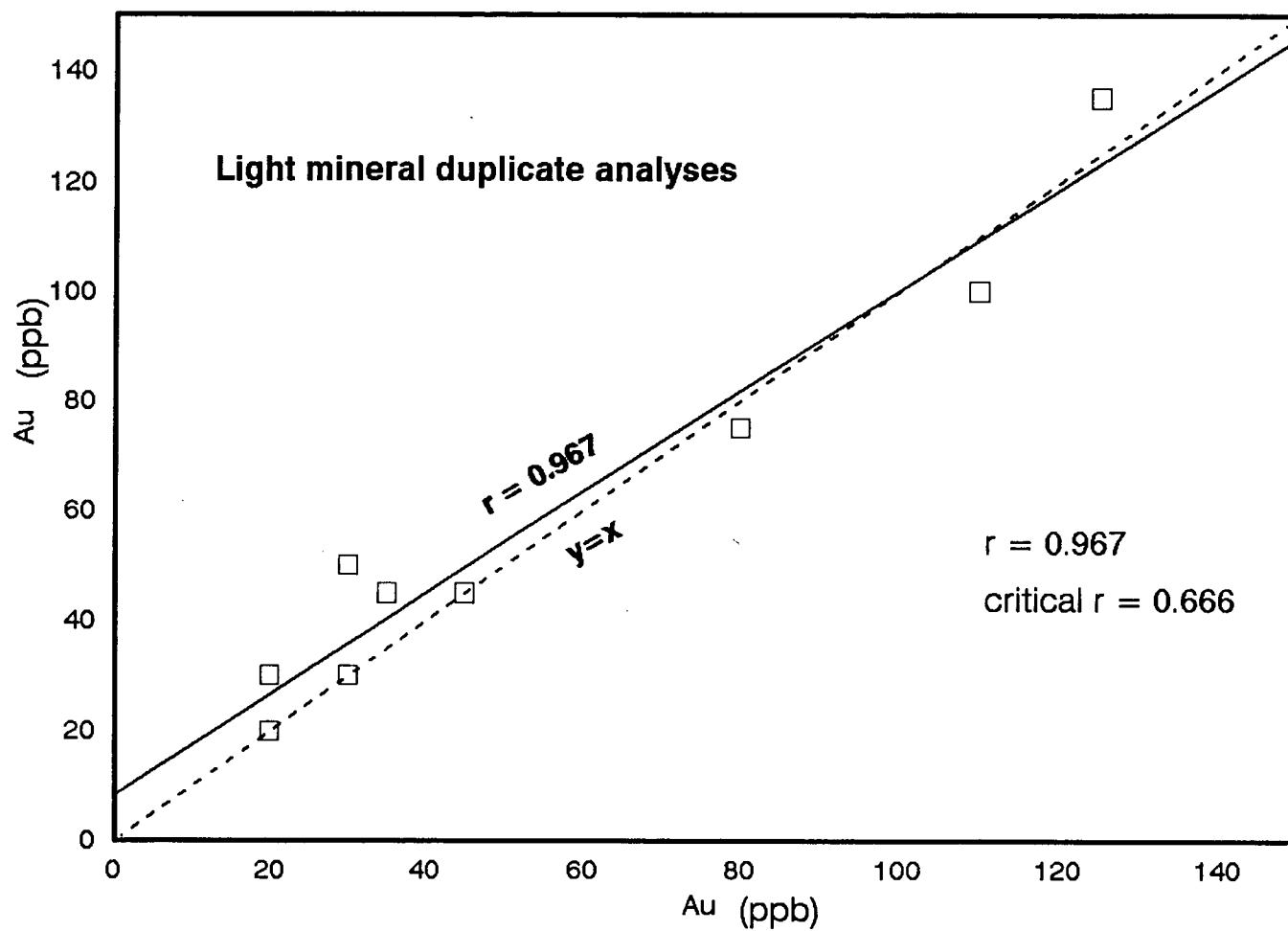
Figure 5.11 – Light mineral fraction duplicate analyses.
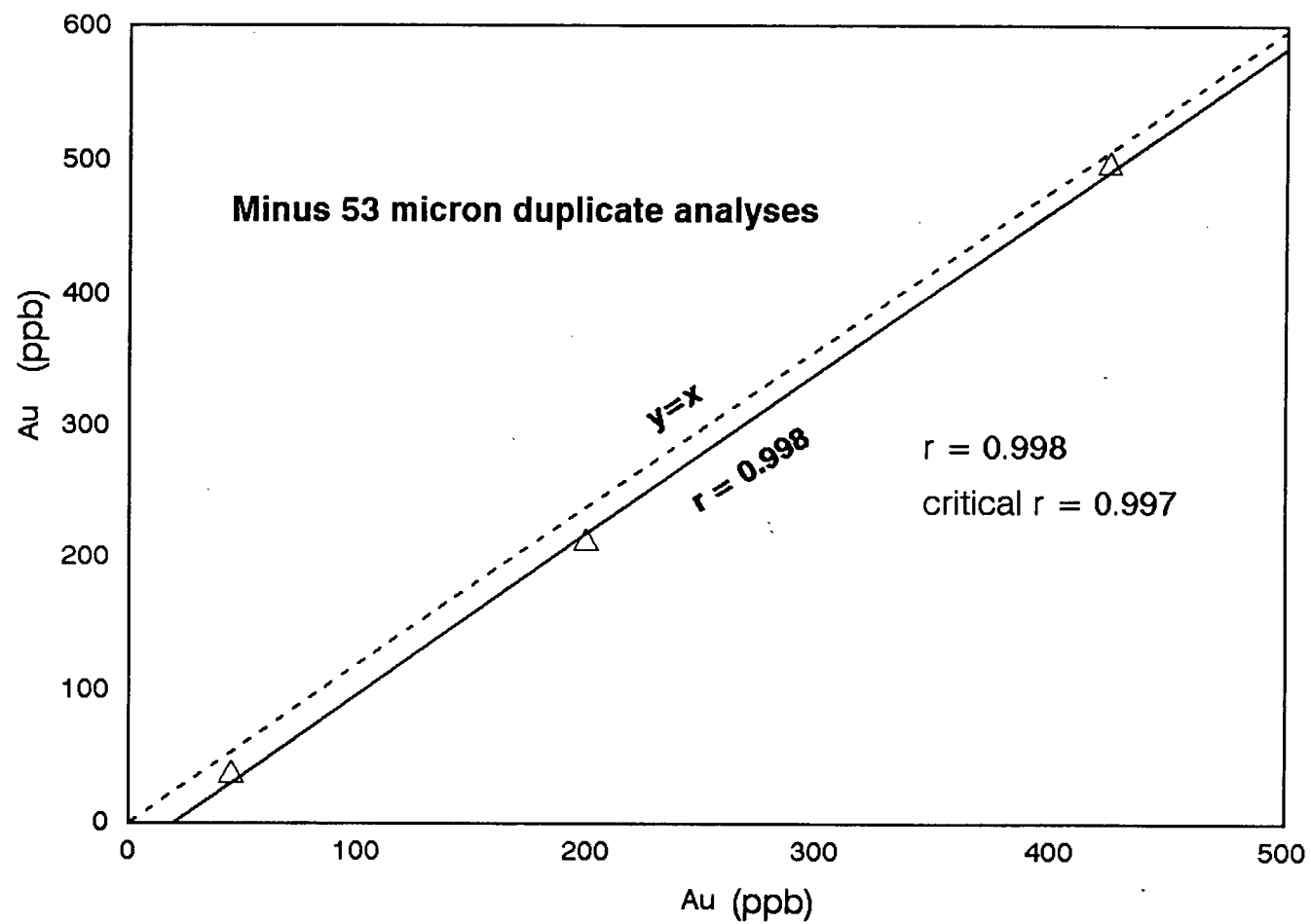
Figure 5.12 - Minus 53 micron fraction duplicate analyses.
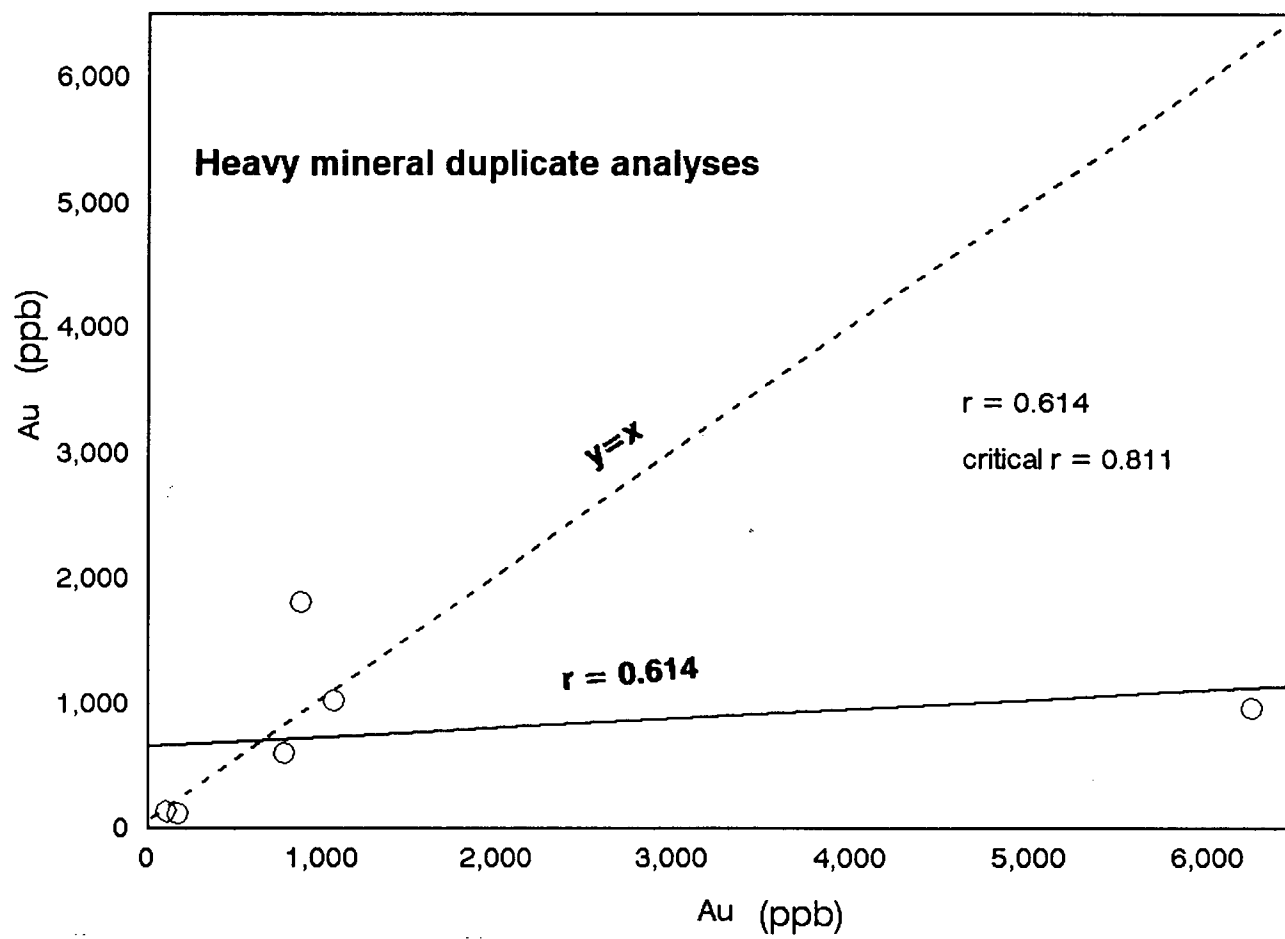
Figure 5.13 – Heavy mineral fraction duplicate analyses.

Light mineral concentrates

Source of Variation	Sum of Squares	Degrees of Freedom	Mean Square
Between groups	12.5	1	12.5008
Within groups	24194.4	16	1512.2
Total	24206.9	17	

$F_{calc} = 0.00027$; $F_{(16,1,0.05)} = 4.49$

Null hypothesis accepted

Heavy mineral concentrates

Source of Variation	Sum of Squares	Degrees of Freedom	Mean Square
Between groups	3461502	1	3461502
Within groups	27809670	10	2780967
Total	31271172	11	

$F_{calc} = 1.245$; $F_{(10,11,0.05)} = 2.85$

Null hypothesis accepted

-53 micron fraction

Source of Variation	Sum of Squares	Degrees of Freedom	Mean Square
Between groups	1350	1	1350
Within groups	180300	4	45075
Total	181650	5	

$F_{calc} = 0.03$; $F_{(4,5,0.05)} = 5.19$

Null hypothesis accepted

Table 5-5 - Analysis of variance results for duplicate light and heavy mineral concentrate and -53 micron Au analyses.

Sample	Soil Horizon	Size Fraction				
		-2000 +420	-420 +212	-212 +106	-106 +53	-53
14	A	22.6	8.8	11.3	8.6	48.5
15	B	24.7	11.2	11.1	7.6	45.4
16	C	29.1	13.9	11.5	7.9	37.7
41	A	28.6	9.8	10.6	7.4	43.6
42	B	29.0	10.3	8.7	5.3	46.7
43	C1	31.5	12.2	7.8	8.3	40.2
44	C2	36.0	14.1	11.1	7.3	31.5
122	A	21.8	8.8	10.4	7.9	51.1
123	B	24.2	10.4	10.1	7.2	48.0
124	C1	29.2	12.0	10.0	6.6	42.1
125	C2	28.0	10.3	10.0	7.0	44.7
127	A	19.7	9.4	10.0	6.9	54.1
128	B	20.7	9.1	9.7	6.1	54.4
129	C1	22.4	10.8	9.2	7.4	50.2
130	C2	26.3	11.9	9.4	6.2	46.3
162	A	19.2	7.3	9.4	5.9	58.2
163	B	27.2	11.5	9.8	6.5	45.0
164	C	31.2	10.5	9.8	8.3	40.2
186	A	15.3	6.1	9.7	6.7	62.3
187	B	15.3	5.7	9.1	7.2	62.8
188	C1	15.5	6.0	7.8	7.3	63.3
189	C2	19.4	7.7	7.7	6.7	58.3
Proximal average		30.1	12.3	10.0	7.3	40.3
Distal average		24.8	8.3	8.8	7.2	53.9
Contrast ratio		1.2	1.5	1.1	1.0	0.7

Table 5-6a - Grain size distribution of the -2000 micron fraction. Values in weight percent. Proximal and distal averages calculated by averaging the B and C horizons of the proximal and distal pits. Contrast ratio equals the proximal average divided by the distal average.

Sample	Soil Horizon	-420+212 L	-420+212 H	-212+106 L	-212+106 H	-106+53 L	-106+53 H	-53
14	A	2.5	8.9	3.0	11.6	2.4	8.7	62.8
15	B	3.6	11.4	4.0	10.8	2.8	7.3	60.2
16	C	4.9	14.8	4.9	11.2	3.5	7.6	53.1
41	A	2.9	10.8	3.3	11.6	2.3	8.0	61.1
42	B	3.2	11.4	2.9	9.4	1.8	5.6	65.8
43	C1	3.9	13.9	3.0	8.3	2.9	9.3	58.6
44	C2	5.2	16.9	4.8	12.6	3.1	8.3	49.1
122	A	1.3	9.9	1.6	11.8	1.1	8.9	65.4
123	B	2.1	11.6	2.2	11.0	1.5	8.1	63.4
124	C1	2.1	14.9	2.1	12.1	1.3	8.0	59.5
125	C2	1.9	12.4	2.2	11.8	1.4	8.2	62.1
127	A	1.3	10.4	1.4	11.0	1.1	7.5	67.3
128	B	1.2	10.3	1.5	10.8	1.0	6.8	68.6
129	C1	1.7	12.2	1.8	10.0	1.6	8.0	64.8
130	C2	2.1	14.1	2.0	10.6	0.7	7.7	63.0
162	A	0.9	8.1	1.1	10.5	0.6	6.7	72.0
163	B	1.1	14.7	1.2	12.2	0.6	8.4	61.8
164	C	0.2	15.1	0.3	14.0	0.2	11.8	58.5
186	A	0.8	6.3	1.2	10.2	0.9	6.9	73.6
187	B	0.9	5.8	1.3	9.4	1.1	7.3	74.2
188	C1	1.2	6.0	1.3	7.9	1.0	7.6	75.0
189	C2	2.2	7.4	1.7	7.9	1.0	7.3	72.5
Proximal ave		13.7	4.2	10.5	4.0	7.6	2.8	57.4
Distal ave		9.8	1.1	10.3	1.2	8.5	0.8	68.4
Contrast ratio		1.4	3.8	1.0	3.3	0.9	3.5	0.8

Table 5-6b - Grain size distribution of the light and heavy fractions of the -420+212, -212+106, -106+53 micron size fractions and the -53 micron fraction. Unlike Table 5-6a, all values in Table 5-6b are expressed as a weight percent of the total mass of the -420 micron fraction.

proportion of heavy mineral concentrate within each size
fraction decreases with distance (Figure 5.14). Percent
contribution of the -2000+420 micron fraction and the -
420+212 micron light mineral fraction also decrease with
distance, whereas the -212+106 and -106+53 micron light
mineral fractions and the -53 micron fraction increase.

5.2.4 <u>Size and density fraction analysis</u>

FA-AAS analysis for Au was carried out on size and
density fractions of selected samples (see section 4.3).
Detection limits for Au determination, which are dependent
upon the mass of sample analysed, varied from 5 (30 gram
sample) to 30 ppb (3.55 gram sample). All heavy mineral
analyses, save one, have Au concentrations above the
detection limit. In every case, light mineral analyses were
also above detection limits. Heavy mineral concentrates
generally returned higher Au values than their light mineral
counterparts (Tables 5-7 and 5-8).

5.2.5 <u>Heavy mineral fraction results</u>

Au concentrations within the heavy mineral fractions
decrease by a factors ranging from 2.2 to 12.5 between line
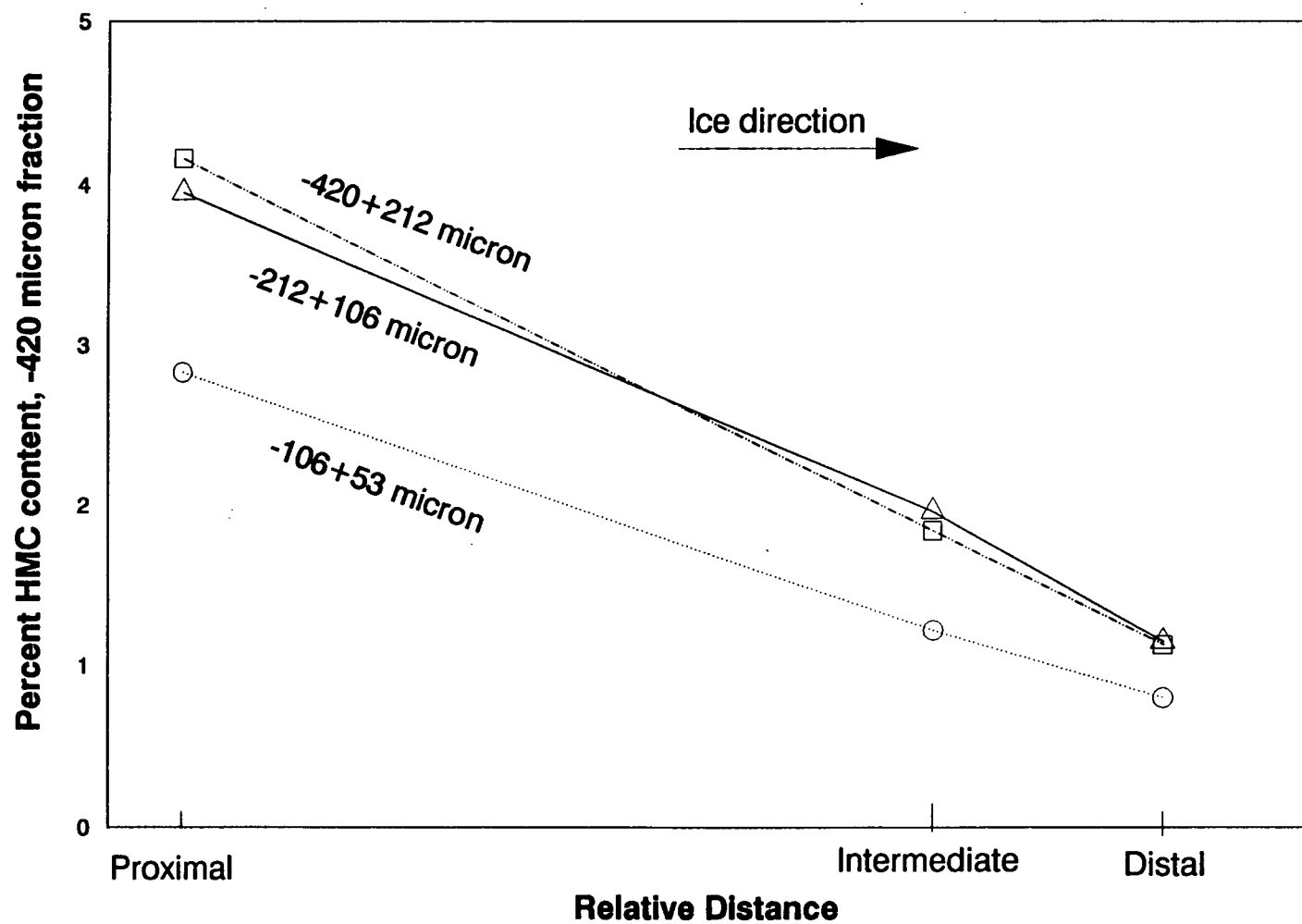
Figure 5.14 – Variation of heavy mineral content of the -420 micron fraction with increase in distance from the minesite.

Sample	Horizon	-420+212	-212+106	-106+53
14	A	110	805	1060
15	B	2200	100	875
16	C	175	505	2210
41	A	130	1115	975
42	B	180	935	1360
43	C1	895	1585	725
44	C2	125	1650	1685
122	A	50	45	330
123	B	6250	385	725
124	C1	40	305	735
125	C2	60	1180	785
127	A	60	420	560
128	B	45	165	1070
129	C1	35	45	585
130	C2	40	365	2120
162	A	20	1720	140
163	B	40	615	1360
164	C	25	70	<30
186	A	25	385	420
187	B	155	465	760
188	C1	20	40	620
189	C2	45	45	335
Proximal average (ppb)		511	682	979
Distal average (ppb)		41	176	441
Contrast ratio		12.5	3.9	2.2

Table 5-7 - Au concentrations (ppb) in heavy mineral concentrates. Proximal and distal averages calculated by averaging the Au contents of the respective B and C horizons. Contrast ratios calculated by dividing the proximal average by the distal average.

Sample	Horizon	-420+212	-212+106	-106+53
14	A	85	70	40
15	B	130	90	80
16	C	150	125	125
41	A	120	65	45
42	B	110	65	50
43	C1	90	105	80
44	C2	105	175	120
122	A	30	40	20
123	B	55	55	45
124	C1	80	60	40
125	C2	65	80	55
127	A	45	20	20
128	B	50	35	40
129	C1	40	50	30
130	C2	70	60	30
162	A	20	20	25
163	B	10	20	10
164	C	10	10	10
186	A	35	35	20
187	B	50	40	30
188	C1	55	50	40
189	C2	40	40	30

	-420+212	-212+106	-106+53
Proximal average (ppb)	84	80	65
Distal average (ppb)	24	23	17
Contrast ratio	3.5	3.5	3.8

Table 5-8 - Au concentrations (ppb) in light mineral concentrates. Proximal and distal averages calculated by averaging the Au contents of the respective B and C horizons. Contrast ratios calculated by dividing the proximal average by the distal average.

1 (proximal to mine) and line 4 (distal to mine) (Table 5-7). Trends in Au content are not observed within the sample pits; values appear to be erratic and unrelated to soil horizons. Overall, the coarse (-420+212 micron) fractions contain less Au than the finer (-212+106 micron, -106+53 micron) fractions.

5.2.6 Light mineral fraction results

The light mineral size fractions contain Au values ranging from 10 to 150 ppb (Table 5-8). Au contents are lowest within the -106+53 micron fraction in 15 of 22 samples, while Au contents of the -420+212 micron fraction are highest in 11 of 22 samples. In contrast to the heavy mineral samples, the Au concentrations of the light mineral fractions appear in many cases to be related to depth within the soil profile. Increasing Au values are observed with increasing depth within the soil profile in thirteen of eighteen cases (Table 5-8). Contrast ratios (the ratio of averaged proximal B and C horizons to averaged distal B and C horizons) for the light fractions are very similar.

5.2.7 Minus 53 micron fraction results

Results of FA-AAS on the -53 micron fraction are

presented in Table (5-9). Au concentrations range from 595
(C horizon sample 87-SS-44, proximal to mine) to 30 ppb (A
horizon sample 87-SS-162, distal to mine). A decline in Au
content by a factor of six is observed with increasing
distance from the mine. Also noticeable is the increase of
Au concentrations with depth in individual soil profiles.

5.2.8 Total Au concentration by size fraction

Au content of the light and heavy mineral fractions
were combined to estimate the concentration of Au within
each size fraction. Calculated Au contents of the -420+212,
-212+106, -106+53 micron size fractions are given in Table
5-10; also listed are the -53 micron Au results. All four
size fractions have similar Au concentrations. Paired t-
tests carried out between size fractions indicate that the
null hypothesis can be accepted in all cases (Table 5-11).

5.2.9 Proportion of total Au contributed from each size-density fraction

Analytical values and sample weights were used to
calculate the mass of Au present in each size-density
fraction. Table (5-12) lists the mass of Au found within
each fraction. Expressed as a percentage of the total, the

Sample	Horizon	Au (ppb)
14	A	305
15	B	390
16	C	425
41	A	200
42	B	225
43	C1	390
44	C2	595
122	A	70
123	B	120
124	C1	150
125	C2	155
127	A	55
128	B	90
129	C1	130
130	C2	120
162	A	30
163	B	55
164	C	40
186	A	45
187	B	70
188	C1	90
189	C2	95

Proximal average (ppb)	405
Distal average (ppb)	70
Contrast ratio	5.78

Table 5-9- Au concentration of the -53 micron fraction. Proximal and distal averages calculated by averaging the Au contents of the respective B and C horizons. Contrast ratios calculated by dividing the proximal average by the distal average.

Sample	Horizon	Size Fraction			
		−420+212	−212+106	−106+53	−53
14	A	90.55	222.05	260.85	305
15	B	622.39	92.71	300.14	390
16	C	156.19	241.01	787.57	425
41	A	122.14	296.93	249.93	200
42	B	125.51	271.04	374.55	225
43	C1	268.52	506.26	232.61	390
44	C2	109.71	582.58	547.02	595
122	A	32.39	40.59	53.94	70
123	B	1015.58	110.57	148.38	120
124	C1	75.10	96.28	135.69	150
125	C2	64.33	250.76	160.79	155
127	A	46.64	65.71	87.86	55
128	B	49.49	51.10	167.22	90
129	C1	39.40	49.23	121.29	130
130	C2	66.18	107.75	205.03	120
162	A	20.00	186.86	33.86	30
163	B	12.15	74.09	95.33	55
164	C	10.22	11.09	10.90	40
186	A	33.83	70.41	66.87	45
187	B	64.60	90.24	129.32	70
188	C1	49.32	48.57	107.20	90
189	C2	41.15	40.88	68.77	95
Proximal average (ppb)		257.3	338.7	448.4	405
Distal average (ppb)		35.4	52.9	82.2	70
Contrast ratio		7.26	6.40	5.45	5.78

Table 5-10 – Calculated Au concentration (ppb) by size fraction. Proximal and distal averages calculated by averaging the Au contents of the respective B and C horizons. Contrast ratios calculated by dividing the proximal average by the distal average.

	-420+212	-212+106	-106+53	-53
-420+212	–	–	–	–
-212+106	-.310	–	–	–
-106+53	-.962	-1.194	–	–
-53	-.637	-.736	1.077	

$$t_{(21,0.05)} = 1.72$$

Table 5-11 – Paired t-test results on comparisons of total Au contents of different size fractions.

Sample	Soil Horizon	Size Fraction −420+212 L	−420+212 H	−212+106 L	−212+106 H	−106+53 L	−106+53 H	−53	Total
14	A	15.9	5.9	17.1	51.4	7.3	53.8	403.8	555.3
15	B	31.9	168.4	20.9	8.7	12.5	52.5	506.5	801.4
16	C	47.1	18.1	29.8	52.9	20.1	165.4	478.7	812.2
41	A	23.4	6.9	13.6	66.3	6.5	40.1	220.8	377.7
42	B	26.7	12.4	13.0	58.0	5.9	53.1	315.8	484.8
43	C1	29.8	84.4	20.8	116.9	17.8	49.9	546.4	866.0
44	C2	38.9	14.3	48.6	174.9	21.9	115.5	641.8	1055.0
122	A	3.8	0.9	6.1	0.9	2.3	4.7	59.0	77.7
123	B	15.7	328.3	14.9	21.1	8.9	25.8	186.5	601.3
124	C1	22.0	1.5	13.4	11.9	5.9	17.4	165.2	237.3
125	C2	26.8	3.9	31.2	84.5	8.0	36.4	318.2	509.4
127	A	9.2	1.5	4.3	11.6	2.9	11.7	72.3	113.5
128	B	8.8	0.9	6.4	4.3	4.6	17.3	105.0	147.3
129	C1	7.3	0.9	7.4	1.2	3.5	13.6	124.8	158.6
130	C2	14.0	1.2	9.0	10.1	3.3	21.1	107.1	165.6
162	A	2.4	0.3	3.2	29.6	2.5	1.2	32.5	71.7
163	B	1.9	0.6	3.1	9.6	1.1	9.8	43.4	69.5
164	C	2.5	0.1	2.3	0.3	2.0	0.1	39.0	46.3
186	A	3.4	0.3	5.6	6.9	2.2	6.0	51.6	76.0
187	B	4.9	2.4	6.3	9.9	3.6	14.6	87.0	128.6
188	C1	4.0	0.3	4.8	0.6	3.7	7.5	81.2	101.9
189	C2	4.8	1.6	5.1	1.2	3.5	5.7	111.0	132.9

Table 5-12 – Calculated mass (micrograms) of Au in each size and / or density fraction.

proportion of Au in each fraction is listed in Table (5-13).
The majority of the Au is found in the -53 micron fraction,
ranging from 31% to 84.3%. Au content of the light mineral
fractions amount to only 1% to 9% of the whole. Conversely,
heavy mineral Au contents display a wide range of Au
content, from 0.1% to 55%. No consistent changes occur in
the partitioning of Au between the light and heavy mineral
fractions with depth. Examination of contrast ratios (Table
5-13) indicates that with increasing distance from the
minesite, the percentage of Au within the heavy mineral
fractions decrease. The percentage of Au in the finer light
mineral fractions (-212+106 and -106+53 micron) and the -53
micron fraction increases with distance, whereas the
proportion of Au within the -420+212 micron light mineral
fraction decreases with distance.

5.2.10 Comparison of light and heavy density fractions of each size fraction

The proportion of Au in the light and heavy density
fractions of the -420+212, -212+106 and -106+53 micron size
fractions are shown in Table (5-14). Comparison of the light
and heavy mineral fractions shows that differences in Au
content between the two fractions increase with decreasing
grain size. Au in the -420+212 micron fraction is
concentrated in the light mineral fraction, which contains

Sample	Soil Horizon	Size Fraction						
		-420+212 L	H	-212+106 L	H	-106+53 L	H	-53
14	A	2.9	1.1	3.1	9.3	1.3	9.7	72.7
15	B	4.0	21.0	2.6	1.1	1.6	6.5	63.2
16	C	5.8	2.2	3.7	6.5	2.5	20.4	58.9
41	A	6.2	1.8	3.6	17.6	1.7	10.6	58.5
42	B	5.5	2.6	2.7	12.0	1.2	10.9	65.1
43	C1	3.4	9.8	2.4	13.5	2.1	5.8	63.1
44	C2	3.7	1.4	4.6	16.6	2.1	10.9	60.8
122	A	4.9	1.1	7.8	1.2	3.0	6.0	76.0
123	B	2.6	54.6	2.5	3.5	1.5	4.3	31.0
124	C1	9.3	0.6	5.7	5.0	2.5	7.3	69.6
125	C2	5.3	0.8	6.1	16.6	1.6	7.1	62.6
127	A	8.1	1.3	3.8	10.2	2.6	10.3	63.7
128	B	6.0	0.6	4.3	2.9	3.1	11.8	71.3
129	C1	4.6	0.6	4.7	0.8	2.2	8.6	78.7
130	C2	8.4	0.7	5.4	6.1	2.0	12.7	64.7
162	A	3.4	0.4	4.4	41.3	3.5	1.7	45.4
163	B	2.7	0.8	4.5	13.8	1.5	14.1	62.5
164	C	5.4	0.2	5.0	0.7	4.2	0.1	84.3
186	A	4.5	0.4	7.3	9.1	2.8	7.9	67.9
187	B	3.8	1.9	4.9	7.7	2.8	11.3	67.6
188	C1	3.9	0.3	4.7	0.6	3.6	7.3	79.6
189	C2	3.6	1.2	3.8	0.9	2.6	4.3	83.5
Proximal ave.		4.5	7.4	3.2	9.9	1.9	10.9	62.2
Distal ave.		3.9	0.9	4.6	4.7	2.9	7.4	75.5
Contrast ratio		1.2	8.4	0.7	2.1	0.7	1.5	0.8

Table 5-13 - Percentage of Au in each size and / or density fraction of the -420 micron fraction.

Sample	Soil Horizon	Size Fraction					
		−420+212		−212+106		−106+53	
		L	H	L	H	L	H
14	A	73.0	27.0	25.0	75.0	12.0	88.0
15	B	15.9	84.1	70.7	29.3	19.3	80.7
16	C	72.3	27.7	36.0	64.0	10.8	89.2
41	A	77.3	22.7	17.1	82.9	14.0	86.0
42	B	68.2	31.8	18.3	81.7	10.0	90.0
43	C1	26.1	73.9	15.1	84.9	26.3	73.7
44	C2	73.2	26.8	21.7	78.3	16.0	84.0
122	A	81.6	18.4	87.0	13.0	33.0	67.0
123	B	4.6	95.4	41.4	58.6	25.7	74.3
124	C1	93.5	6.5	53.1	46.9	25.4	74.6
125	C2	87.4	12.6	27.0	73.0	19.9	80.1
127	A	85.9	14.1	27.0	73.0	18.0	82.0
128	B	90.8	9.2	60.0	40.0	21.0	79.0
129	C1	89.3	10.7	86.0	14.0	20.7	79.3
130	C2	92.3	7.7	47.0	53.0	13.4	86.6
162	A	89.6	10.4	9.7	90.3	68.1	31.9
163	B	76.4	23.6	24.5	75.5	9.8	90.2
164	C	96.4	3.6	88.5	11.5	97.4	2.6
186	A	91.4	8.6	44.7	55.3	26.4	73.6
187	B	66.6	33.4	39.1	60.9	20.0	80.0
188	C1	93.4	6.6	88.3	11.7	33.0	67.0
189	C2	74.8	25.2	80.7	19.3	38.1	61.9
Proximal average		51.1	48.9	32.4	67.6	16.5	83.5
Distal average		81.5	18.5	64.2	35.8	39.7	60.3
Contrast ratio		0.6	2.7	0.5	1.9	0.4	1.4

Table 5-14 − Distribution of Au between the light and heavy fractions of each size fraction. All values in percent.

(on average) 74% of the Au. Nineteen of twenty-two -420+212

micron samples contain more Au in the light fraction than in

the heavy fraction. Heavy mineral proportions of Au in three

-420+212 micron samples (15, 43, 123) are higher than the

remaining samples by a factor of two, but due to the coarse

grain size, this is likely a result of nugget effect. Eight

of twenty-two -212+106 micron samples contain a greater

proportion of Au in the lights than in the heavies, whereas

only two of the -106+53 micron samples display the same

tendency. Thus, the largest proportion of Au within the

three size fractions shifts from the light fraction (-

420+212 micron) to the heavy fraction (-106+53 micron) with

decreasing grain size (Figure 5.15).

With increasing distance of transport, the proportion

of Au shifts from the heavy to light mineral fraction for

each size fraction (Figure 5.15). No consistent changes with

depth in the proportional distribution of Au between light

and heavy density fractions of individual size fractions are

present.

5.2.11 Number of gold particles in each size fraction

Estimates of the number (N) of gold particles present

in each sample size fraction were made by assuming that each

size fraction contained spherical gold grains with a
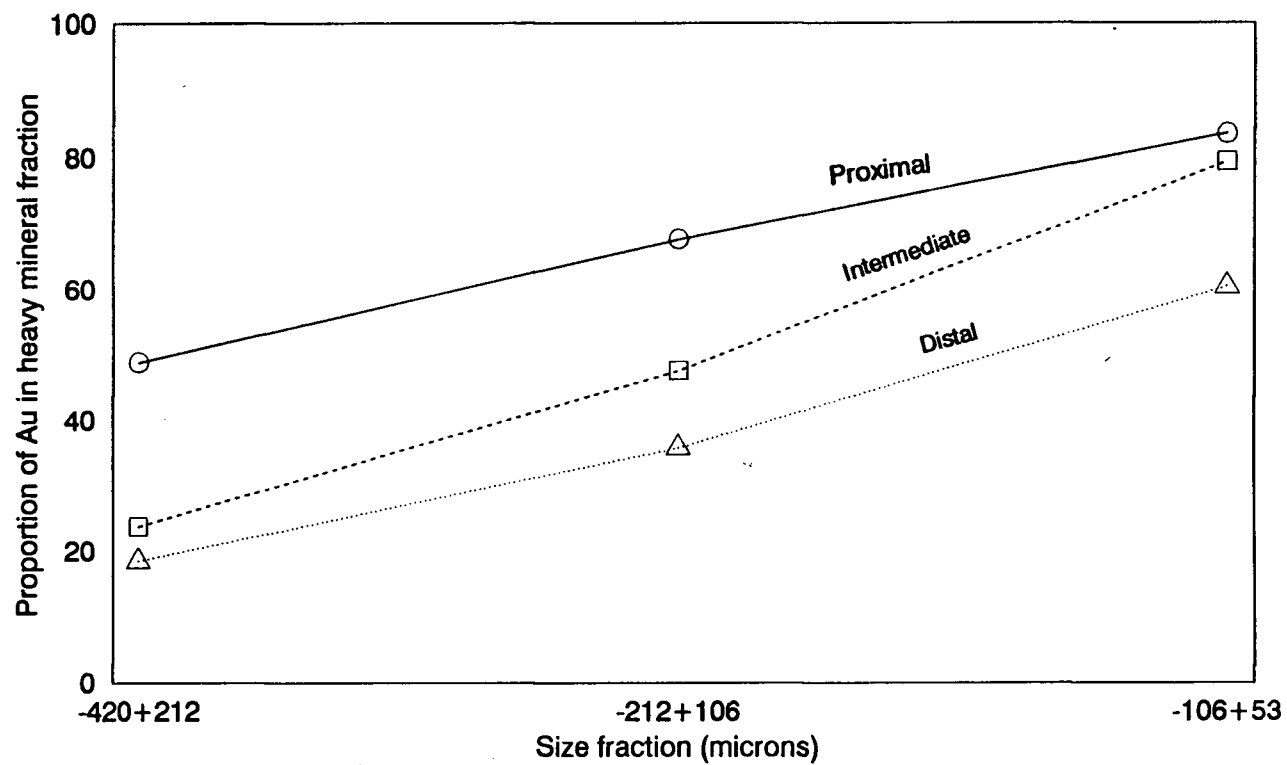
Figure 5.15 - Proportion of Au within the heavy mineral fraction of each size fraction. Points calculated using data from the B and C horizons of the Proximal, Intermediate and Distal pits.

diameter equal to the geometric mean of the bounding sieve diameters. Averaged measurements of gold grain shapes extracted from the -212+53 micron fraction of selected samples indicated a nearly spherical grain shape (see section 5.4). Based upon the results of electron microprobe analysis of grain cores (section 5.5), a density of 15.45 g/cm^3 was assumed, corresponding to a fineness of 700.

Table 5-15a and Table 5-15b list the calculated number of gold grains (per analysed sample weight and per 30 gram subsample, respectively) in the -420+212, -212+106, -106+53 micron heavy mineral fractions. Also listed are the calculated number of gold grains found within the -53 micron fraction, assuming that all Au within this fraction occurs as free gold grains 50 microns in diameter. The number of gold grains in each heavy mineral sample increases with decreasing grain size. In all fractions, proximal samples (14, 15, 16, 41, 42, 43, 44) contain more grains than the intermediate or distal samples. None of the samples contain more than the minimum number of gold grains (20) required to insure a precision of 50% (Clifton, et al., 1969).

5.3 Cyanide extraction results

Analyses of cyanide extracted Au carried out on splits of the -53 micron fraction are shown in Table 5-16. Au

Sample	Horizon	-420+212	-212+106	-106+53	-53
14	A	0.0	0.9	9.4	9.1
15	B	0.3	0.1	7.7	11.6
16	C	0.0	0.6	19.5	2.6
41	A	0.0	1.2	8.6	5.9
42	B	0.0	1.0	12.0	6.7
43	C1	0.1	1.7	6.4	11.6
44	C2	0.0	1.8	14.9	17.7
122	A	0.0	0.0	0.4	0.0
123	B	0.9	0.4	6.4	3.6
124	C1	0.0	0.3	5.1	4.5
125	C2	0.0	1.3	6.9	4.6
127	A	0.0	0.4	3.5	1.6
128	B	0.0	0.2	5.1	2.7
129	C1	0.0	0.0	4.0	3.9
130	C2	0.0	0.4	6.2	3.6
162	A	0.0	1.1	0.4	0.9
163	B	0.0	0.4	2.9	1.6
164	C	0.0	0.0	0.0	1.2
186	A	0.0	0.3	1.8	1.4
187	B	0.0	0.4	4.3	2.1
188	C1	0.0	0.0	2.2	2.7
189	C2	0.0	0.0	1.7	2.8
Proximal average		0.0	1.0	12.1	10.0
Distal average		0.0	0.2	2.2	2.1
Contrast ratio		0.0	5.0	5.5	4.8

Table 5-15a- Calculated number of gold grains in each heavy mineral size fraction and the -53 micron fraction per weight of analyzed sample (30 gram maximum). Anomalous and background averages calculated by averaging the Au contents of the respective B and C horizons. Grain sizes for the heavy mineral concentrates are assumed to be equivalent to the geometric mean of the bounding sieve diameters. Grain size of the -53 micron fraction is conservatively estimated to be 50 microns, approximately the upper grain size limit.

Sample	Horizon	-420+212	-212+106	-106+53	-53
14	A	0.0	.9	9.4	9.1
15	B	0.3	0.1	7.7	11.6
16	C	0.0	0.6	19.5	12.6
41	A	0.0	1.2	8.6	5.9
42	B	0.0	1.0	12.0	6.7
43	C1	0.1	1.7	6.4	11.6
44	C2	0.0	1.8	14.9	17.7
122	A	0.0	0.0	2.9	2.1
123	B	0.9	0.4	6.4	3.6
124	C1	0.0	0.3	6.5	4.5
125	C2	0.0	1.3	6.9	4.6
127	A	0.0	0.5	4.9	1.6
128	B	0.0	0.2	9.4	2.7
129	C1	0.0	0.0	5.2	3.9
130	C2	0.0	0.4	18.7	3.6
162	A	0.0	1.9	1.2	0.9
163	B	0.0	0.7	12	1.6
164	C	0.0	0.0	0.0	1.2
186	A	0.0	0.4	3.7	1.3
187	B	0.0	0.5	6.7	2.1
188	C1	0.0	0.0	5.5	2.7
189	C2	0.0	0.0	3.0	2.8
Proximal average		0.0	1.0	12.1	12.0
Distal average		0.0	0.3	5.4	2.1
Contrast ratio		0.0	3.3	2.2	5.7

Table 5-15b - Calculated number of gold grains in each heavy mineral size fraction and the -53 micron fraction per 30 gram sample weight. Proximal and distal averages calculated by averaging the Au contents of the respective B and C horizons. Grain sizes for the heavy mineral concentrates are assumed to be equivalent to the geometric mean of the bounding sieve diameters. Grain size of the -53 micron fraction is conservatively estimated to be 50 microns, approximately the upper grain size limit.

Sample	Horizon	Cyanide Extracted Au (ppb)	Residual Au (ppb)	% Au Extracted
14	A	90	45	66.7
15	B	450	145	75.6
16	C	350	105	76.9
41	A	95	145	39.6
42	B	130	115	53.1
43	C1	370	115	76.3
44	C2	510	145	77.9
122	A	<15 (7.5)	20	27.3
123	B	145	35	80.6
124	C1	145	35	80.6
125	C2	145	35	80.6
127	A	145	35	80.6
128	B	80	15	84.2
129	C1	175	45	79.5
130	C2	110	65	62.9
162	A	<15 (7.5)	20	27.3
163	B	65	15	81.25
164	C	<15 (7.5)	5	60.0
186	A	30	5	85.7
187	B	110	40	73.3
188	C1	80	15	84.2
189	C2	130	25	83.9
Proximal average (ppb)		362	125	72.0
Distal average (ppb)		80	20	76.5
Contrast ratio		4.6	6.3	0.9

Table 5-16 - Cyanide extractable Au and residual Au contents of the -53 micron fraction. (% Au Extracted = cyanide extractable Au/(cyanide extractable + residual Au)). For calculations , one-half the detection limit was used for results below detection limit.

values range from <15 to 510 ppb for cyanide extractable Au whereas the sample residues (material remaining after cyanide leaching) contain 5 to 145 ppb Au. Comparison of the results with "total Au" FA-AAS analyses of representative -53 micron sample splits (see section 5.2.6) reveals several interesting patterns. Except for three low analyses (<15 ppb), cyanide extracted Au results have a comparable distribution of values to those analysed for total Au by FA-AAS (Figure 5.16), including a high correlation coefficient of r = 0.902. On average, cyanide leaching extracted 70% of the gold within the -53 micron samples. The mean extraction efficiency of A horizon soils is 54%, while B and C horizon soils have a higher mean efficiency of 76%. With the exception of three A horizon samples (41, 122 and 162) and one C horizon sample (164), the Au contents of the sample residues are less than the cyanide extracted Au concentrations.

5.4 Grain morphology

Scanning electron microscopy was used to study the morphological characteristics of free gold grains extracted from select samples. Samples were chosen to represent the complete soil profiles of two pits: one proximal (Pit #6) and one distal (Pit #38) to the minesite. Axial dimensions of each gold grain were measured from photographs and
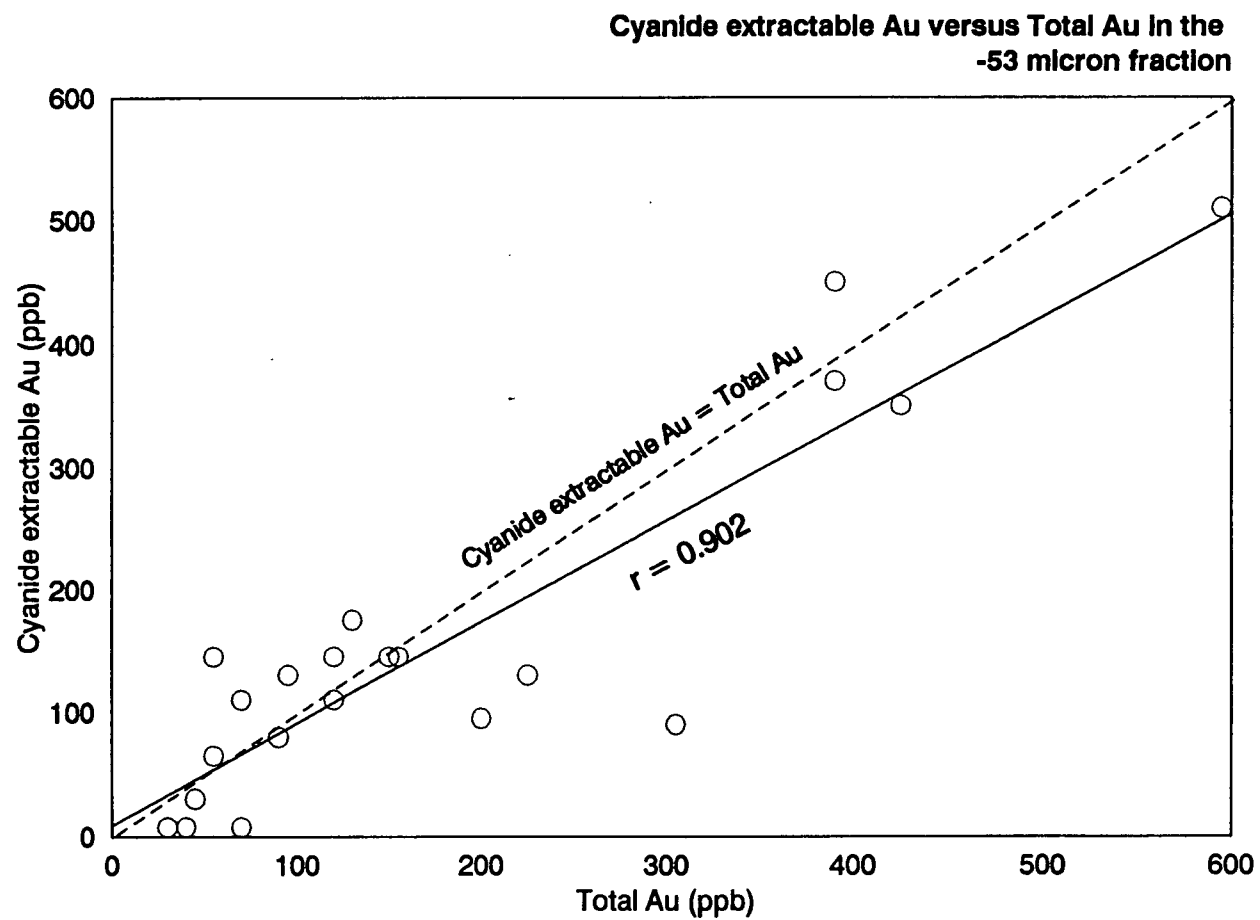
Figure 5.16 - Cyanide extractable Au versus Total Au (FA-AAS), -53 micron fraction.

directly from SEM imagery. Axial measurements of each grain are listed in the Appendix. Grain shape was determined using two methods; quantitatively, using an arbitrary shape factor, and qualitatively, using a system of grain classification developed by Averill and Zimmerman (1984) and modified by DiLabio (1989).

Calculation of a shape factor for each grain was carried out using a formula similar to the Cory shape factor (Cory, 1949) but modified to allow for the identification of long, cylindrical particles (Day, 1988). The ratio used is :

$$SF = (dS*dL)^{-1/2}/dX \qquad (5-4)$$

where dS, dX and dL are the smallest, intermediate and longest diameters respectively (Day, 1988). An SF value of 1 will represent a sphere, SF>1 represents long cylindrical particles ("needles"), and SF<1 represents flat cylindrical particles ("flakes").

Modelling of the population distribution with a probability plot (Figure 5.17) indicates that three separate populations of grain shapes can be defined. Population 1 has a mean SF = 0.678 (standard deviation = 0.161) and comprises 49.4% of the grains. This corresponds to a disc shaped grain
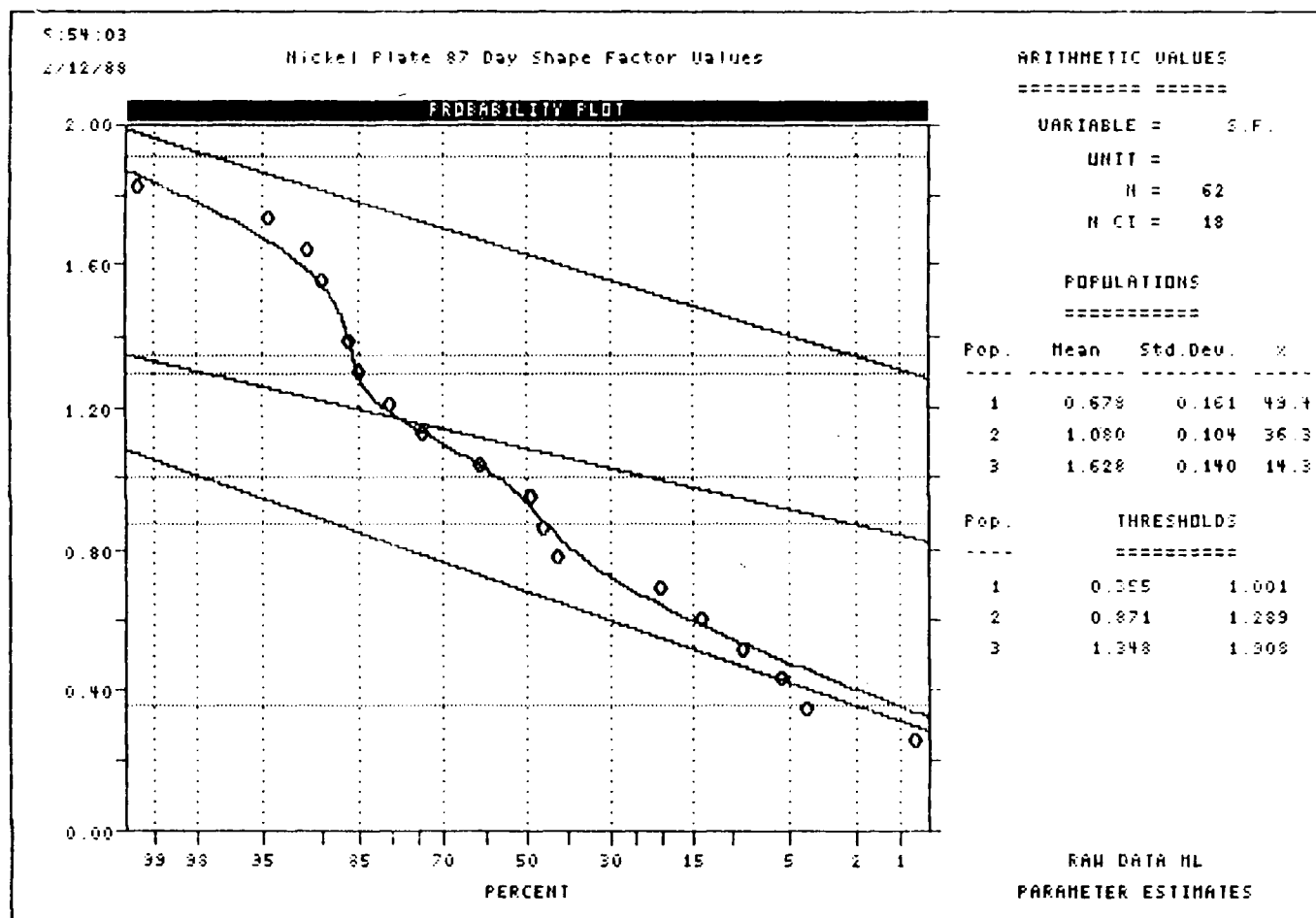
Figure 5.17 - Probabiliity plot of shape factor values.

with a diameter to thickness (largest to smallest diameters) ratio of 2.18. Grains found within the Population 2 group have a mean SF = 1.080 (standard deviation = 0.104) and compose 36.3% of the grains. The mean grain shape for this group is spherical, with a mean ratio of largest to smallest diameters of 1.16. Population 3 grains make up 14.3% of the grains and have a mean SF = 1.628 (standard deviation = 0.140). For all particles (n = 62), the mean SF is 0.950 (standard deviation = 0.365), which is equivalent to a nearly spherical particle.

Shape factor data by horizon for the proximal pit is shown in Table 5-17. Shape factors generated for the distal pit grains are not considered due to the low number of grains recovered from each horizon (eight grains total). Means and standard deviations of each horizon are very similar to the mean and standard deviation of the entire sample set. Analysis of variance carried out on the data (horizon vs. horizon) indicates that at the 95% confidence level, the null hypothesis is accepted in all cases (Table 5-18). Comparison of shape factors between the proximal and distal pits was also performed using analysis of variance. In this instance, a comparison was made between all proximal pit grains (54) and all distal pit grains (8). Results of the analysis of variance (Table 5-19) reveals that the null hypothesis is valid at the 95% confidence level.

Horizon	Number of Grains	Shape Factor Mean	Standard Deviation
A	19	.933	.372
B	19	.979	.375
C	15	.931	.417
Totals	53	.949	.379

Table 5-17 – Shape factor data, proximal pit grains.

Group	Mean	N
1	.933	19
2	.979	19
3	.931	15
Grand mean	.949	53

Source of Variation	Sum of Squares	Degrees of Freedom	Mean Square
Between groups	.026	2	.013
Within groups	7.466	50	.149
Total	7.492	52	

$$F_{calc} = 0.088; \quad F_{(2,60,0.05)} = 3.15$$

Null hypothesis accepted

Table 5-18 - Analysis of variance results on shape factors, by horizon.

Group	Mean	N
1	.963	56
2	.854	7
Grand mean	.951	63

Source of Variation	Sum of Squares	Degrees of Freedom	Mean Square
Between groups	.074	1	.074
Within groups	8.065	61	.132
Total	8.139	62	

$$F_{calc} = 0.56; \quad F_{(1,60,0.05)} = 4.00$$

Null hypothesis accepted

Table 5-19 - Analysis of variance results on shape factor values for proximal versus distal grain shapes.

Qualitative assessment of grain shape was conducted using a three-tiered categorical system developed by S.A. Averill (Averill and Zimmerman, 1986; Averill, 1988; Sopuck, et.al., 1986) and modified by DiLabio (1989). Table (5-20) lists the three shape classes and their accompanying shape and textural characteristics. Using SEM photographs, the sixty-two grains from both pits were classified as being either pristine, modified or reshaped. The Appendix lists the results of this evaluation. Tests of significance carried out using the Chi-squared distribution (Table 5-21) indicate that no difference in shape exists between horizons or between the proximal and distal pits.

5.5 Electron microprobe data

Results of electron microprobe Au, Ag analyses of the cores of 41 sectioned gold grains are presented in Table (5-22). Also listed are the corresponding Au and Ag analyses for twenty-three grain edges. All grains were analysed for Au, Ag, Cu and Hg. Cu and Hg analyses generally are less than their respective detection limits (Cu: 0.025%; Hg: 0.65%) and therefore cannot be considered reliable. Wide ranges in gold composition are present within the analysed grains. Fineness (the ratio of Au/(Au+Ag) X 1000) ranges from 999.7 (pure gold) to 379.5 (Ag-rich electrum). Mean fineness for the 41 grain cores is 698.6 (standard deviation

Type	Shapes	Surface Textures
Pristine	block rod wire leaf crystal star globule	-smooth surfaces -grain molds clearly visible -thin edges not curled -some striae
Modified	all shapes, damaged	-primary shapes visible -leaf edges and wires bent -blunted and thickened edges -grain molds preserved where protected -some striae -felty texture when damaged

Reshaped	folded rod,
	wire, flake
	rounded blocks
	typical discoid
	placer flake
		-primary shapes visible
		-well rounded grain outline
		  -some striae
		  -porous, scaly, felty, or
		  spongy

Table 5-20 – Classification of shapes and surface textures of gold grains. Reproduced from DiLabio (1989).

Proximal Pit

Horizon	Pristine	Modified	Reshaped	Totals
A	6	8	5	19
B	4	11	4	19
C	3	5	8	16
Totals	13	24	17	54

$X^2 = 4.69$ $X^2_{(4,0.05)} = 9.48$

No significant difference

Distal vs Proximal Pits

Pit	Pristine	Modified	Reshaped	Totals
Distal	1	3	4	8
Proximal	13	24	17	54
Totals	14	27	21	62

$X^2 = 1.19$ $X^2_{(2,0.05)} = 5.99$

No significant difference

Table 5-21 - Results of gold grains classified using the Averill (1988) and DiLabio (1989) system for qualitative grain evaluation. Included are Chi-squared tests of significance at the 95% confidence level.

Grain Number	Core Au	Core Ag	Edge Au	Edge Ag
23-02	74.74	24.88	70.74	28.93
23-04	57.57	41.86	59.36	40.37
23-05	61.86	37.57	66.98	33.04
23-09	63.03	36.40	62.75	36.53
23-11	60.10	39.40	-	-
23-12	55.99	43.09	-	-
23-13	93.17	6.44	-	-
23-14	90.77	7.30	92.54	7.335
23-15	45.10	54.47	45.32	54.27
23-17	73.26	26.42	-	-
24-02	58.95	40.56	57.05	42.43
24-11	37.54	61.38	-	-
24-13	91.29	8.27	-	-
24-16	78.49	21.11	78.04	21.37
24-18	73.12	26.51	-	-
24-19	64.49	35.03	63.00	36.83
24-01	92.63	6.77	-	-
24-04	89.83	9.61	-	-
24-06	41.80	57.64	-	-
24-14	89.97	9.44	89.77	9.40
24-17	79.51	20.07	-	-
25-01	93.85	5.82	-	-
25-02	75.34	24.09	-	-
25-03	80.68	18.73	81.17	19.21
25-05	38.56	60.87	37.87	61.40
25-06	62.27	36.98	61.43	37.76
25-07	46.70	52.57	43.01	55.82
25-09	91.50	8.29	-	-
25-10	99.21	0.03	98.39	0.08
25-11	86.38	13.07	86.41	12.95
25-12	38.91	60.50	-	-
25-13	49.11	50.21	48.05	50.78
25-14	61.20	38.46	61.11	38.28
25-16	68.12	31.37	68.18	31.44
25-17	77.08	22.80	76.91	22.52
181-01	41.86	57.58	-	-
181-03	44.60	53.66	44.48	54.07
182-02	99.66	0.06	-	-
183-02	86.23	36.51	-	-
183-03	184-0	11.26	88.05	11.68
184-02	68.70	30.43	69.59	29.83

Table 5-22 - Results of electron microprobe analyses on the cores and edges of 41 gold grains.

= 189.3), whereas the mean fineness of the 23 edges is 677.8
(standard deviation = 171.7). Examination of the 41 grain
sections using backscatter electron imaging revealed the
presence of minor, patchy rimming along the edges of seven
grains. An eighth grain (25-5) displayed a complete Ag-poor
rim. Comparison of core and edge compositions shows
excellent correlations for core Au / rim Au (0.994) and core
Ag / rim Ag (0.996).

No changes are observed in core composition between the
proximal and distal pits. Figure (5.18) shows the
scatterplot distribution of Au, Ag grain core values for
both the proximal and distal pits: the distal pit values
(six total) plot evenly along the linear trend with no
apparent bias towards a particular composition. Similarily,
no variation in grain edge or grain core Au-Ag composition
is observed with change in soil profile depth (Figures 5.19
and 5.20).
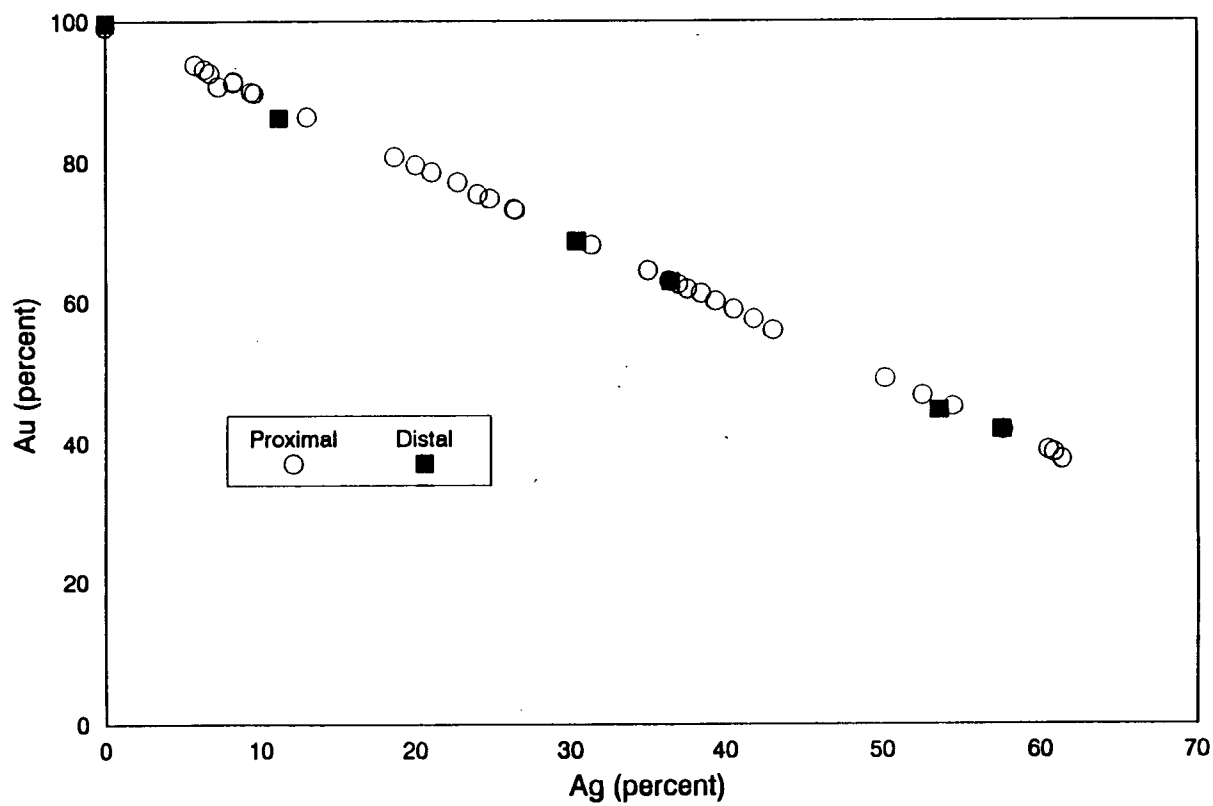
Figure 5.18 - Plot of core Au vs core Ag analyses, Proximal and Distal pits.
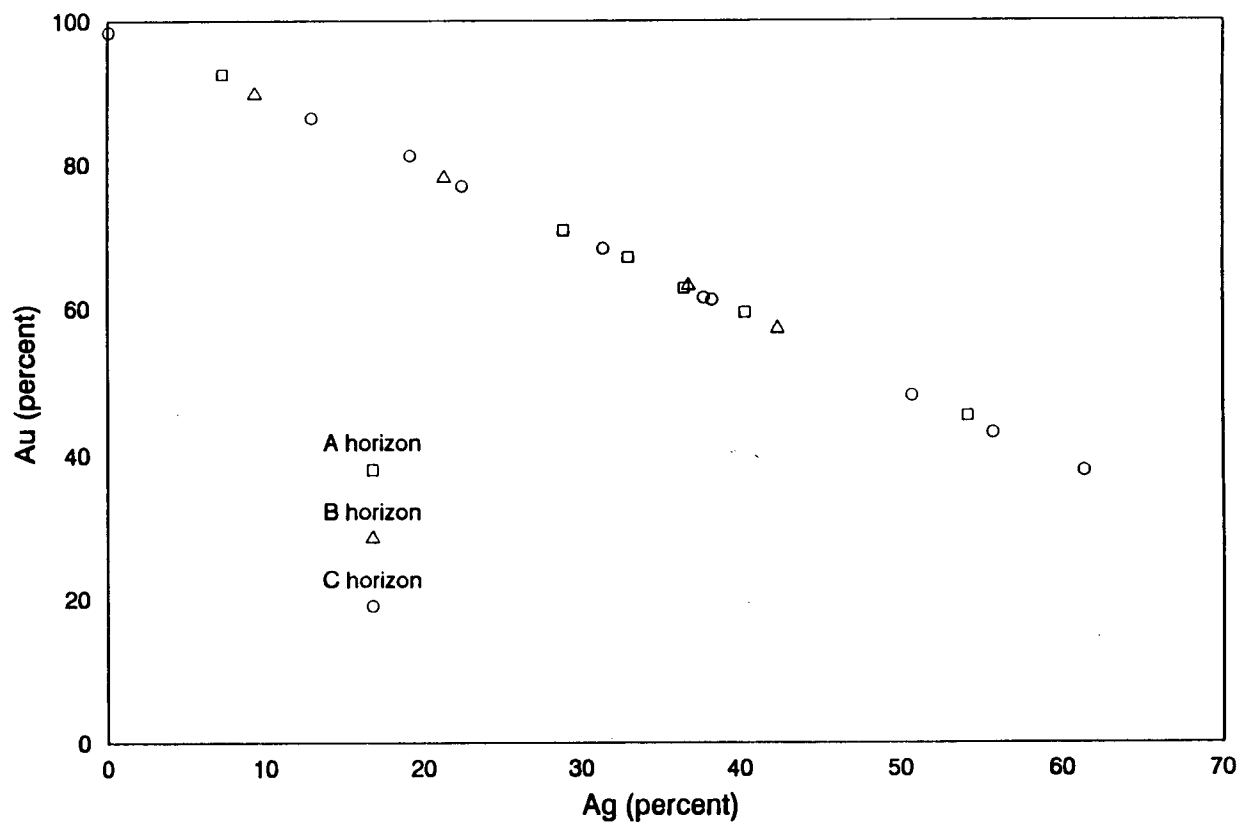
Figure 5.19 – Plot of edge Au vs edge Ag analyses of the A, B and C horizons, Proximal pit.
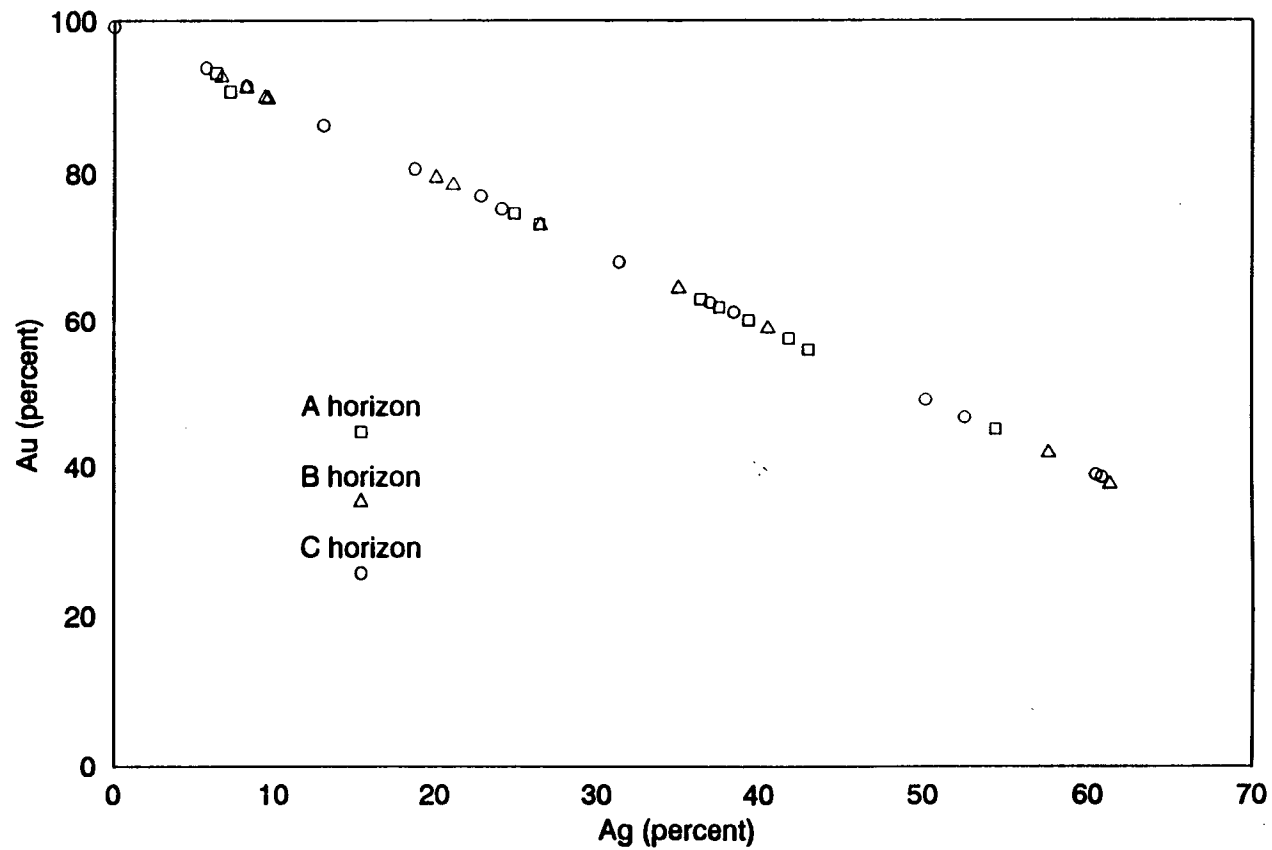
Figure 5.20 - Plot of core Au vs core Ag analyses of the A, B and C horizons, Proximal pit.

Chapter Six

Discussion

6.1 <u>Gold grain shape and composition</u>

The effect of soil formation on the morphology and composition of gold grains in temperate environments is poorly understood. Work by Freyssinet et.al. (1989), Mann (1984), Webster and Mann (1984), and Wilson (1984) has dealt with gold in lateritic or saprolitic tropical environments. Investigations of gold shape in temperate environments have been restricted to studies of gold grains in till with an emphasis on the effects of glacial transport (Averill and Zimmerman, 1984; Sauerbrei et al., 1987; Thorleifson and Kristjansson, 1988). MacEachern and Stea (1985) carried out detailed work on the shape and composition of gold grains extracted from tills downice from gold mineralization, but did not investigate the overlying soil layers. Comparison with these data sets is therefore difficult.

At the Nickel Plate mine, the similarity in composition of the gold grain cores and rims between soil profiles is in contrast to the results found within tropical lateritic soil profiles. Within lateritic soils, dissolution, upwards transport and reprecipitation of Au results in the formation of pure Au crystals, grains or nuggets. The chemically intense nature of laterite formation over long (several Ma) periods versus the short (10 Ka) duration of chemical activity associated with soil formation at the Nickel Plate

mine obviously is a major factor in gold grain behaviour. Ag depleted rims, seen in lateritic profiles and a common feature of placer gold, are not prevalent. Only one grain displayed a complete rim, whereas five other grains showed minor rimming. It is likely that the scarcity of rimming is a result of the non-chemical (ie. mechanical) transport of the grains, and their limited residence time within the till. However, it is also possible that abrasion of the grains during transport has removed any developed rims.

Use of gold grain shape to estimate transport distance is difficult due to the low number of grains removed from the two soil profiles (Proximal pit, 54 grains; Distal pit, 8 grains). However, the abundance of the grains between the two pits is a relative indicator of proximity to the minesite. The different distances of transport between the two pits cannot be determined through the use of a quantitative shape factor (equation 5-4), possibly because of the low number of grains in the distal pit, and likely because no difference exists. Application of a simple, qualitative method of grain shape classification (Dilabio, 1989; Sauerbrei, et.al, 1987) also indicates that no difference exists in grain shape with either increased transport distance or location within the soil profile. However, the small population size for the A, B and C horizons (n= 19, 19, 16 grains, respectively) may influence these results.

6.2 <u>Residence sites of Au in soil and till</u>

Size fraction analysis of twenty-two samples indicates that total Au content remains constant with decreasing grain size (Table 5-10). Analysis of light and heavy mineral fractions for the -420+212, -212+106 and -106+53 micron size fractions indicates that a significant proportion of the Au (10 to 175 ppb) is concentrated within the light fraction, as inclusions of fine gold grains (Table 5-8).

Increase in the Au content of the heavy mineral size fraction with diminishing grain size is a function of the abundance of free gold grains within the heavy mineral fraction. Au concentrations of the -420+212 micron light and heavy mineral fractions are equivalent (Tables 5-7 and 5-8), indicating that no free gold exists within the heavy mineral fraction (Table 5-15). Concentration of Au within the -212+106 and -106+53 micron heavy mineral fractions increase with decreasing grain size. This is a reflection of the distribution of gold grain sizes within the deposit, the effects of glacial abrasion upon the orebodies during glaciation and the effect of comminution on the entrained clasts during glacial transport.

Results of cyanide extraction on the -53 micron samples reveal that approximately 70% of the Au exists as free gold grains or as gold weakly bound to clays / secondary iron

oxides. A lower average extraction efficiency of 54% for Au

from the A horizon samples is likely due to the higher

organic content of these samples relative to the B and C

horizons. Organic (carbonaceous) material is known to impede

the efficiency of the cyanide extraction process for Au

(Avraamides, 1982).

Paired t-tests carried out on the Au content of each

size fraction (light and heavy fractions combined) indicate

that all size fractions have a similar Au concentration.

These results are in disagreement with the work of DiLabio

(1982a, 1982b, 1985 and 1988) who studied the size fraction

distribution of Au within several till dispersion trains

associated with gold mineralization. Au analysis was carried

out on ten to fifteen gram subsamples of size fractions

sieved from a field sample of unspecified weight. Size

fractions greater than 63 microns in diameter were ground to

-63 microns prior to analysis (DiLabio, 1988). No attempt

was made to separate and analyse the heavy mineral fraction

of each size fraction. From this, DiLabio (1982a, 1982b,

1985 and 1988) concluded that Au concentrations were

enriched in the finer fractions of the tills, possibly

through hydromorphic redistribution. However, as shown in

section 1.3, use of undersized coarse sample fractions will

impart a strong bias on the analytical results. Coarse

grained fractions which are not representative will

consistently return Au contents lower than their true

concentrations, due to the low probability of encountering a
gold grain (or grains) within the sample. Finer fractions,
having a more representative distribution of gold grains,
will return Au values more characteristic of the true
concentration of the size fraction. The end result will be
the perception of an increase in Au content with decreasing
grain size. Use of heavy mineral concentration techniques on
large samples can alleviate this problem by concentrating
all free gold grains within a single analytical subsample.
Analysis of the heavy mineral concentrate, combined with an
analysis of the light mineral fraction, will give a result
with a significantly higher degree of representivity.

6.3 Variation of Au concentration with depth

Within soil profiles, Au concentrations of the -212
micron fraction increase with depth. Increases in Au content
with depth are also noted for the -53 micron fraction, the -
212+106 micron light mineral fraction and the -106+53 micron
light mineral fraction. No comparable patterns are observed
with the -420+212 micron light mineral fraction or the heavy
mineral size fractions. Except for the samples of pit 10
(sample #'s: 41, 42, 43, 44), results obtained from cyanide
extraction do not display a consistent pattern of Au
increase with depth.

Several possible mechanisms exist to explain the increase down profile of Au within soils. These mechanisms can be separated into two categories: i) primary agents (those occurring during the deposition or immediately after the deposition of the till) and ii) secondary agents (modification of the Au content of the till by soil forming processes which occur after deposition).

i) Primary Agents (Glacial/Periglacial)

Features of this category involve processes which take place during the actual physical transport and deposition of the till beneath the glacier sole, or immediately after exposure of the till to the atmosphere, but before the onset of significant soil forming processes. An example of this would be the deposition of a non-auriferous, exotic ablation till on a basal till of local derivation. Similar results would be expected if an auriferous basal till were to be overlain by either a second, nonauriferous basal till or Au poor colluvium derived from unmineralized bedrock.

Field observations of the soil profiles, do not however support this interpretation. No significant changes were observed in gross physical characteristics of the soil profiles with depth; no paleosols, erosion layers, or changes in overall clast (grains >1 cm diameter) shape or composition were observed. Observed changes in compaction

and soil colour with depth are attributed to soil forming
processes.

No information is available on the influence
periglacial effects, such as sheetwash and cryoturbation,
could have upon the distribution of gold grains within
modern-day soil profiles. However, periglacial activity does
not appear to have altered the soil profiles of the thesis
area. Periglacial activity is generally restricted to arctic
or alpine environments where permafrost exists. As
deglaciation in the region occurred rapidly (Ryder, 1978)
and was quickly followed by temperatures warmer than the
present day (Lowdon et.al, 1971), the amount of time
available for periglacial processes to operate was limited.
Cryoturbation features were not observed within the thesis
area, although solifluction lobes were noted nearby
(approximately one kilometre distant) within a small creek
valley.

The most probable cause of the observed Au distribution
is also the simplest; the downward increase in Au content is
a primary feature related to the dispersion of Au during
glacial transport. Gold grains from the Nickel Plate mine
entrained within the glacier sole would preferentially
remain near the base of the till until sufficient new
material was incorporated to disperse the grains. A small
component of vertical mixing of the auriferous till during

transport would result in upwards dispersion of the gold grains through the till unit resulting in the observed distribution of Au values. Such models of glacial dispersal are common within the literature (Rose, Hawkes and Webb, 1979). Probability plots of the distribution of Au values for each horizon (section 5.1.5) indicate that contrast between anomalous and background populations decreases upwards through the soil profile. These differences are probably a result of vertical mixing of the till during glacial transport.

ii) Secondary Agents

Assuming that the initial concentration of Au within the basal till was uniform, then several processes exist which would account for the observed variations in Au content. Addition of organic material to the upper layers of the soil profile during soil formation would result in the dilution of the primary glacial material (till) and a commensurate decrease in the Au content. However, dilution of the upper soil horizons cannot account for the observed variations in Au content with depth. For the detailed samples, the decrease of the weight proportion with depth of -53 micron material ranges from approximately 5 to 20%. A similar range of decreasing weight proportions (8 to 30%) is observed for the -212 micron fraction. Decrease in Au concentrations within the soil profiles range from 26.1 to 58.5%, too great a range to be explained simply by dilution.

Lakin et al.(1974) suggested downward movement of gold grains within the soil profile during soil creep as a possible device for increasing Au concentrations with depth. Gradual downslope movement and the accompanying churning motion of the soils might progressively lower dense minerals, such as gold, through the soil profile by density sorting. Less dense, more readily dislodged minerals adjacent to the gold grains would be moved a greater distance during downslope movement of the soil. Repetition of this process would lead to the partial segregation of dense grains within the lower horizons of the soil profile. This process, however, cannot explain the increase in Au content of the light mineral fraction with depth nor does it explain the erratic behavior of Au in the heavy mineral fraction. Soil creep does not appear to be a cause for increased Au content with depth.

6.4 Variation of Au concentration with distance

All sample media display the same characteristic pattern of Au distribution: a decrease in concentration with increasing distance from the mine. No downice displacement of elevated Au values is observed. Displacement of the anomaly may have occurred, but as the study area begins approximately 200 meters downice of the minesite,

displacement is impossible to determine with the available data. The observed dispersal curves for the A, B, C horizon pit samples and the roadcut C horizon samples approximate negative exponential curves. These are analogous to data obtained by Shilts (1976) on the regional glacial dispersion of nickel in till from the Thetford Mines area, and Bird and Coker (1987) on the local glacial dispersion of gold in till from the Owl Creek mine, Timmins, Ontario.

Behaviour of the Au distribution of the till with increasing distance of transport can be inferred through the use of contrast ratios. Contrast ratios (the ratio of proximal to distal Au values) for various size and density fractions are shown in Table 6-1. The percent heavy mineral content contrast ratios are similar for all three size fractions (-420+212, -212+106, -106+53 microns); a decrease by a factor of approximately 3.5. Assuming that the source of heavy minerals (i.e. garnet, diopside) is restricted to zones of alteration within the Marble Line (see sections 3.4 and 3.5), then the decrease of the percentage of heavy minerals is a result of dilution. The similarity of the contrast ratios of the size fractions indicates that comminution has not significantly influenced the heavy mineral grains. Had comminution played a significant role during glacial transport, then contrast ratios would decrease with a decrease in size fraction, reflecting the preferential comminution of coarse grains into finer grains.

Sample Media	-420+212	-212+106	-106+53	-53
Percent heavy minerals	3.8	3.3	3.5	-
Percent light minerals	1.4	1.0	0.9	0.8
Au content HMF	12.5	3.9	2.2	-
Au content LMF	3.5	3.5	3.8	-
Percent Au heavy mineral fraction	8.4	2.0	1.5	-
Percent Au light mineral fraction	1.2	0.7	0.7	0.8

Table 6-1 - Contrast ratios for a variety of sample media.
Ratios are taken from Tables 5-6b, 5-7, 5-8 and 5-13. Minus
53 micron ratios are listed as a light mineral fraction, but
are assumed to contain a significant heavy mineral
component.

Contrast ratios for the Au content of the heavy mineral
fraction and the proportion of Au in the heavy mineral
fraction are all greater than one, indicating a decrease
with distance. Gold grains from the Nickel Plate mine were
dispersed within the till as they were transported downice.
However, contrary to the light mineral fraction Au
concentrations or the percentage of heavy minerals, the
contrast values of the heavy mineral fraction Au contents
also lessen with a decrease in size fraction. This decrease
in contrast values is a result of the comminution of
sulphide and / or limonite grains within the heavy mineral
fractions, reflecting the tendency for comminution to grind
down coarse grained material at a faster rate than fine
grained material. During glacial transport, these relatively
soft, coarse grained sulphides or limonitic materials were
reduced in size, liberating finer gold contained within
their matrix, thereby increasing the proportion of gold
within the finer fractions.

Nearly identical contrast ratios for the Au content of
the light mineral size fractions are a result of the nearly
identical Au concentrations of all three size fractions.
This similarity of the Au content is a manifestation of the
fine grained (<10 micron) gold, typical of the Nickel Plate
orebodies, encapsulated within grains of the light mineral
fraction. Assuming an even distribution of this fine grained
gold throughout the grains, variation of the size fraction

analysed should not alter the results. Comminution of coarse grains to smaller grain diameters also should not alter the contrast ratios. Only until the size fraction analysed is near to or less than the diameter of gold grains being analysed will significant changes in the representivity of an analysis occur. Since the contrast ratios are independent of grain size or comminution effects, then the decrease in Au content with distance is a result of dilution. The similarity of these contrast ratios to the percent heavy mineral content contrast ratios suggests that dilution is a more significant effect than comminution.

A three dimensional dispersion train, like those described by Drake (1983) or Miller (1984) is not present within the depth of till sampled. High Au values are not observed to ascend towards the surface with increasing distance from the mine. Rather, they consistently increase in value with depth (see section 5.1.3). Lack of a rising dispersion train may be due to several factors: 1) the till is thin (1 to 5 meters) and the underlying bedrock sufficiently uneven to prevent or disrupt a rising dispersion train; 2) post glacial processes have destroyed the presence of a train; or, 3) the material composing the till did not originate directly from the mineralized bedrock of the mine, but is reworked colluvium or till from pre Fraser glaciation times. It is likely that 1) and 3) are the

factors which prevented the formation of a rising dispersion train.

6.5 Origin of the dispersion train

Relationships between the shape of the dispersion train, the restriction of mineralization within the Marble Line and the local ice movement direction indicate that the dispersion train did not originate directly from the Nickel Plate mine area (see Figure 4.1). Rather, the dispersion train is offset from a direct downice path from the mine by several hundred metres. The ice which deposited the dispersion train did not flow directly over the deposit, but flowed over mineralized colluvium which originated from the mine area. A moraine located across the Cahill Creek valley, downslope from the mine, indicates that the glacier residing within the valley was stationary for a period sufficient for supraglacial till to develop. During glacial retreat, this overlying blanket of till was deposited upon the previously deposited basal till.

6.6 Recommendations for Mineral Exploration

6.6.1 Determination of a representative field sample
size

As discussed in section 1.3, the size of sample required to give a minimum precision of 50% at the 95% confidence level is one which contains 20 particles of gold (Clifton et al., 1969). Precision of an analysis varies with the number of gold grains in the sample; a decrease in the number of grains results in a reduction of the precision. Based on the work of Clifton et al. (1969), Nichol et al. (1989) demonstrated how the relative standard deviation (coefficient of variation) of a set of (50) duplicate analyses could be utilized to determine the number of gold grains within a particular sample weight, and therefore the size of sample required to contain 20 particles of gold. However, the primary goal of a geochemical soil survey is not to obtain reproducible Au analyses for each individual sample, but to reliably identify a pattern of anomalous values which reflects bedrock mineralization. Stanley and Smee (1988, 1989) demonstrated that samples containing 1 grain of gold, on average, could be used to define a geochemical soil anomaly.

A similar approach was taken here, such that the amount of -53 micron fraction soil containing 1 grain of gold was

calculated for each of the twenty-two detailed samples. The -53 micron fraction was selected as it contains approximately sixty to seventy percent (by mass) of the Au within the -420 micron fraction. Of this proportion, an average of seventy percent exists as free gold (see section 5.3). Therefore, the greatest chance of encountering a single free grain of gold will occur within the -53 micron fraction. Table (6-2) lists the calculated sample sizes containing a minimum of 1 grain of gold for the -53 micron size fraction. Also listed is the mass of -2000 micron (-2 mm) fraction containing the required amount of -53 micron material. The number of grains in the -53 micron size fraction was calculated under the very conservative assumption that all gold exists as free grains 50 microns in diameter.

Only one sample (#162) requires more than 30 grams of -53 micron material to obtain, on average, 1 grain of gold. In general, less than 30 grams of -2000 micron material is required to obtain a single gold grain in the -53 micron fraction. The maximum calculated -2000 micron sample size (63 grams) is a reasonable minimum field sample size limit; all samples are then guaranteed to contain at least 1 grain of gold, on average.

The wet sieving technique used to partition the various size fractions is up to seven times more efficient at

Sample	Horizon	# grains of gold in -53 micron fraction	mass for 1 grain in -53 micron fraction	mass for 1 grain in -2000 micron fraction
14	A	9.1	3.3	6.8
15	B	11.6	2.6	5.7
16	C	12.6	2.4	6.3
41	A	5.9	5.1	11.6
42	B	6.7	4.5	9.6
43	C1	11.6	2.6	6.4
44	C2	17.7	1.7	5.4
122	A	2.1	14.4	28.2
123	B	3.6	8.4	17.5
124	C1	4.5	6.7	16.0
125	C2	4.6	6.5	14.6
127	A	1.6	18.4	33.9
128	B	2.7	11.2	20.6
129	C1	3.9	7.8	15.5
130	C2	3.6	8.4	18.2
162	A	0.9	33.7	57.8
163	B	1.6	18.4	40.8
164	C	1.2	25.3	62.8
186	A	1.3	22.4	36.0
187	B	2.7	14.4	23.0
188	C1	2.7	11.2	17.7
189	C2	2.8	10.6	18.2

Table 6-2 - Estimates of the number of gold grains in the minus 53 micron fraction (assuming a grain diameter of 50 microns), the mass of -53 micron sample required to contain 1 grain of gold, and the mass of -2000 micron material necessary to provide the required mass of -53 micron sample. Mass of each sample is reported in grams.

extracting the -53 micron fraction than conventional dry sieving (Day, 1988). Sampling programs which utilize standard commercial labratory dry sieving techniques instead of wet sieving should increase in the amount of -2000 micron material sampled in the field to approximately 400 grams.

6.6.2 Analysis of heavy mineral concentrates versus the -53 micron fraction

Use of heavy mineral concentrates in gold exploration is a relatively common practice. Analysis of a ten or thirty gram heavy mineral concentrate derived from a bulk sample (hundreds to thousands of grams) effectively represents the analysis of the entire bulk sample, provided all the Au exists as free gold. Au retained within the light mineral fraction will not be detected through this technique. Results of heavy mineral concentrate analyses were erratic with poor definition between anomalous and background populations, undoubtedly a result of the nugget effect.

Use of the -53 micron (-270 mesh) fraction, however, was more reliable and provided better definition of anomalous and background populations. The -53 micron fraction is superior to heavy mineral concentrates (or any other sampling media) since its fine grain size reduces the nugget effect and yet still provides good contrast between

sampling sites located at proximal and distal locations from the minesite.

6.6.3 <u>Analysis by fire assay - atomic absorption versus cyanide extraction</u>

Cyanide extraction offers comparable results to those obtained through conventional FA-AAS performed on -53 micron samples. Unlike FA-AAS, cyanide extraction is incapable of analyzing for Au held within silicates; micron or submicron sized gold grains trapped within a silicate grain would not be detected. However, since seventy percent of the Au within the -53 micron fraction exists as free grains and is detectable by the cyanide extraction technique, the adverse effects of the encapsulated gold is negligible. Cyanide extraction would be more advantageous than FA-AAS on bulk samples greater than thirty grams in weight. Nugget effects would be minimized if 100 to 1000 gram samples could be analysed by cyanide extraction. However, care should be taken to exclude A horizon soils, as the higher organic content of these horizons impedes the ability of cyanide to dissolve gold.

6.6.4 Optimum method for indicating source location of
the geochemical anomaly

Attempts to use gold grain shapes to determine
transport distance and therefore, source location (Averill
and Zimmerman, 1986; DiLabio, 1989), were not successful.
Comparison of the geochemical response of the various size
and density fractions indicates that the strongest
geochemical gradient (contrast ratio) would be found by
analysis of the -53 micron C horizon fraction. The C horizon
is the unit most representative of the original, unweathered
till. Both the A and B horizons have undergone sufficient
modifications by soil forming processes to disrupt their
original Au distribution, thereby decreasing their anomalous
to background contrast. Use of the -53 micron fraction would
enhance contrast by increasing the representivity of each
sample and attenuating the chance of nugget effect.

6.6.5 Optimum field sample

Based on the above results, a field sampling program at
the Nickel Plate mine should attempt to recover samples
which will provide a minimum of 30 grams of -53 micron (ASTM
-270 mesh) material from the C horizon. In order to obtain
30 grams of -53 micron material through wet sieving, a
minimum of 63 grams of -2000 micron (ASTM -10 mesh) material

should be sampled in the field. If dry sieving techniques are to be used, then an approximate sample weight of 400 grams of -2000 micron material should be field sampled. This soil sampling technique will provide the best contrast and sample representivity of all the size and density fractions considered.

Chapter Seven

Conclusions and Recommendations

7.1 Conclusions and Recommendations

1) At the Nickel Plate mine, a gold dispersion train is hosted within a thin (<1 to 5 metre thick) unit of oxidized basal till. This dispersion train extends approximately one kilometre from the minesite and parallels the direction of local ice movement.

2) Au concentrations of the soil profiles increase with depth, while the Au content of each horizon decrease with distance. Both are primary features related to the mechanical dispersion of till during glacial transport. Post glacial soil development does not appear to have influenced the distribution of Au within the till.

3) Heavy mineral concentrates and light mineral fraction Au abundances indicate that dilution by a factor of 3.5 occurs within the till over a distance of approximately 800 metres. This is a result of the entrainment of new material into the till during glacial transport. However, Au contents of the heavy mineral size fractions indicate that gold grains are both diluted and comminuted during transport.

4) Au content of the total size fractions are equivalent; no changes in Au abundance are observed with a change in grain size.

5) Cyanide extraction - atomic absorption spectometry indicates that approximately 70% of the Au in the -53 micron fraction exists as free gold or gold weakly bound to clays and / or secondary iron oxides. Lower extraction efficiencies for A horizon samples are likely a result of higher levels of organic material within the A horizon.

6) Chemical activity has not altered the composition of gold grains found within the soil profiles. Au enriched edges (rims) are generally absent; grain core compositions are identical to grain edge Au-Ag values.

7) Compositional and / or morphological differences in gold grains are not indicative of distance of transport or location within the soil profile. However, the relative abundance of grains between locations can be used as an indicator of proximity to the minesite.

8) In order to obtain the best sample representivity and contrast between anomalous and background Au populations in the vicinity of the Nickel Plate mine, FA-AAS analysis for Au should be carried out on 30 grams of -53 micron C horizon material. If conventiomal dry sieving techniques are used, the optimum field sample should have a minimum mass of 370 grams of -2000 micron (-2 mm) material.

References

References

Allen, J. and Strobel, G. (1966) The assimmilation of $HC^{14}N$ by a variety of fungi. Can. J. Microbiol. 12 , p. 414 - 416.

Alley, N.F. (1976) The palynology and palaeoclimatic significance of a dated core of Holocene peat, Okanagan Valley, southern British Columbia. Can. Journ. Earth Sci., v. 13, p. 1131 - 1144.

Ambrose, J.W. (1964) Exhumed paleoplains of the Precambrian Shield of North America. Amer Jour. Sci., v.262, p. 817 - 857.

Averill, S.A (1988) Regional variations in the gold content of till in Canada; in Prospecting in areas of glaciated terrain - 1988. D.R. MacDonald and K.A. Mills (eds.). Canadian Institute of Mining and Metallurgy, p. 271 - 284.

Averill, S.A and Zimmerman, J.R. (1984) The Riddle resolved: the discovery of the Partridge gold zone using sonic drilling in glacial overburden at Waddy Lake, Saskatchewan. C.I.M.M Geological Journal, v. 1, p. 14 - 20.

Avraamides, J. (1982) Prospects for alternative leaching systems for gold: a review. in The Austrailian I.M.M. Perth and Kalgoorlie branches and Murdoch University, Carbon-in-pulp seminar. p. 369 - 391.

Baker, W.E. (1973) The role of humic acids from Tasmanian podzolic soils in mineral degradation and metal mobilization. Geochim. Cosmochim. Acta, v.37, p. 269 - 281.

Baker, W.E. (1978) The role of humic acid in the transport of gold. Geochim. Cosmochim. Acta, v.42, p. 645 - 649.

Billingsley, P. and Hume, C.B.(1941) The ore deposits of Nickel Plate Mountain, Hedley, B.C., Canadian Institute of Mining and Metallurgy, Bulletin, Vol.44, p. 524 - 590.

Bird, D.J. and Coker, W.B. (1987) Quaternary stratigraphy and geochemistry at the Owl Creek gold mine, Timmins, Ontario, Canada. J. Geochem. Explor., v. 28, p. 267 - 284.

Bolviken, B. and Gleeson, C.F. (1979) Focus on the use of soils for geochemical exploration in glaciated terrain. *in* Geophysics and Geochemistry in the Search for Metallic Ores. Geol. Surv. Can. Econ. Geol. Rept. 31, p. 295 - 326.

Bostock, H.S. (1930) Geology and Ore Deposits of Nickel Plate Mountain Hedley, B.C., Geological Survey of Canada, Summary Report, 1929 Part A.

Bostock, H.S. (1940) Map 568A, Hedley Area, Geol. Surv. Can.

Boulton, G.S. (1968) Flow tills and related deposits on some Vestspitsbergen glaciers. Jour. Glaciol., v.7, p. 391 - 412.

Boulton, G.S. (1970) The deposition of subglacial and melt out tills at the margins of certain Svarlbard glaciers. Jour. Glaciol., v. 9, p. 231 - 245.

Boulton, G.S. (1971) Till genesis and fabric in Svarlbard, Spitsburgen. in Till: A Symposium., R.P. Goldthwait (ed.) Ohio State University Press. p. 41 - 72.

Boyle, R.W., Alexander, W.M., and Aslin, G.E.M. (1975) Some observations on the solubility of gold. Geol. Surv. Can. Paper 75-24.

Boyle, R.W. (1979) The Geochemistry of Gold and its Deposits. Geol. Surv. Can. Bull. 280.

Bradshaw, P.M.D. (ed.) (1975) Conceptual models in exploration geochemistry. J. Geochem. Explor., v.4(1), 213 p.

Camsell, C. (1910) Geology and Ore Deposits of Hedley Mining District, B.C., Geol. Surv. Can. Mem. 2.

Clague, J.J. (1980). Late quaternary geology and geochronolgy of British Columbia. Part 1: Radiocarbon Dates; Geol.Surv. Can., Paper 80-13. 28 p.

Clague, J.J., Armstrong, J.E. and Mathews, W.H. (1980) Advance of the late Wisconsin Cordilleran ice sheet in southern British Columbia since 22,000 yr BP.. Quater. Res., v. 13, p. 322 - 326.

Clifton, H.E., Hunter, R.E., Swanson, F.J. and Phillips, R.L. (1969) Sample size and meaningful gold analysis. U.S. Geol. Surv. Prof. Paper 625C, p. C1 - C17.

Coker, W.B. and DiLabio, R.N.W. (1989) Geochemical exploration in glaciated terrain: geochemical responses. *in* Proceedings of Exploration '87: third decennial conference on geophysical and geochemical exploration for minerals and groundwater. G.D. Garland (ed.). Ontario Geological Survey, Special Volume 3. p. 336 - 385.

Coker, W.B., Sexton, A., Lawyer, I. and Duncan, D. (1988) Bedrock, till and soil geochemical signatures at the Beaver Dam gold deposit, Nova Scotia, Canada. *in* Prospecting in areas of glaciated terrain - 1988. D.R. MacDonald and K.A. Mills (eds.). Canadian Institute of Mining and Metallurgy, p. 241 - 254.

Corey, A.T. (1949) Influence of shape on the fall velocity of sand grains. Unpub. M.Sc. thesis, Colorado A & M college, 102 p.

Day, S.J. (1988) Sampling stream sediments for gold in mineral exploration, southern British Columbia. Unpub. M.Sc. thesis, The University of British Columbia, 233 p.

DiLabio, R.N.W (1982a) Gold and tungsten abundance vs. grain size in till at Waverly, Nova Scotia. *in* Current Research, Part B, Geol. Surv. Can., Paper 82-1B.

DiLabio, R.N.W. (1982b) Drift prospecting near gold occurences at Onaman River, Ontario and Oldham, Nova Scotia. in Geology of Canadian gold deposits. R.W. Hodder and W. Petruk (eds.). Can. Inst. Min. Metall. Special Volume 24. p. 261 - 266.

DiLabio, R.N.W. (1985) Gold Abundance vs. Grain Size in Weathered and Unweathered Till. Geol. Surv. Can. Paper 85-1A, p. 117 -119.

DiLabio, R.N.W. (1988) Residence sites of gold, PGE, and rare lithophile elements in till; in Prospecting in areas of glaciated terrain - 1988. D.R. MacDonald and K.A. Mills (eds.). Canadian Institute of Mining and Metallurgy. p. 121 - 140.

DiLabio, R.N.W. (1989) Classification and interpretation of the shapes and surface textures of gold grains from till. Unpub. manuscript, Terrain Sciences Division, Geol. Surv. Can..

Dolmage, V. and Brown, C.E. (1945) Contact Metamorphism at Nickel Plate Mountain, Hedley, B.C., Canadian Institute of Mining and Metallurgy, Bulletin, Vol. 48.

Downing, B.W and Hoffman, S.J. (1987) A multidisciplinary exploration case history of the Shasta epithermal gold-silver deposit, British Columbia, Canada. *in* Geoexpo 86 - exploration in the North American Cordillera. I.L. Elliot and B.W. Smee (eds.). Association of Exploration Geochemists, 222 p.

Drake, L.D. (1983) Ore plumes in till. Journ. Geol.. v. 91, p. 707 - 713.

Dreimanis, A. (1976) Tills: their origins and properties. *in* Glacial Till., R.F. Legget (Ed.), Roy. Soc. Can. Spec. Publ. No. 12 , p. 11 - 49.

Dreimanis, A. and Vagners, U.J. (1971) Bimodal distribution of rock and mineral fragments in basal tills. *in* Till: A Symposium., R.P. Goldthwait (Ed.). Columbus Pub. p. 237 - 250.

Ettlinger, A.D. and Ray, G.E. (1989) Precious metal enriched skarns in British Columbia: an overview and geological study. B.C. Ministry of Energy, Mines and Petroleum Resources, Paper 1989-3, 128 p.

Evenson, E.B., Pasquini, T.A., Stewart, R.A. and Stephens, G. (1979) Systematic provenance investigations in areas of alpine glaciation: applications to glacial geology and mineral exploration. *in* Moraines and Varves. Ch. Schlucter (ed.). p. 25 - 42.

Flint, R.F. (1971) Glacial and Quaternary Geology. Wiley, New York p. 892.

Fox, P.E, Cameron, R.S. and Hoffman, S.J. (1987) Geology and soil geochemistry of the Quesnel River gold deposit, British Columbia. *in* Geoexpo 86 - Exploration in the North American Cordillera. I.L. Elliot and B.W. Elliot (eds.). Association of Exploration Geochemists, 222 p.

Freise, F.W. (1931) The transportation of gold by organic underground solutions. Econ. Geol. 26, p. 421 - 431.

Freyssinet, Ph., Zeegers, H. and Tardy, Y. (1989) Morphology and geochemistry of gold grains in lateritic profiles of southern Mali. Journ. Geochem. Explor., v. 32, p. 17- 31.

Fulton, R.J. and Smith, G.W. (1978) Late Pleistocene stratigraphy of south-central British Columbia. Can. Journ. Earth Sci. v. 15, p. 971 - 980.

Girling, C.A. and Peterson, P.J. (1978) Uptake, transport and localization of gold in plants. *in* Trace Substances *in* Environmental Health XII, D.D. Hemphill (ed.)., Univ. of Missouri Press.

Goldthwait, R.P. (1971) Introduction to till, today. *in* Till: A Symposium., R.P. Goldthwait (Ed.). Ohio State University Press. p. 3 - 26.

Govett, G.J.S. (1973) Geochemical exploration studies in glaciated terrain, New Brunswick, Canada. *in* Prospecting in Areas of Glaciated Terrain. M.J. Jones (ed.). p. 11 - 24.

Groen, J.C. (1987) Gold-enriched rims on placer gold grains: an evaluation of formational processes. Unpub. M.Sc. thesis, Virginia Polytechnic Institute and State University, 72 p.

Hicock, S.R. (1986) Pliestocene glacial dispersal and history in Buttle valley, Vancouver Island, British Columbia: a feasibility study for alpine drift prospecting. Can. J. Earth Sci., v. 23, p. 1867 - 1879.

Hoffman, S.J. (1987) Soil Sampling. *in* Exploration Geochemistry: design and interpretation of soil surveys., J.M. Robertson (ed.). Reviews in Economic Geology Vol. 3., The Economic Geology Publishing Company, El Paso, Tx. p. 39 - 76.

Holmes, C.D. (1952) Drift dispersion in west-central New York. Bull. Geol. Surv. Am., v. 63, p. 993 - 1010.

Howarth, R.J. and Thompson, M. (1976) Duplicate analysis in geochemical practice. Part 2. Examination of proposed method and examples of its use. Analyst. v. 101, p. 699 - 709.

Ingamells, C.O. (1981) Evaluation of skewed exploration data - the nugget effect. Geochim. et Cosmochim. Acta, v.45, p. 1209 - 1216.

Kerr, F.A. (1936) Quaternary glaciation in the Coast Range, northern British Columbia and Alaska. Jour. Geol., v.44. p. 681 - 700.

Klassen, R.A. (1987) Relationship between glacial history and drift composition. J. Geochem. Explor., v.29., p. 421 - 422.

Knight, J. and McTaggart, K.C. (1986) The composition of placer and lode gold from the Fraser River drainage area, southwestern British Columbia. C.I.M.M Geol. Journ., v.1, no.1, p. 21 - 30.

Koch, J.S. and Link, R.F. (1970) Statistical analysis of geological data. John Wiley and Sons. 375 p.

Krauskopf, K.B. (1951) The solubility of gold. Econ. Geol. v.46. p. 858 - 870.

Lakin, H.W., Curtin, G.C., and Hubert, A.F. (1974) Geochemistry of gold in the weathering cycle. U.S. Geol. Surv. Bull. 1330. 80 p.

Lee, J.W. (1951) The Geology of Nickel Plate Mountain, B.C., Unpub. Ph.D Thesis, Stanford University. 89 p.

Lowdon, J.A., Robertson, I.M., and W. Blake, Jr. (1971). Geological Survey of Canada radiocarbon dates XI: Radiocarbon, v. 13, no. 2, p. 255-324.

MacEachern, I.J. (1983) The distribution, character and composition of gold in till at the Fifteen Mile Stream Gold District, Halifax County, Nova Scotia. Unpub. B.Sc. thesis, Dalhousie University, Halifax. 63 p.

MacEachern, I.J. and Stea, R.R. (1985) The dispersal of gold and related elements in tills and soils at the Forest Hills Gold District, Guyasborough County, Nova Scotia. Geol. Surv. Can. Publ. 85-18, 31 p.

Mackie, W.H. (1961) Climate of British Columbia. Tables of temperature, precipitation and sunshine. Report for 1962. B.C. Dept. of Agriculture, Victoria, B.C..

Mann, A.W. (1984) Mobility of gold and silver in lateritic weathering profiles: some observations from Western Austrailia. Econ. Geol. v. 79, p. 38 - 49.

Mathews, W.H. (1944) Glacial lakes and ice retreat in south -central British Columbia. Trans. Royal Soc. Can., ser. 3, v. 38, sec. 4, p. 39 - 57.

Matysek, P.F. and Sinclair, A.J. (1984) Statistical evaluation of duplicate samples, regional sediment surveys (Map-area 92H, 92I and 92J), British Columbia. B.C. Ministry of Energy, Mines and Petroleum Resources, Geological Fieldwork, 1983, Paper 1984-1, p. 186 - 196.

Matysek, P.F. (1985) An evaluation of regional stream sediment data by advanced statistical procedures., Unpub. M.Sc. Thesis. The University of British Columbia. 95 p.

Milford, J.C. (1984) Geology of the Apex Mountain Group, north and east of the Similkameen River, south central B.C., Unpub. M.Sc. Thesis. The University of British Columbia. 108 p.

Miller, J.K. (1984) Model for clastic indicator trains in till. *in* Prospecting in Areas of Glaciated Terrain, 1984., The Institution of Mining and Metallurgy. 232 p.

Mineyev, G.G. (1976) Organisms in the gold migration -accumulation cycle. Geochem. Int., v. 13., p. 164 - 168.

Moran, S.R. (1971) Glaciotectonic structures in drift. *in* Till: A Symposium. R.P. Goldthwait (ed.). Ohio State University Press. p. 127 - 148.

Mullineaux, D.R., Waldron, H.H. and Rubin, M. (1965) Stratigraphy and chronology of late interglacial and early Vashon glacial time in the Seattle Area, Washington. U.S.G.S. Bull. 1194-O, 10 p.

Northern Miner Magazine.(Feb. 1987) Mascot Gold Mines. *in*: 1987 Gold Report. p. 27 - 29.

Nichol, I., Closs, L.G. and Lavin, O.P. (1987) Sample representivity with reference to gold exploration. *in* Proceedings of Exploration '87: third decennial international conference on geophysical and geochemical exploration for minerals and groundwater. G.D. Garland (ed.). Ontario Geological Survey, Special Volume 24. p. 609 - 624.

Ong, H. and Swanson, V.E. (1969) Natural organic acids in the transportation, deposition and concentration of gold. Colorado School of Mines Quarterly. v. 64., p. 395 - 425.

Ray, G.E., Simpson, R., Wilkinson, W. and Thomas, P. (1986) Preliminary report on the Hedley Mapping Project. B.C. Ministry of Energy, Mines and Petroleum Resources, Geological Fieldwork, 1985, Paper 1986-1, p. 101 - 105.

Ray, G.E., Dawson, G.L., and Simpson, R. (1987) The geology and controls of skarn mineralization in the Hedley Gold Camp, southern British Columbia (92H/8, 82E/5). British Columbia Ministry of Energy, Mines and Petroleum Resources, Geological Fieldwork, 1986, Paper 1987-1.

Ray, G.E. and Dawson, G.L. (1988) Geology and mineral occurrences in the Hedley Gold Camp. B.C. Ministry of Energy, Mines and Petroleum Resources, Open File 1988-6.

Ray, G.E. and Dawson, G.L. (1990) The geology and mineralization of the Hedley gold skarn district, southern British Columbia. (in press).

Rice, H.M.A. (1947) Geology and mineral deposits of the Princeton map-area, B.C., Geol. Surv. Can. Mem. 243.

Rice, H.M.A. (1960) Map 889A, Princeton, British Columbia. Geol. Surv. Can. Mem. 243.

Roddick, J.C., Farrar, E. and Procyshyn, E.L. (1972) Potassium-argon ages of igneous rocks from the area near Hedley, Southern B.C., Can. Journ. Earth Sci., v. 9, p. 1632 - 1639.

Rose, A.W., Hawkes, H.E. and Webb, J.S. (1979) Geochemistry in Mineral Exploration. Academic Press, 657 p.

Roslyakov, N.A. (1984) Zonality of gold forms in the surficial environment as a criterion for buried gold deposits. J. Geochem. Explor., v. 21., p. 95 - 117.

Ryder, J.M. (1978) Geology, landforms and surficial materials ; *in* The soil landscapes of British Columbia. K.W.G. Valentine, P.N. Sprout, T.E. Baker and L.M. Lavkulich (eds.). British Columbia Ministry of Environment, Resource Analysis Branch. p. 11 - 33.

Sauerbrei, J.A., Pattison, E.F., and Averill, S.A. (1987) Till sampling in the Casa Berardi gold area, Quebec: a case history in orientation and discovery. J. Geochem. Explor., v. 28., p. 297 - 314.

Shacklette, H.T., Lakin, H.W., Hubert, A.E., and Curtin, G.C. (1970) Absorption of gold by plants. U.S. Geol. Surv. Bull. 1314-B.

Sharp, R.P. (1949) Studies of superglacial debris on valley glaciers. Amer. Jour. Sci., v. 247., p. 289 - 315.

Sharpe, A.G. (1976) The chemistry of the cyano complexes of the transition metals. Academic Press, 302 p.

Shelp, G.S. and Nichol, I. (1987) Distribution and dispersion of gold in glacial till associated with gold mineralization in the Canadian Shield. J. Geochem. Explor., v. 27., p. 315 - 336.

Shilts, W.W. (1973) Glacial dispersal of rocks, minerals and trace elements in Wisconsin till, southeastern Quebec, Canada. Geol. Soc. Am. Mem. 136., p. 189 - 219.

Shilts, W.W. (1975) Common glacial sediments of the Shield, their properties, distribution and possible uses as geochemical sampling media. J. Geochem. Explor., v. 4., p. 189 - 199.

Shilts, W.W. (1976) Glacial till and mineral exploration. *in* Glacial till. An interdisciplinary study. R.F. Legget (ed.). Roy. Soc. Can. Spec. Pub. no. 12., p. 205 - 224.

Sopuck, V.J, Schreiner, B.T.,and Averill, S.A. (1986) Drift prospecting for gold in the southwestern Shield of Saskatchewan, Canada; *in* Prospecting in areas of glaciated terrain - 1986. Institution of Mining and Metallurgy, London. p. 217 - 240.

St. Arnaud, R.J. (1976) Pedological aspects of tills. *in* Glacial Till. An interdisciplinary study. R.F. Legget, (ed.). Roy. Soc. Can. Spec. Pub. no. 12., p. 133 - 155.

Stanley, C.R. (1987) PROBPLOT, an interactive program to fit mixtures of normal (or log-normal) distributions with maximum likelihood optimization procedures. Association of Exploration Geochemists Spec. Vol. 14.

Stanley, C.R. and Smee, B.W. (1988) A test in pattern recognition: defining anomalous patterns in surficial samples which exhibit severe nugget effects. Explore, no. 63, p. 12 - 14.

Stanley, C.R. and Smee, B.W. (1989) A test in pattern recognition: defining anomalous patterns in surficial amples which exhibit severe nugget effects - II. Explore, no. 65, p. 12 - 14.

Stoffregen, R. (1986) Observations on the behavior of gold during supergene oxidation at Summitville, Colorado, USA, and implications for electrum stability in the weathering environment. Appl. Geoch., v. 1, p. 549 - 558.

Strobel, G.A. (1967) Cyanide utilization in soil. Soil Sci. v. 103, p. 299 - 302.

Thompson, M. and Howarth, R.J. (1973) The rapid estimation and control of precision by duplicate determinations. Analyst. v. 98 no. 1164. p. 153 - 160.

Thompson, M. and Howarth, R.J. (1976) Duplicate analysis in geochemical practice. Part 1. Theoretical approach and estimation of analytical reproducibility. Analyst. v. 101, p. 690 - 698.

Thompson, M. and Howarth, R.J. (1978) A new approach to the estimation of analytical precision. J. Geochem. Explor., v.28, p. 23 - 30.

Thomson, I., Burns, J.G., and Faulkner, F.H. (1987) Gold exploration in deep glaciated overburden: experiences from the Belore case history. J. Geochem. Explor., v.29., p. 435 - 436.

Thorleifson, L.H. and Kristjansson, F.J. (1988) Visible gold content and lithology of till from overburden drillholes, Beardmore - Geraldton area, District of Thunder Bay, northern Ontario. Geol. Surv. Can. Open File 1756. 21 p.

Warren, H.V. and Cummmings, J.M. (1936) Mineralogy at the Nickel Plate Mine, Miner, v. 9, p. 27 - 28.

Warren, H.V. (1982) The significance of a discovery of gold crystals in overburden. Levinson, A.A. (ed.). Precious Metals in the Northern Cordillera. p. 45 - 51.

Webster, J.G and Mann, A.W. (1984) The influence of climate, geomorphology and primary geology on the supergene migration of gold and silver. J. Geochem. Explor., v. 22, p. 21 - 42.

Wilson, A.F. (1984) Origin of quartz-free gold nuggets and supergene gold found in laterites and soils - a review and some new observations . Austrailian Journ. Earth Sci. v. 31, p. 303 - 316.

Young, R.J. (1984) Geochemistry - 1984: Good Hope Option V-194, Primont Option V-199, Osoyoos Mining Division, Latitude $49^\circ22'$N, Longitude $120^\circ00'$W. Unpub. rept., Placer Development Limited.

Zar, J.H. (1984) Biostatistical analysis. Prentice-Hall, Inc. 718 p.

Appendix

Analytical Data and Sample Weights

Nickel Plate 1987
Sample data

Size Fraction

Samp #	Horzn	Pit	Depth (cm)	pH	+2000 (grams)	-2000 +420 (grams)	-420 +212 (grams)	-212 (grams)	Au (ppb)
2	2	1	30	7.10	619.36	284.18	115.93	789.92	275
3	3	1	55	7.10	883.46	259.41	99.46	567.47	380
4	4	1	110	7.20	781.14	317.93	83.61	413.12	325
6	2	2	20	7.10	479.25	132.55	42.20	320.63	6350
7	3	2	70	7.40	978.15	254.21	97.80	518.01	495
8	4	2	100	7.40	826.07	244.54	81.10	701.72	280
10	2	3	13	6.60	579.14	181.02	78.90	556.54	200
11	3	3	67	6.90	648.89	231.20	102.83	661.43	250
12	4	3	100	7.20	629.82	281.77	135.63	565.88	15
14	2	4	25	7.45	699.81	245.35	100.94	696.02	410
15	3	4	72	7.15	936.27	259.08	117.13	660.87	115
16	4	4	110	7.75	832.93	327.22	174.21	558.59	225
18	2	5	18	7.00	697.19	242.72	99.02	522.93	95
19	3	5	55	7.20	481.43	247.74	108.77	370.76	270
20	4	5	93	7.00	725.62	265.98	106.43	410.14	520
21	4	5	100	7.15	554.69	294.96	145.69	623.86	285
23	2	6	20	6.50	695.43	186.72	76.98	475.29	225
24	3	6	57	7.40	667.65	235.88	100.61	667.64	200
25	4	6	100	7.15	842.33	273.17	122.08	642.21	305
27	2	7	42	6.65	663.04	282.55	134.69	869.84	1580
28	3	7	63	7.00	748.88	277.26	133.92	582.18	285
29	4	7	110	7.30	1132.68	439.98	239.53	897.40	435
31	2	8	25	6.05	839.71	312.29	134.36	786.24	135
32	3	8	58	7.00	670.99	306.17	139.18	683.47	310
33	4	8	110	7.05	867.35	329.42	109.91	547.62	485
34	4	8	120	7.20	771.69	271.38	108.62	647.46	260
36	2	9	24	6.60	836.58	278.89	110.56	649.29	425
37	3	9	58	6.95	1015.65	341.48	147.54	698.00	240
38	4	9	90	7.00	836.12	534.39	165.15	510.36	535
39	4	9	105	7.20	1346.22	365.30	215.02	884.30	485
41	2	10	13	6.65	967.97	338.03	120.11	683.13	155
42	3	10	47	6.80	872.69	296.69	112.12	573.29	150
43	4	10	80	6.90	1050.20	365.04	140.73	665.06	360
44	4	10	130	7.20	1399.98	457.93	195.86	660.74	400
46	2	11	23	6.90	871.40	263.38	83.47	496.73	185
47	3	11	52	7.00	964.25	339.28	140.80	661.55	-10
48	4	11	115	7.00	773.39	346.11	152.30	482.00	465
49	4	11	130	7.10	655.61	346.85	145.03	707.20	675
51	2	12	19	6.65	864.81	218.34	102.18	592.63	210
52	3	12	58	6.70	1023.22	326.21	118.15	653.56	195
53	4	12	140	7.15	1067.45	376.89	162.67	835.00	810
55	2	13	13	7.10	1156.36	341.23	104.66	574.75	80
56	3	13	60	6.85	1350.86	450.50	137.08	784.70	480

Nickel Plate 1987
Sample data

Size Fraction

Samp #	Horzn	Pit	Depth (cm)	pH	+2000 (grams)	-2000 +420 (grams)	-420 +212 (grams)	-212 (grams)	Au (ppb)
57	4	13	104	6.90	970.70	403.74	158.48	469.55	485
58	4	13	115	6.90	1433.23	481.31	208.74	707.66	1025
60	2	14	18	6.75	1282.51	280.89	78.84	436.25	100
61	3	14	50	7.00	1270.35	452.80	150.37	661.09	135
62	4	14	115	7.40	1338.44	325.54	128.51	463.64	295
64	2	15	8	6.90	858.67	203.23	61.49	345.47	155
65	3	15	55	6.70	1068.00	372.93	121.32	588.95	210
66	4	15	90	6.90	1183.49	565.21	184.77	672.39	445
67	4	15	125	7.15	1170.81	510.34	217.49	610.48	285
70	2	16	18	6.85	757.77	207.54	69.47	448.33	60
72	4	16	115	6.90	1741.49	448.97	143.13	524.32	145
73	4	16	130	7.10	712.69	266.36	90.22	421.11	150
75	2	17	14	7.00	634.23	194.40	69.00	427.40	75
99	4	17	60	6.70	1126.68	272.07	110.20	417.00	150
100	4	17	80	6.90	1227.74	419.32	166.71	473.36	225
101	4	17	115	6.60	1226.68	343.83	132.70	665.37	220
79	2	18	30	6.75	825.37	280.99	80.80	549.75	60
80	3	18	69	6.90	782.15	326.92	122.97	658.78	130
81	4	18	108	6.85	837.89	378.34	158.25	0.00	0
82	4	18	132	7.15	508.51	252.53	104.44	619.75	265
83	4	18	140	7.20	732.49	342.15	141.24	805.69	255
85	2	19	8	6.80	931.57	207.61	62.49	0.00	0
86	3	19	55	6.90	761.83	244.50	80.84	385.26	65
87	4	19	106	6.90	926.14	415.02	178.09	577.05	145
88	4	19	110	6.70	907.49	443.14	164.94	451.67	320
90	2	20	8	7.15	615.65	247.55	84.58	416.12	90
92	4	20	115	7.20	1513.90	688.86	285.69	622.35	275
93	4	20	125	6.90	922.32	368.90	155.72	421.98	155
95	2	21	44	7.00	840.24	298.35	112.48	497.87	410
96	3	21	75	7.00	1018.04	394.65	140.93	480.98	165
97	4	21	100	7.05	1186.51	637.23	244.37	574.55	185
98	4	21	130	7.00	756.83	386.03	186.77	511.02	225
103	2	22	22	6.90	704.33	224.34	84.13	653.09	110
104	3	22	55	7.00	942.48	387.43	162.62	968.13	105
105	4	22	95	7.60	1570.89	630.64	239.45	897.13	195
106	4	22	130	7.60	682.52	284.09	112.72	677.18	110
108	2	23	35	6.70	970.30	224.89	82.01	699.33	50
109	3	23	60	7.20	633.65	146.52	63.06	418.47	145
110	4	23	85	7.50	692.82	286.60	119.28	606.92	115
111	4	23	115	7.20	894.63	297.17	79.98	239.90	190
113	2	24	22	7.00	551.56	183.94	71.89	583.96	35
114	3	24	50	7.15	560.09	194.74	83.08	673.36	85
115	4	24	70	6.80	1090.53	373.42	148.62	874.60	155

Nickel Plate 1987
Sample data

Size Fraction

Samp #	Horzn	Pit	Depth (cm)	pH	+2000 (grams)	-2000 +420 (grams)	-420 +212 (grams)	-212 (grams)	Au (ppb)
116	4	24	115	7.30	433.16	185.47	76.09	580.78	60
118	2	25	21	7.15	482.75	163.68	65.43	554.02	45
119	3	25	42	7.20	544.30	192.19	84.67	585.45	250
120	4	25	85	7.15	595.84	258.55	100.68	788.54	175
122	2	26	20	6.80	649.14	163.13	50.98	523.76	35
123	3	26	45	7.00	974.76	293.78	116.33	788.75	90
124	4	26	90	7.10	1034.08	323.28	120.77	701.89	105
125	4	26	135	6.90	1792.59	608.29	172.03	115.92	85
127	2	27	18	6.85	549.42	187.47	72.51	686.04	65
128	3	27	42	7.20	533.03	180.87	66.91	515.66	60
129	4	27	65	7.20	737.14	247.49	88.41	660.01	105
130	4	27	95	6.75	824.97	269.61	86.97	569.66	90
132	2	28	35	6.90	453.55	178.36	69.73	589.05	55
133	3	28	57	7.30	368.72	187.58	74.15	512.13	95
134	4	28	85	7.00	764.11	324.23	136.55	488.45	285
135	4	28	115	7.20	1447.06	560.59	187.75	507.65	250
137	2	29	38	7.10	747.66	188.62	80.34	614.07	100
138	3	29	65	7.10	747.74	258.70	105.30	614.72	175
139	4	29	90	7.15	550.02	243.99	86.40	529.07	65
140	4	29	115	7.25	877.50	285.42	110.38	574.84	830
142	2	30	25	6.90	474.97	166.04	57.41	450.50	155
143	3	30	49	7.10	536.53	209.27	79.77	605.23	30
144	4	30	82	7.15	579.48	154.34	62.71	417.28	130
145	4	30	115	7.15	1234.21	483.01	165.12	926.20	70
147	2	31	15	7.00	400.85	137.81	41.45	424.06	65
148	3	31	49	7.25	902.80	243.70	84.84	843.01	35
149	4	31	79	7.15	1068.38	346.12	127.68	958.92	75
150	4	31	115	7.60	786.46	313.76	115.29	716.70	45
152	2	32	25	7.35	388.24	127.61	46.05	437.36	85
153	3	32	50	7.50	387.25	185.32	66.90	589.05	60
154	4	32	75	7.50	555.60	206.51	85.20	717.12	65
155	4	32	100	7.85	1085.51	412.74	151.39	878.74	50
157	2	33	26	7.30	534.08	156.26	54.47	523.34	40
158	3	33	48	7.50	687.07	127.65	48.26	352.07	100
159	4	33	75	7.50	860.31	286.90	114.32	758.91	55
160	4	33	115	7.50	760.17	386.27	134.13	787.13	75
162	2	34	35	7.65	477.34	160.17	52.94	584.00	40
163	3	34	55	7.60	828.91	185.44	72.92	519.21	65
163	3	34	55	7.50	828.91	185.44	72.92	519.21	65
164	4	34	100	7.70	928.46	287.80	87.77	566.18	35
166	2	35	30	7.60	555.36	127.03	45.17	557.67	20
167	3	35	50	7.60	503.91	172.17	68.13	752.91	25
169	4	35	100	7.95	617.25	212.57	86.46	725.76	35

Nickel Plate 1987
Sample data

Size Fraction

Samp #	Horzn	Pit	Depth (cm)	pH	+2000 (grams)	-2000 +420 (grams)	-420 +212 (grams)	-212 (grams)	Au (ppb)
171	2	36	28	7.00	416.25	119.61	37.41	511.31	15
172	3	36	48	7.50	488.80	126.07	44.73	531.55	25
173	4	36	70	7.45	303.88	137.18	56.01	384.32	245
174	4	36	110	7.60	436.52	174.82	72.08	375.63	45
176	2	37	11	7.20	769.57	171.87	55.35	623.21	10
177	3	37	45	7.00	414.08	184.71	66.84	648.97	40
178	4	37	80	7.60	571.76	226.13	86.58	563.44	65
179	4	37	125	7.50	1496.97	285.62	152.12	746.99	35
181	2	38	34	7.30	427.61	141.20	42.24	435.47	15
182	3	38	55	7.35	485.78	185.04	72.70	590.00	40
183	4	38	80	7.70	1025.85	174.81	61.88	507.93	45
184	4	38	110	7.85	579.82	165.54	59.57	519.65	20
186	2	39	30	7.18	376.18	117.92	43.23	583.85	30
187	3	39	50	7.30	323.20	136.92	49.41	695.34	45
188	4	39	72	7.50	399.10	85.25	28.30	418.13	55
189	4	39	105	7.80	677.19	189.49	71.32	684.28	95
191	2	40	35	7.15	364.23	182.95	73.54	845.29	65
192	3	40	53	7.45	567.76	184.50	70.88	610.20	115
193	4	40	80	7.45	974.22	256.05	86.64	502.57	310
194	4	40	110	7.80	786.86	296.05	124.50	588.16	70
196	2	41	30	7.70	670.79	185.45	68.89	658.96	70
197	3	41	60	7.65	301.37	106.13	43.98	498.55	35
198	4	41	90	7.90	306.93	110.82	53.76	788.42	30
200	2	42	28	7.15	457.79	185.32	67.35	674.26	70
201	3	42	52	7.25	484.44	176.48	68.89	460.68	95
202	4	42	77	7.00	283.92	146.90	71.70	638.22	70
203	4	42	105	7.75	215.15	92.90	53.82	531.83	55
206	3	43	45	7.70	12.51	26.33	14.30	584.37	10
207	4	43	75	7.30	636.95	170.05	59.19	280.72	85
208	4	43	100	7.40	681.34	142.08	45.10	259.56	55
211	2	44	27	7.60	1.55	4.25	4.19	233.17	45
212	3	44	38	7.70	6.28	13.20	3.23	223.70	-15
213	4	44	50	7.25	5.27	16.25	7.31	170.91	105
214	4	44	70	7.50	797.82	180.88	71.43	328.88	60
216	2	45	15	7.60	47.32	21.05	13.86	569.89	20
217	3	45	35	7.70	51.32	17.15	8.34	639.84	20
218	4	45	65	7.80	539.57	157.35	69.43	394.88	40
219	4	45	100	7.35	428.13	161.66	75.25	446.74	45
221	2	46	30	7.80	35.00	25.78	14.61	283.91	20
222	4	46	65	7.70	784.58	385.28	174.34	637.49	55
223	4	46	100	7.70	752.41	231.43	85.95	346.76	75
225	2	47	12	7.65	45.87	22.27	14.07	466.18	35
227	9	47	42	7.70	4.58	9.68	8.60	455.56	140

Nickel Plate 1987
Sample data

Size Fraction

Samp #	Horzn	Pit	Depth (cm)	pH	+2000 (grams)	-2000 +420 (grams)	-420 +212 (grams)	-212 (grams)	Au (ppb)
228	4	47	63	7.60	334.64	64.30	17.98	259.77	50
229	4	47	100	7.80	346.04	177.60	65.57	564.98	75
231	2	48	10	7.85	18.90	13.79	11.03	183.44	15
233	4	48	85	7.85	611.95	167.27	63.18	397.22	300
235	2	49	10	7.50	47.28	23.02	20.00	322.35	20
236	3	49	25	7.20	181.16	74.89	26.55	591.36	60
237	4	49	55	7.40	896.13	158.93	58.12	360.62	200
240	2	50	40	7.60	523.91	58.36	104.68	546.19	170
244	2	51	26	7.50	118.77	33.11	19.15	466.48	10
245	4	51	63	7.70	814.99	353.12	149.51	480.19	80
246	4	51	100	7.60	445.76	202.63	86.15	682.71	40
250	4	52	62	8.00	389.96	207.20	85.78	576.26	70
258	2	53	100	6.80	322.97	123.28	42.52	269.98	320
259	3	53	45	6.90	473.28	155.52	52.63	283.83	140
260	4	53	80	7.20	1128.38	365.53	108.14	380.47	860
261	4	53	115	7.40	957.34	255.40	67.57	247.05	470
262	4	54	180	7.90	682.22	393.36	137.28	239.98	720
264	4	55	130	7.75	825.62	396.36	134.05	418.70	1060
266	4	56	150	7.60	830.33	429.38	126.74	244.37	1030
267	4	56	200	7.70	1129.37	433.15	77.16	101.31	5070
268	4	57	185	7.40	1069.40	312.48	123.99	323.59	470
269	4	57	230	7.50	1253.23	302.22	103.75	226.94	590
272	4	59	145	6.90	807.34	325.34	115.13	464.69	400
273	4	59	185	7.40	520.75	258.15	84.31	210.96	400
275	4	60	240	7.25	342.11	99.23	35.09	543.15	1280
277	4	61	250	7.40	1096.85	443.93	204.18	689.77	610
278	4	62	200	7.30	1036.37	589.08	140.82	635.21	770
279	4	63	200	7.50	875.25	377.17	140.79	763.68	290
280	4	64	150	7.65	1059.59	468.60	196.68	954.47	290
283	4	66	140	7.50	1004.85	449.17	131.57	419.50	345
284	4	66	260	7.50	544.90	243.89	76.18	520.98	80
287	4	68	200	8.00	1042.08	211.23	47.09	128.85	60
289	4	70	200	7.50	598.03	279.06	380.91	540.29	370
290	4	72	80	7.15	452.27	126.54	63.57	421.98	20
292	4	73	160	7.70	749.83	309.58	46.95	154.53	40
293	4	74	130	7.60	1261.28	323.55	122.14	502.86	160
294	2	76	15	7.30	322.97	154.88	70.03	681.84	90
295	3	76	45	7.75	422.63	136.54	58.55	502.72	100
296	4	76	120	7.50	381.32	241.14	99.90	896.42	185
297	2	77	30	7.45	325.33	88.45	35.44	449.75	60
299	4	77	105	7.50	555.22	197.54	65.48	653.25	50
300	4	78	53	7.50	349.59	176.54	76.11	608.31	130
301	4	78	140	7.90	561.77	188.44	73.94	654.88	80

Nickel Plate 1987
Sample data

Size Fraction

Samp #	Horzn	Pit	Depth (cm)	pH	+2000 (grams)	-2000 +420 (grams)	-420 +212 (grams)	-212 (grams)	Au (ppb)
302	2	80	30	7.25	255.09	74.84	29.17	327.57	20
304	4	81	110	7.05	516.37	141.88	60.15	364.11	40
305	2	82	50	7.55	364.19	167.09	63.24	582.26	80
306	3	82	70	7.65	502.36	204.80	77.80	476.27	170
308	2	83	30	7.40	353.90	137.09	52.32	471.41	30
310	4	83	125	7.80	943.22	401.87	84.52	378.75	60
311	2	84	35	7.60	711.88	154.34	49.42	339.73	120
312	4	84	170	7.90	432.43	144.60	49.05	608.02	60
313	4	84	240	7.80	465.53	228.44	98.07	791.65	160
315	4	85	210	7.60	381.55	188.59	67.10	541.24	100
316	2	86	40	7.60	548.45	163.86	50.90	397.16	100
317	3	86	60	7.50	839.65	320.81	93.79	262.53	270
318	4	86	130	7.55	1185.48	313.41	93.46	429.93	230
320	4	87	0	8.10	283.34	114.56	53.65	377.62	10

Nickel Plate 1987
Size Fraction weight data
Detailed Samples

Samp #	Pit	Horzn	-2000 +420 (grams)	-420 +212 (grams)	-212 +106 (grams)	-106 +53 (grams)	-53 (grams)	Total (grams)
14	4	2	617.75	241.05	309.34	235.33	1324.02	2727.49
15	4	3	706.00	321.31	318.22	216.93	1298.82	2861.28
16	4	4	869.64	417.24	342.84	235.56	1126.47	2991.75
41	10	2	723.98	248.00	269.37	187.38	1104.15	2532.88
42	10	3	870.61	310.56	261.60	157.91	1403.52	3004.20
43	10	4	1097.57	424.63	272.18	289.88	1400.92	3485.18
44	10	4	1235.72	482.34	382.05	250.26	1078.65	3429.02
122	26	2	359.58	145.05	171.67	129.95	842.92	1649.17
123	26	3	784.52	337.09	325.19	234.07	1554.42	3235.29
124	26	4	763.95	313.67	262.37	172.26	1101.19	2613.44
125	26	4	1287.22	475.98	461.19	321.06	2056.42	4601.87
127	27	2	477.43	228.03	243.09	167.19	1313.92	2429.66
128	27	3	443.67	195.33	208.97	131.70	1167.01	2146.68
129	27	4	427.84	206.60	175.42	142.32	959.68	1911.86
130	27	4	507.82	229.15	181.02	119.08	892.54	1929.61
162	34	2	357.45	136.22	175.76	110.70	1084.65	1864.78
163	34	3	477.36	201.60	172.07	114.90	789.54	1755.47
164	34	4	757.88	255.12	237.73	200.95	975.70	2427.38
186	39	2	281.79	111.75	177.67	123.49	1146.37	1841.07
187	39	3	301.78	113.02	179.54	141.50	1242.22	1978.06
188	39	4	221.43	86.26	111.63	104.66	901.90	1425.88
189	39	4	389.59	155.19	154.96	134.99	1168.88	2003.61

Nickel Plate 1987
Size and Density fraction
weight data

Samp #	-420 +212 light	-420 +212 heavy	-212 +106 light	-212 +106 heavy	-106 +53 light	-106 +53 heavy
14	187.37	53.48	244.95	63.89	183.53	50.72
15	245.30	76.56	232.37	86.51	156.63	59.98
16	314.31	103.46	238.38	104.76	160.69	74.85
41	194.99	53.00	209.77	59.47	145.38	41.09
42	242.42	68.98	199.76	61.99	118.48	39.02
43	331.06	94.34	198.32	73.77	221.91	68.78
44	370.58	114.10	277.61	106.00	182.60	68.52
122	127.72	17.33	151.72	20.11	115.32	14.18
123	285.16	52.53	270.86	54.85	198.39	35.57
124	275.52	38.51	223.65	38.88	148.12	23.65
125	412.21	64.25	389.68	71.61	273.30	46.32
127	203.55	24.96	214.53	27.68	145.55	20.92
128	175.40	19.80	182.92	25.85	114.89	16.19
129	181.42	24.96	147.97	26.82	117.95	23.22
130	199.53	29.12	149.49	27.75	108.64	9.93
162	121.80	14.10	158.13	17.21	101.56	8.48
163	187.20	14.48	156.21	15.62	106.86	7.21
164	251.15	3.73	232.90	4.32	196.66	3.55
186	98.34	13.01	159.04	17.90	108.11	14.35
187	97.03	15.67	158.08	21.19	121.60	19.15
188	71.86	13.92	95.24	15.85	91.95	12.05
189	119.10	35.65	127.39	27.06	117.08	17.05

Nickel Plate 1987
Size and Density fraction
Au analyses

Samp #	-420 +212 light	-420 +212 heavy	-212 +106 light	-212 +106 heavy	-106 +53 light	-106 +53 heavy	-53
14	85	110	70	805	40	1060	305
15	130	2200	90	100	80	875	390
16	150	175	125	505	125	2210	425
41	120	130	65	1115	45	975	200
42	110	180	65	935	50	1360	225
43	90	895	105	1585	80	725	390
44	105	125	175	1650	120	1685	595
122	30	50	40	45	20	330	70
123	55	6250	55	385	45	725	120
124	80	40	60	305	40	735	150
125	65	60	80	1180	55	785	155
127	45	60	20	420	20	560	55
128	50	45	35	165	40	1070	90
129	40	35	50	45	30	585	130
130	70	40	60	365	30	2120	120
162	20	20	20	1720	25	140	30
163	10	40	20	615	10	1360	55
164	10	25	10	70	10	-30	40
186	35	25	35	385	20	420	45
187	50	155	40	465	30	760	70
188	55	20	50	40	40	620	90
189	40	45	40	45	30	335	95

Nickel Plate 1987
Cyanide extraction - AAS results

Sample	Horzn	Cyanide Extractable Au (ppb)	Residual Au (ppb)
14	A	90	45
15	B	450	145
16	C	350	105
41	A	95	145
42	B	130	115
43	C1	370	115
44	C2	510	145
122	A	-15	20
123	B	145	35
124	C1	145	35
125	C2	145	35
127	A	145	35
128	B	80	15
129	C1	175	45
130	C2	110	65
162	A	-15	20
163	B	65	15
164	C	-15	5
186	A	30	5
187	B	110	40
188	C1	80	15
189	C2	130	25

Sample Location Map

5150

5000

L1

L2

L3

L4

L5

57

85

N

Roadcut soil site

L1 —— Soil line

100m